HOLOCENE OSTRACOD PALEOECOLOGY OF THE
SOUTHWESTERN BLACK SEA SHELF

LORNA R. WILLIAMS

HOLOCENE OSTRACOD PALEOECOLOGY OF THE SOUTHWESTERN

BLACK SEA SHELF

by

© Lorna R. Williams

A Thesis submitted to the

School of Graduate Studies

in partial fulfillment of the requirements for the degree of

Master of Science

Earth Sciences Department

Memorial University of Newfoundland

September 2012

St. John's   Newfoundland

ABSTRACT

The Black Sea is an essentially isolated sea connected to the Mediterranean Sea through two narrow and shallow straits. The Bosphorus Strait connects the Black Sea to the Marmara Sea and the Dardanelles Strait connects the Marmara Sea to the eastern Mediterranean Sea. Today, a two-way flow exists between the Mediterranean Sea and the Black Sea via the Marmara Sea and the Dardanelles and Bosphorus Straits. During glacial periods when water levels in the World Ocean dropped, the Black Sea became periodically isolated. There are three conflicting hypotheses regarding the timing and mechanism of the last reconnection of the Black Sea to the Mediterranean Sea: the Flood Hypothesis, the Outflow Hypothesis and the Oscillating Hypothesis.

Cores MAR05-50P and MAR05-51G were raised in 91 m water depth from the southwestern Black Sea shelf on the eastern levee of a saline underflow channel. Composite core MAR05-50 was constructed from the above cores to accommodate core top loss and an age model was created based on 11 radiocarbon dates. Core MAR05-50 recovered sediments from virtually the entire Holocene from 11490 cal yr BP to present.

A total of 45 individual ostracod species were found in the above cores and 43 were identified with the aid of taxonomic literature. From 11400 to7450 cal yr BP the ostracod assemblage is completely dominated by Ponto-Caspian species, mainly *Loxoconcha sublepida*, *Loxoconcha lepida* and *Tyrrhenocythere amnicola donetziensis*. From 7580 to 6410 cal yr BP the assemblage is almost equal abundances of a new Mediterranean species *Loxoconcha littoralis* and the Ponto-Caspian species. After 7450 cal yr BP to the top of the core, the assemblage is fully dominated by Mediterranean

species, including *Palmoconcha agilis*, *Carinocythereis carinata*, *Hiltermannicythere rubra* and *Pterygocythereis jonesii*. CONISS cluster analysis revealed 6 Bio-zones where there are distinct changes in the ostracod assemblage. The lower, Ponto-Caspian interval is divided into Bio-zones 1 and 2. The "mixed" assemblage is Bio-zone 3. The upper, Mediterranean interval of the core is divided into Bio-zones 4, 5 and 6 where new Mediterranean species are introduced and previous species decrease in abundance or disappear. The changes in the ostracod assemblages from one bio-zone to the next suggests that progressive ecological changes took place on the southwestern Black Sea shelf from 11400 cal yr BP to present. Sedimentological data and geochemical data from core MAR02-45, ~70 km northeast of the study area, place the timing of the last post-glacial reconnection between the Black Sea and the Mediterranean Sea at ~8500 cal yr BP.

The ostracod data indicate a ~1000 year salinization lag between the reconnection and the first Mediterranean species to colonize the area. The step-wise Bio-zones further suggest that the post-reconnection salinization of the Black Sea was a gradual process and took ~5000 years to reach near-modern salinity conditions. The results conflict with the catastrophic Flood Hypothesis in that the changes in the ostracod assemblages seem to reflect a more ordered reconnection and stepwise salinization process. The ostracod results can neither confirm nor refute the Oscillating Hypothesis. There are no conflicts between the ostracod data and the Outflow Hypothesis which argues for a gradual reconnection and salinization. Both the Outflow Hypothesis and the Oscillating Hypothesis are entirely plausible based on the ostracod evidence from core MAR05-50.

Acknowledgements

I am truly grateful to many people who made this thesis not only possible but also a truly rewarding experience. First and foremost I extend my sincerest gratitude to my supervisors, Ali Aksu and Richard Hiscott for giving me the opportunity to work with them on such an interesting research project. I wish to thank them for their financial support and for their constant guidance, encouragement and their faith in me.

I would like to express my deepest thanks to ostracod experts David Horne of Queen Mary University in the United Kingdom and Marius Stoica of the University of Bucharest in Romania. Without their ongoing advice, and especially their help with ostracod identifications, this thesis would never have been possible.

I wish to thank the Earth Sciences Department and the School of Graduate Studies at Memorial University of Newfoundland for all their assistance, in particular I am grateful for their financial support during my research and for providing funding for travel necessary to my research.

I would like to extend my appreciation to the people I saw every day, had a chat or a cup of tea with and who made my time as a graduate student something I will miss and remember fondly. I would especially like to thank my friend Bahar Kutboğan and my officemates Anna Linegar and Katey Roberts who helped me so much along the way. I extend my heartfelt thanks to my officemate Anna Linegar whose desk was next to mine from the very first day and for sharing all the triumphs, stresses and many cups of tea.

Finally, I wish to thank my partner Paul who paid the rent and encouraged me and my family who have supported me in every way during my program and always.

Table of Contents

List of Tables

List of Figures

CHAPTER 7

List of Plates

CHAPTER 1

INTRODUCTION

This thesis is part of continuing research in the area of the Aegean, Marmara and Black seas with regard to tectonic events, sea-level and climatic changes during the Quaternary in central and northern Europe. The goal of this study is to develop a paleoecological reconstruction of the southwest Black Sea shelf area using the calcareous microfossil Ostracoda. The Ostracoda are a class of the Crustacea (phylum Arthropoda) which are commonly preserved in marine sediments. The main purpose of this research is to support and add to an existing body of data regarding the post-glacial environment of the Black Sea. This thesis also highlights Black Sea ostracod taxonomy as well as the value and increasing use of ostracods as paleoenvironmental indicators.

1.1. Thesis Objectives

The primary scientific objectives of this thesis are:

1. to construct a chronostratigraphic framework for the latest glacial to Recent sediments recovered in a 737 cm-long piston core (MAR05-50) and its 157 cm-long gravity core (MAR05-51G) raised in 91 m water depth from the southwestern Black Sea shelf.

2. to identify ostracod species collected from 89 samples extracted from the above piston and gravity cores.

3. to determine the abundance and distribution of 45 ostracod species found in the above 89 samples.

4. to delineate the paleoclimatic and paleoceanographic evolution, with emphasis

1

on salinity changes, of the southwestern Black Sea shelf based on the ecological affinities (where known) of the above 45 ostracod species and

     5. to evaluate the validity of three existing and internally conflicting hypotheses regarding the post-glacial reconnection of the Black Sea with the eastern Mediterranean Sea.

1.2. Oceanography of the Black Sea

The Black Sea is an essentially isolated sea situated between the Pontic Mountains of Turkey to the south, the Caucasus and Crimea Mountains of Russia and Ukraine to the north and northeast and the Danube alluvial plain to the west (Fig.1.1). It is bordered by Bulgaria, Georgia, Romania, Russia, Turkey, and Ukraine.

The Black Sea is connected to the World Ocean through two shallow and narrow straits. The Bosphorus Strait connects the southwestern Black Sea to the Marmara Sea; the Marmara Sea in turn is connected to the Aegean Sea through the Dardanelles Strait (Fig. 1.1). The sill depth of the Bosphorus Strait is ~40 m and the Dardanelles Strait sill depth is ~70 m (Aksu et al., 2002a). The Black Sea is also connected to the Sea of Azov by the Strait of Kerch in the north. It has an elliptical shape trending west-east with a surface area of ~436,000 km^2, a maximum west-east length of approximately 1210 km and a maximum width of 560 km. The volume of water contained in the Black Sea is ~534,000 km^3. The maximum depth is 2212 m (Panin and Strechie, 2006). The level of the Black Sea oscillates seasonally by ~10–15 cm in response to freshwater river input from large rivers such as the Danube, Don, Dnieper, Dniester and Bug (Stanev et al., 2000) and no significant tides. In the southwestern Black Sea waves generated by 100-

2
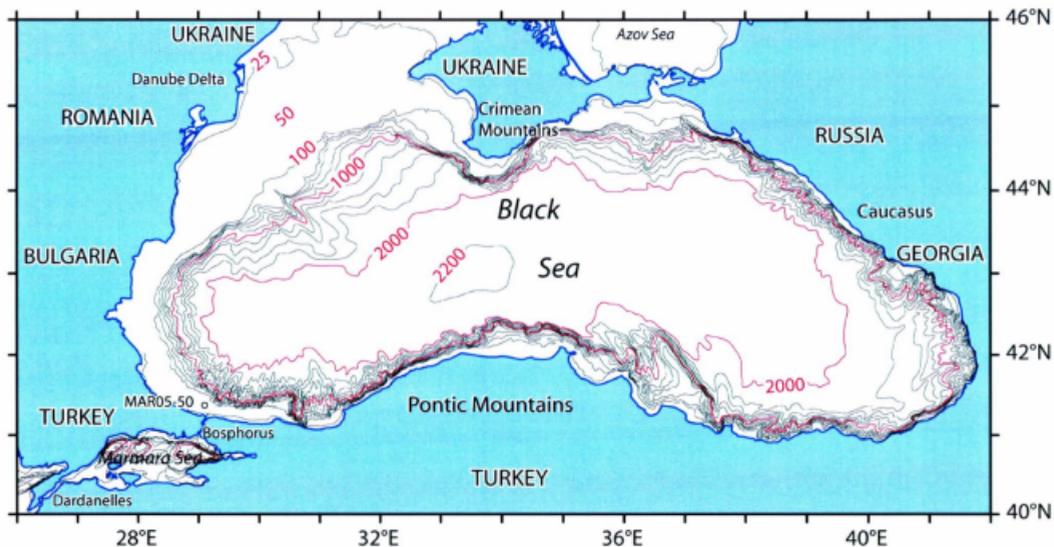
Figure 1.1. Bathymetric map of the Black Sea showing its location within Europe and connections to the Azov Sea to the north and the Marmara Sea to the southeast. Isobaths in meters (modified from Aksu et al., 2002b).

year storms influence the seafloor to depths of up to 95 m (Aksu et al., 2002a).

1.2.1. Water Masses

The Black Sea is the world's largest meromictic water body, meaning it has layers which do not mix. A two-way flow exists between the Mediterranean Sea, Aegean Sea and Black Sea via the Marmara Sea and the Dardanelles and Bosphorus Straits (Fig.1.2; Latif et al., 1992). A low-salinity (17–20 psu) 25–100 m thick layer flows at a velocity of 10–30 cm s^{-1} into the northern Aegean. This water mass is known as the Black Sea outflow. In the winter the Black Sea outflow is cool (5–15 ºC) and in the summer is warm (20–25 ºC). Higher salinity (38–39 psu) warm (15–20 ºC) Mediterranean water flows north along the eastern Aegean. This water mass is known as the Mediterranean inflow. This water mass descends beneath the low-salinity surface water of the northern Aegean, transits the Dardanelles Strait and Marmara Sea and eventually crosses the Bosphorus Strait at a velocity of 5–15 cm s^{-1} and flows into the Black Sea where it contributes to a bottom water mass below the low-salinity, low-density surface water layer (Özsoy et al., 1995). At the Bosphorus exit the underflow salinity is ~ 35 psu and at the shelf edge is reduced to ~ 31 psu by entrainment of surface water (Özsoy et al., 2001).

The seasonally varying temperature in the surface layer decreases with depth to a minimum which can be traced throughout the Black Sea and is known as the cold intermediate layer. The cold intermediate layer ranges from depths of 50 m in the center to 100 m at the margins of the Black Sea basin. Below this layer at depths of 50–200 m is the permanent halocline which separates the upper and bottom water masses (Murray et al., 1991). The Black Sea water column exhibits strong vertical stratification and there is

4
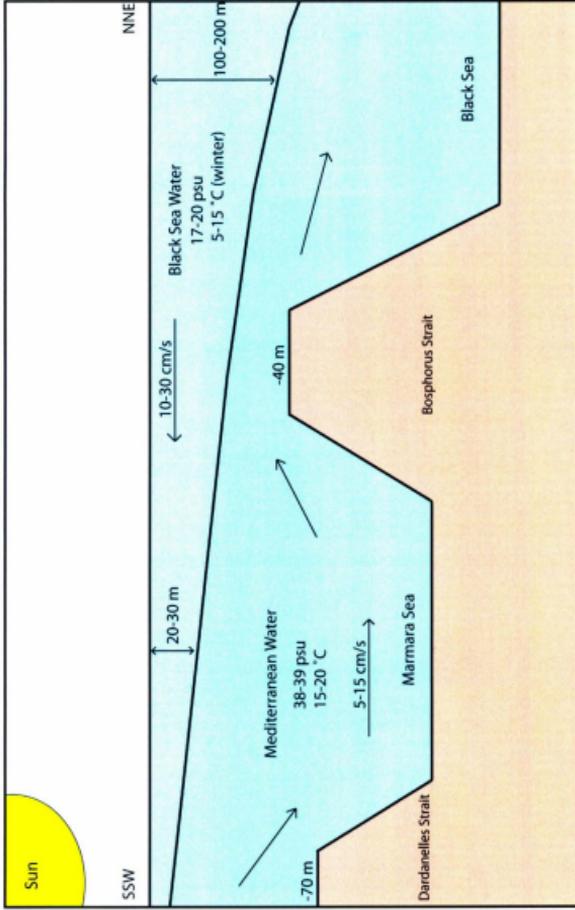
Figure 1.2. A schematic diagram of the two-way water exchange that exists between the Mediterranean Sea and the Black Sea via the Marmara Sea.

5

little mixing between the bottom water layer and the upper oxygen-rich layer because the intervening halocline is deeper than storm wave base. Thus, the warmer, high-salinity, high-density bottom water layer below a depth of 150–200 m is permanently anoxic and enriched in enriched in hydrogen sulfide (Panin and Strechie, 2006). The Black Sea is the largest permanently anoxic basin in the world (Murray and İzdar, 1989).

1.2.2. Hydrological Exchanges

Today, there is a net export of ~300 km^3 yr^{-1} of water from the Black Sea to the Aegean Sea (Özsoy et al., 1995). The volume of Black Sea surface water outflow is ~600 km^3 per year. The volume of water lost through evaporation is ~350 km^3 yr^{-1}. The volume of bottom water inflow from the Mediterranean is approximately ~300 km^3 yr^{-1}. Precipitation contributes ~300 km^3 yr^{-1}. The Black Sea receives a high input of river discharge. In the northwestern Black Sea alone the Danube, Dniestr, Dniepr and Southern Bug rivers contribute a total water volume of ~255.7 km^3 yr^{-1}. Rivers such as the Don and Kuban which flow into the Sea of Azov bring the total freshwater fluvial input into the Black Sea to ~370 km^3 yr^{-1} (Balkas et al., 1990).

1.2.3. Currents

The surface water circulation of the Black Sea is dominated by two large central cyclonic gyres, one western and one eastern (Fig. 1.3; Oğuz et al., 1993) and several smaller anticyclonic eddies along the coast. The cyclonic basinal gyres and anticyclonic coastal eddies are separated by the Rim Current which is < 75 km wide and transports water counter clockwise around the periphery of the Black Sea basin at a velocity of ~20 cm s^{-1} (Oğuz et al., 1993).
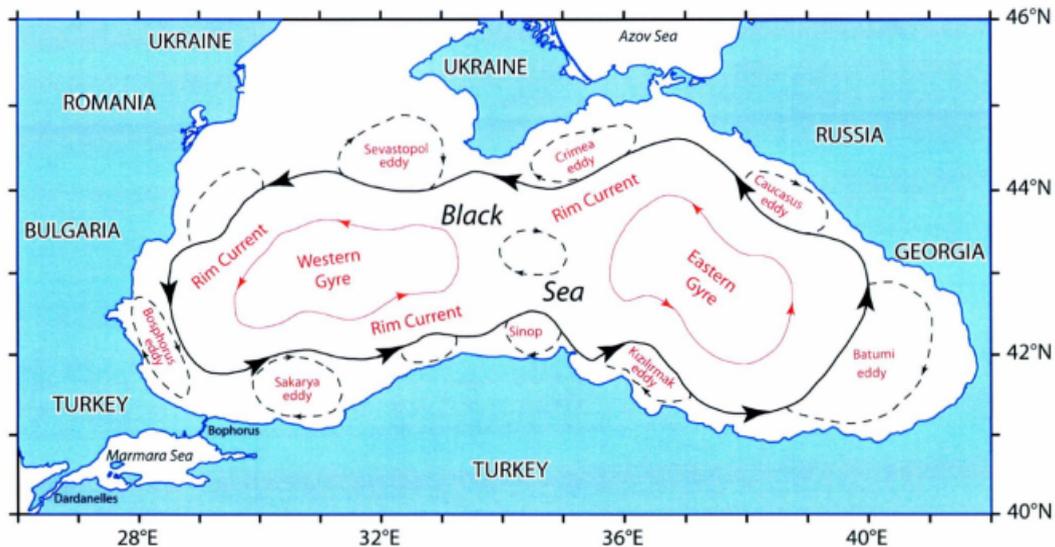
Figure 1.3. A map of the Black Sea showing the Rim Current which travels counter clockwise around the entire basin, western and eastern cyclonic gyres and numerous anticyclonic eddies (modified from Aksu et al., 2002b).

1.3. Geological Setting of the Black Sea

The Black Sea is part of the Ponto-Caspian basins which also include the Sea of Azov, the Caspian Sea and the Aral Sea (Boomer et al., 2010). These basins are the remnants of the Paratethys Sea, which existed from the Late Jurassic (~150 Ma) to Early Pliocene (~5 Ma). The Tethys Ocean, to which the Paratethys Sea was connected, closed during the Paleogene with the subduction of the Tethyan plate (Robinson, 1997) and the western part of this ocean became the Mediterranean Sea (Rögl, 1999). The Paratethys Sea to the north became progressively shallower during the Pliocene and was partitioned into the Ponto-Caspian basins.

The Black Sea floor is separated into the Western and Eastern basins, which are separated by the Mid-Black Sea Ridge (Finetti et al., 1988). These basins originated as two back arc basins in the Early Cretaceous as the Neo-Tethys Ocean floor was subducted beneath the Balcanides-Pontides volcanic arc (Letouzey et al., 1977; Robinson, 1997).

1.3.1. Geomorphology of the Study Area

Sediment cores studied in this thesis were collected on the southwest Black Sea shelf (Fig. 1.4). This area is generally flat and dips gently to the north. It is dissected by a prominent channel that begins at the Bosphorus Strait and extends to the shelf edge west of the Bosphorus Canyon and accommodates Mediterranean bottom water inflow to the Black Sea (Fig. 1.4; Flood et al. 2009). The channel is 200–500 m wide and 10–25 m deep and separates the shelf region into two parts: a western shelf which is 25–35 km wide and an eastern shelf which is 10–17 km wide. On both sides of the channel the shelf break occurs at ~115–120 m water depth. The shelf slopes are steep at 5–9° and
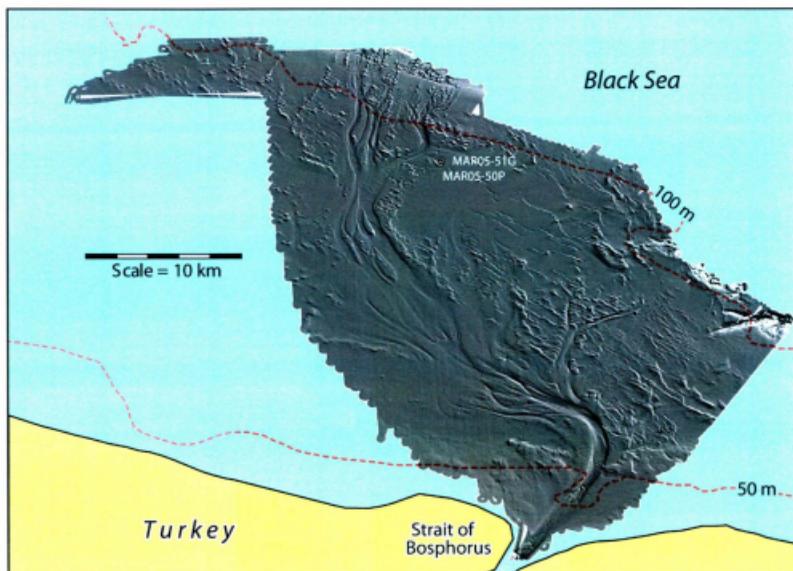
Figure 1.4. Sun-illuminated image of the channel network which accommodates inflow of saline Mediterranean water. The locations of cores MAR05-50P and MAR05-51G to the east of the channel are also shown (Aksu and Hiscott, unpublished data).

are dissected by numerous submarine canyons and gullies. Eventually the slope levels off at the floor of the Black Sea basin at ~2200 m water depth (Aksu et al., 2002a).

1.4. Summary of Quaternary Glaciation and Deglaciation in the Black Sea

The Black Sea region has felt the repercussions of glaciations and deglaciations which are recorded by cycles of transgressions and regressions and changes in seabed geomorphology (e.g., Ostrovsky et al., 1977 (in Russian), in Panin and Strechie, 2006; Chepalyga, 1984; Skene et al., 1998). During glacial periods the Black Sea became periodically isolated from the World Ocean as the sealevel fell below the sill depth of the Bosphorus Strait. Geomorphological, geochemical and paleontological evidence records these events and the effects on the environment. The last glacial period ended approximately 16000 years ago (Panin and Strechie, 2006). This thesis is concerned with the post-glacial paleoceanographic evolution of the southwestern Black Sea shelf.

1.4.1. Brief Glacial-Interglacial History of the Black Sea from 125 ka Years Ago

The following summary of glacial/deglacial effects in the Black Sea region is largely summarized from Panin and Strechie (2006).

During the Riss-Würm interglacial (125–65 ka BP) the Black Sea level was higher than it is today. At that time the Black Sea was connected to the Caspian Sea through the Manych Strait and had a surface salinity of 30–37 psu (Nevesskaya, 1970 (in Russian), in Panin and Strechie, 2006). After this highstand there was a 100–110 m drop in sea level in the Black Sea associated with glaciation correlated with the marine isotopic stage 4 (Chepalyga, 1984). During this period the water in the Black Sea became brackish to fresh (5–10psu) and the fauna living there were low-salinity Caspian types. During the

following interstadial some ~40–25 ka BP (i.e., marine isotopic stage 3; Imbrie et al., 1984) the water level in the Black Sea rose again to breach the Bosphorus Strait. Thus, the Black Sea flowed out to the Marmara Sea and became reconnected with the Mediterranean once again (Aksu et al., 2002a).

At around 25 ka BP the Würm glaciation (i.e., marine isotopic stage 2) lead to a dramatic regression and extreme drop in sea level. There is some debate regarding the actual amount of this drawdown: Ryan et al. (1997) estimated a Black Sea level of -140 m, whereas Aksu et al. (2002a) and Hiscott et al. (2002) estimated a level of -110 m. The last glacial maximum occurred at ~19–18 ka BP. At this time the Black Sea once again became an isolated brackish lake. Between 16–15 ka BP post-glacial melting associated with the transition from the Würm glacial to the Holocene interglacial began in northern Eurasia and Alpine mountain belts and by ~5000 yr BP the Black Sea level had attained approximately its present level. There is some debate regarding the effect of the post-glacial ice cap melting on the Black Sea level and the ensuing reconnection with the Mediterranean Sea, as explained below.

1.5. Hypotheses Regarding Mechanisms and Timing of Reconnection

There are three basic hypotheses regarding the Holocene connection history of the Black Sea to its neighbouring basins and the World Ocean. They are known as: the Flood Hypothesis, the Outflow Hypothesis and the Oscillating Sealevel Hypothesis.

1.5.1. The Flood Hypothesis

The Flood Hypothesis was first proposed by Ryan et al. (1997). The authors argue against the conventional story of a gradual reconnection of the Black Sea to the

Mediterranean Sea. Instead, they argued for a catastrophic reconnection when the Mediterranean waters invaded the Black Sea in less than 2-3 years. In Ryan et al. (1997) this "flood" is to have taken place at ~ 7150 yr BP (~7570 cal yr BP). This was later revised in Ryan et al. (2003) to 8360 yr BP (~9140 cal yr BP). The hypothesis was made famous by Ryan and Pitman (1998) in their book "Noah's Flood: The Scientific Discoveries About the Event that Changed History". As the title suggests, they argue that the possible flooding event in the Black Sea might have inspired the Biblical story of Noah and the flood.

The Flood Hypothesis diverges from the more conventional story at the point where the glacial maximum ends and ice caps begin to melt at ~15–16 ka BP. Some scientists (e.g., Aksu et al., 2002a; Hiscott et al., 2002) believe that meltwater led to the refilling of the Black Sea through heavy river input and Caspian spillover and as early as ~11500–12500 cal yr BP the Black Sea began flowing out through the Bosphorus Strait and has not been isolated from the Mediterranean Sea since.

As first presented, The Flood Hypothesis postulated that instead of refilling the Black Sea, the meltwater from the ice caps was redirected northward to the Baltic and North Seas. The isolated Black Sea became a giant freshwater lake and continued to regress to a lowstand of -150 m (Ryan et al., 1997). When the Mediterranean water level rose high enough to break through a hypothetical unconsolidated sediment dam across the Bosphorus Strait, the Mediterranean waters catastrophically flooded the isolated freshwater Black Sea with saline Mediterranean water at 7570 cal yr BP (Ryan et al., 1997). The authors calculated that this flooding could have been completed in just a couple of years at the rate of 15 cm water-level rise per day, or instantaneously by

geological standards. This resulted in the submergence of 100,000 km^2 of previously exposed shelves around the Black Sea (Ryan et al. 1997; Ryan and Pitman, 1998).

Ryan et al. (2003) subsequently revised the details of the Flood Hypothesis. The authors now believe there were actually two lowstands and two flood events instead of one. First, there was a lowstand of -120 m at ~15200–12400 cal yr BP. Ryan et al. (2003) as well as Major et al. (2002) explained that Black Sea outflow at this time was possible. They said the outflow then ceased again between ~12500 and 10100 cal yr BP and the Black Sea fell to a new lowstand of -95 m. At ~9140 cal ka BP the second and more significant flooding event took place as indicated by marine strontium isotopic signals (Major et al., 2006). This hypothesis directly precludes the possibility of a continuous outflow from the Black Sea by ~11900 cal ka BP as argued by Aksu et al. (2002a), Hiscott et al. (2002), Hiscott et al. (2007) and others (see the Outflow Hypothesis below).

Ryan et al. (2003) described evidence from sediment cores which suggests that the shelves surrounding the Black Sea were subaerially exposed from ~12500 to 10100 cal yr BP, after post-glacial melting. They report mud cracks at -99 m and shrub roots in place in desiccated mud at -123 m. They report seeing no evidence of landward onlap which is characteristic of transgression. The original date of the flooding event was based on radiocarbon dating of the first marine species of mussels and bivalves to colonize the area. In five cores dates were obtained which cluster at 7150 ± 100 yr BP (7570 ka cal BP; Ryan et al., 1997).

Ballard et al. (2000) supported Ryan et al. (1997) reporting evidence of an ancient shoreline at -155 m. Mollusks collected from this ancient inferred beach were dated at

8050 ± 60 to 7335 ± 55 cal yr BP. The authors believed this date supported the timing of the flood as first proposed by Ryan et al. (1997). However, the timing of the flood event was later changed by Ryan et al. (2003) to 9140 cal yr BP. The previous date of 7570 cal yr BP was reinterpreted as the onset of water conditions suitable to marine fauna.

High-resolution seismic reflection profiles across the outer Ukraine shelf revealed an erosional unconformity which Ryan et al. (2003) labeled Unconformity 1 and interpreted to represent a shelf-wide exposure surface resulting from regression. At -120 m, Unconformity 1 is represented by a wave-cut surface which is draped by coquina shells dated at ~12200 cal yr BP. Lericolais et al. (2009, 2010) support the idea of a lowstand of around -100 m between ~12400 and 9100 cal yr BP based on their interpretation of a "pronounced shoreline" on the Romanian shelf. They also support the idea of a rapid transgression (< 100 years) which was fast enough to preserve these coastal features.

1.5.2. The Outflow Hypothesis

An alternative Black Sea hypothesis advocates a more gradual and progressive Holocene reconnection of the Black Sea with the eastern Mediterranean Sea. Aksu et al. (1999, 2002a, 2002b), Kaminski et al. (2002), Mudie et al. (2007) and Hiscott et al. (2007) presented evidence that there could not have been a catastrophic flood of the Black Sea at 9150 cal yr BP. These authors believe that the Black Sea was fully transgressed. and water was flowing out of the Black Sea by ~ 11900 cal yr BP (Aksu et al., 2002a; Hiscott et al., 2002) and its level has not changed significantly since that time.

Brackish surface water conditions prevailed in the Black Sea as it flowed out to

the Marmara Sea until ~8100 cal yr BP (Marret et al., 2009; Mertens et al., 2012). A short pulse of Mediterranean water entered the Black Sea at ~9100 cal BP (Marret et al., 2009) and then ceased, or was greatly reduced, due to strengthening in Black Sea outflow. Sometime between ~8500 and 8000 cal yr BP, a two-way flow was established through the Bosphorus Strait.

Hiscott et al. (2002) used high resolution seismic profiles to show the presence of two south-prograded delta lobes at the southern exit of the Bosphorus Strait. They argued that these deltas are the result of persistent Black Sea outflow because there are no rivers in the area that could account for the observed volume of sediments (Hiscott et al., 2002). The younger delta was constructed between ~11200–9900 cal yr BP based on radiocarbon dates. After ~10000–9400 cal yr BP the delta became inactive because two-way flow with the Mediterranean had been initiated. When Mediterranean water began flowing northward underneath the Black Sea outflow, the sediment supply to the delta was cut off. This strongly suggests that water was already vigorously flowing out of the Black Sea at a time when the Flood Hypothesis would have the Black Sea isolated and at a maximum lowstand.

In response, Eriş et al. (2007) said that the sediment supply for this delta was the Kurbağalıdere River, which today flows into the Marmara Sea near the western side of İstanbul, and not Black Sea outflow through the Bosphorus Strait. Hiscott et al. (2008) rebutted this criticism, calculating that the sediment flux provided by the Kurbağalıdere River is entirely inadequate and stand by their initial conclusion that the delta strongly suggests that water was flowing out of the Black Sea during the early Holocene.

Furthermore, radiocarbon dating of a sapropel layer (mud with >~2 % organic

carbon deposited under reduced-oxygen conditions) in Marmara Sea cores showed it was deposited between ~11850 to ~6500 cal yr BP suggesting that water was flowing out of the Black Sea into the Marmara Sea forming a low salinity lid over the Marmara Sea water during that interval (Aksu et al., 2002a). Flora and fauna found within the sapropel (labeled M1) are of Black Sea affinity, strongly suggesting they were deposited by a Black Sea outflow (Mudie et al., 2002; Aksu et al., 2002a). Sperling et al. (2003) and Vidal et al. (2010) disagreed that sapropel M1 is evidence for Black Sea outflow. Vidal et al. (2010) states that oxygen isotopic evidence from carbonate shells shows rising Marmara Sea surface salinity until ~9900 cal yr BP confirming that Black Sea outflow was not significant enough to contribute to sapropel deposition and that Black Sea outflow only began in earnest after this date as indicated by decreasing salinity.

Hiscott et al. (2007) presents sedimentological and paleontological evidence for a progressive Holocene reconnection of the Black Sea with the Mediterranean Sea. They recovered 9.5 m-long core MAR02-45 from a post-transgressive succession on the southwestern Black Sea shelf. The water depth at the core site is 69 m. The base of the core was dated at 10325 ±80 cal yr BP. The underlying unconformity α (Unconformity 1 of Ryan et al., 2003) deepens toward the shelf edge showing that the core site was never isolated from the open Black Sea suggesting there could not have been a drawdown greater than -70 m after at least 10325 cal yr BP.

There is also evidence that the early Holocene Black Sea was brackish and not freshwater. Based on ostracods from core MAR02-45 Evans (2004) suggests a brackish salinity (~5 psu) before a faunal turnover beginning at ~7500 cal yr BP indicating saline inflow from the Mediterranean (Hiscott et al., 2007). Dinocysts also indicate a rising

salinity (>10–12 psu) after this time (Marret et al., 2009). Mudie et al. (2002, 2007) found that pollen from Black and Marmara Sea cores indicated warm and humid conditions with year-round precipitation by 10500 cal yr BP. This conflicts with the cold, dry conditions necessary for a -100 m drawdown in the Black Sea. Also, they found no unique peak of terrigenous matter indicating rapid flooding of a coastal plain.

Temporary changes in salinity-diagnostic groups of dinocysts and freshwater algae are evidence of the short-lived pulse of saline water. Between ~9400 and 8600 cal yr BP these freshwater/brackish types temporarily gave way to marine flora. This replacement was interrupted between 8400 cal yr BP and ~7900–7500 cal yr BP after which brackish flora and fauna were finally permanently replaced (Hiscott et al., 2007; Marret et al., 2009). These authors therefore believe that reconnection occurred sometime between ~8500 and 8000 cal yr BP.

1.5.3. The Oscillating Sealevel Hypothesis

Yanko-Hombach (2007) questioned the evidence used by Ryan et al. (1997, 2003) and Ryan and Pitman (1998). She commented that the core and seismic data used in the Flood Hypothesis were "limited". In particular she was critical of the use of *Dreissena* species to date a submerged coastline at -100 m. The fossil *Dreissena* actually has a much wider stratigraphic distribution than living specimens and is therefore a weak paleobathymetric indicator. Based on benthic foraminiferal assemblages in the Black Sea Yanko-Hombach et al. (2007) concluded that the Holocene reconnection of the Black Sea to the Mediterranean Sea was "neither rapid, nor gradual, nor catastrophic. Instead, it occurred in an oscillating manner, permitting periodic immigration of Mediterranean

organisms into the Pontic basin". After the last glacial maximum when the climate warmed a large water input, from high river discharge, melting permafrost and Caspian Sea spillover, raised the isolated Black Sea level from -100 to -20 m but then temporarily dropped again to -50 m during the Younger Dryas cold period from ~12700 cal yr BP to ~11200 cal yr BP. At ~10800 cal yr BP the Black Sea then began to spill over the Bosphorus sill and enter the Marmara Sea and inflowing Mediterranean waters raised the level gradually to -20 m. The Black Sea level never again dropped below -50 m, never experienced fluctuations greater than about ±20 m and occasionally rose a few meters higher than present sealevel during the Holocene (Yanko-Hombach et al., 2007). The level gradually rose at a rate of 3 cm yr^{-1}, oscillating between these levels, periodically allowing Mediterranean organisms to make their way into the Black Sea. The first "wave" of immigrants entered the Black Sea at ~10500 cal yr BP. This first connection may not have been through the Bosphorus Strait, but another route (i.e., Sakarya Valley via the Izmit Bay, also known as the Sakarya Bosphorus; Yanko-Hombach et al., 2004; Kerey et al., 2004). Marine colonization was slow but gradual, becoming pronounced at ~7600 cal yr BP which coincides with the "Flood" date of 7570 cal yr BP (Ryan et al., 1997). A Black Sea level which never fell below -20 m directly precludes the -95 m water level drawdown and subsequent flooding event proposed by the Flood Hypothesis.

Martin et al. (2007) also said that the Black Sea Holocene water levels rose and fell periodically due to changes in freshwater discharge and repeated marine incursions and these oscillations decreased in magnitude through the Holocene. Filipova-Marinova (2007) and Ivanova et al. (2007) also presented paleontological evidence for Holocene Black Sea level oscillations which became increasingly attenuated and closer to the

18

modern level in the last ~5000 years. Giosan et al. (2006) stated that immediately before the reconnection to the Mediterranean Sea the Black Sea level was around -30 m based on cores from the Danube Delta and it has not fluctuated more than ±1-2 m in the last 5000 years.

1.6. Dating Methods Used in this Thesis

It is important to convert radiocarbon dates from fossil material into calendar years so that an accurate chronostratigraphic framework can be constructed and the paleoclimatic and paleoceanographic evolution of the study area can be compared with other studies. Radiocarbon dates obtained from fossil material cannot be considered as calendar ages because of changes in atmospheric ^{14}C through time and reservoir effects whereby "old" carbon is recycled and partitioned into marine shells resulting in a date that is inaccurate by 100s of years. In this thesis most dates are given in calendar years before present (cal yr BP). Where radiocarbon dates were obtained from fossil material the dates were calibrated or re-calibrated using the OxCal Marine09 calibration procedure. Approximate ages from the literature which are not directly tied to specific radiocarbon dates were converted to calendar years using the Marine09 "global" marine calibration curve constructed with reservoir corrections for the Black Sea (Fig. 1.5).

1.7. Introduction to the Ostracoda

The Ostracoda are a class of the subphylum Crustacea in the phylum Arthropoda. Commonly referred to as ostracods or ostracodes, living specimens were first described by O.F. Müller in 1776 (Athersuch et al., 1989). Crustaceans also include such well-known animals as lobsters and shrimp and the ostracoda bear a resemblance to these but

19
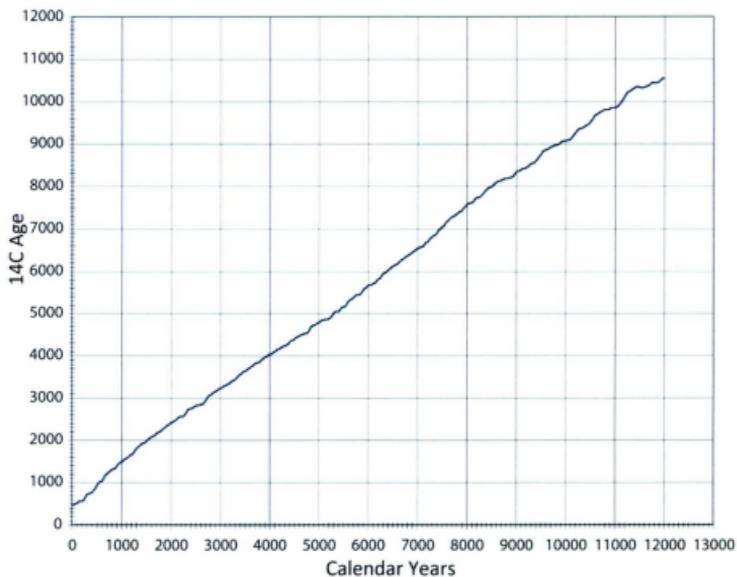
Figure 1.5. Graph of calendar age (cal yr BP) versus conventional radiocarbon age (^{14}C yr BP) based on the Marine09 database downloaded from c14.arch.ox.ac.uk and incorporating Black Sea reservoir corrections of 415 yr for ages younger than 7100 ^{14}C yr and 280 yr for dates older than 7100 ^{14}C yr.

they are much smaller. Generally a microscope is required for detailed observation.

Ostracods are a very diverse group. It is estimated that at least 25,000 species are living today, of which ~8000 have been described (Morin and Cohen, 1991; Cohen et al., 1998). The estimated total of all living and fossil species is 33,000 (Kempf, 2001, personal communication, in Horne et al., 2002). These creatures are amongst the most complex of the organisms studied by micropaleontologists.

On average, these aquatic microcrustaceans range in size from 0.5 to 2.0 mm. Their bodies consist of a head and thorax and 5–8 pairs of appendages used for locomotion (Athersuch et al., 1989). These body parts are often referred to by paleontologists as "soft parts". The ostracod secretes a low-Mg calcite bivalved carapace which encloses its body. This calcified portion of the ostracod is commonly referred to as its "hard parts". Generally, the term carapace is used to denote two valves which are still articulated. The term valve is used to refer to one half of a carapace (Holmes and Chivas, 2002b).

The strongly calcified carapace or valve is typically the only part of the ostracod that is preserved as a fossil. Occasionally internal parts are preserved. Zoologists who work with living ostracods may use internal parts in addition to valve morphology for taxonomic identification. However, a paleontologist has the disadvantage of working with only the empty valves and must make identifications based on gross morphology of the valves alone. Morphological features of ostracods valve are presented in Chapter 4.

The ostracod lives for approximately a few months up to four years and grows by moulting, or ecdysis (Horne et al., 2002). There are 9 growth stages, also called instar stages, including the final adult stage (Athersuch et al., 1989). The juvenile stages are

21

referred to as A-1 (last juvenile stage; read as "A minus 1") through to A-8. The earliest of the juvenile valves are commonly not represented in a fossil assemblage due to the fragile nature of these tiny shells. As the ostracod grows, its physical features develop progressively with each moult (see Chapter 4, Plate 3, figs 10–15 for example) and therefore the adult stage is best suited for identification.

Some ostracods may swim for part or all of their lives (Horne et al., 2002). However, most are benthic, living on or burrowing a few centimetres into the seafloor sediment. Some ostracods are phytal and are commonly associated with algae. The type of substrate preferred by the ostracod is often reflected in its morphology; for example sleek, smooth types are suited to swimming freely in dense aquatic plants (Van Morkhoven, 1962). Athersuch et al. (1989) and Horne et al. (2002) provide detailed information about ostracod morphology and biology. Ostracods are highly sensitive to changes in water chemistry and for this reason they are increasingly being recognized as valuable proxies for environmental and paleoenvironmental studies.

1.8. The Use of Ostracods in (Paleo)environmental Studies

To be able to derive information about past and modern environments, reliable proxies are needed. A proxy is an organism or chemical signal which responds to, and thus records, changes in the environment. Over the past three or four decades ostracods have been recognized as excellent proxies suitable for reconstructing paleoenvironments. Ostracod distribution is highly dependent on water conditions, mainly salinity but also depth, substrate, water chemistry, nutrient availability and temperature. Because ostracods are very sensitive to changes in these conditions they can be studied to interpret

environmental changes over time (Frenzel and Boomer, 2005).

Ostracods are found in almost every conceivable type of aquatic environment. Shallow seas to deep oceans, lakes, rivers, caves, lagoons, estuaries, temporary ponds and even hot springs are all inhabited by these tiny crustaceans. Ostracods have even been found in semi-aquatic environments, specifically damp vegetation. Ostracods are typically divided into marine, brackish and freshwater types (Athersuch et al., 1989).

In addition to being ubiquitous in aquatic environments, ostracods have an excellent fossil record. Their preservation potential is high due to their small size, abundance and strongly calcified low Mg-calcite valves. They are found in the fossil record certainly from the Ordovician, although some sources say the Cambrian (Athersuch et al., 1989). Depending on the species, the degree of calcification of the carapace varies. Furthermore, preservation is affected by the environment. If the pore waters in the sediment are acidic, the valves may be dissolved. Therefore, it should be noted that weakly calcified species are under-represented in fossil assemblages. Therefore, as Boomer et al. (2003) describes, the task of the paleoecologist is to *approximately* reconstruct the living assemblage, or biocoenosis, from which the paleoenvironmental interpretation can be derived.

The application of ostracods to paleoenvironmental reconstruction is best done as part of a multidisciplinary approach. The study of these organisms can be done by both quantitative and qualitative methods. It is possible to obtain geochemical information from ostracod valves through microprobe or laser-ablation techniques. In this thesis, a more qualitative approach is used. The following section gives a brief overview of the applications of ostracod fossils in paleoenvironmental studies.

1.8.1. Information Derived From Ostracod Valves

Ostracod studies may be done both quantitatively and qualitatively. Boomer et al. (2003) and Danielpol et al. (2002) give succinct overviews of the various applications of ostracods in paleoenvironmental studies. This thesis focuses mainly on qualitative methods but does use some of the quantitative methods described below.

1.8.1.1. Quantitative Analyses: Ratios

Female: male ratios may reveal something about the stability of the environment. Abe (1990) suggested that a high female: male ratio may indicate r-strategy reproduction in response to an unstable environment (i.e., many females facilitate quick and certain reproduction. On the other hand, a more equal number of males and females could indicate k-strategy reproduction in a stable environment. Reproduction is sexual in most taxa (Smith and Horne, 2002).

Adult:juvenile ratios and population age structures are commonly used for environmental reconstructions. The ratios of all instars of a species within a sample has been shown to be a reliable indicator of whether the sample is a life or death assemblage and the degree of *post-mortem* transport (Boomer et al., 2003). This type of observation can also be made qualitatively. Simply observing fully grown adults as well as lots of juveniles of different stages is adequate to infer an *in situ*, life assemblage (D. Horne, personal communication).

Valve:carapace ratios yield limited information regarding reworking or *post-mortem* transport. One can deduce that a high number of disarticulated valves could indicate a high energy environment. One must take into account that some species have a

24

stronger hinge than others. Also, sample processing will certainly cause some degree of carapace disarticulation. It is therefore advisable to compare these ratios only for the same or closely related species within a sequence (Boomer et al., 2003).

Ostracod shell chemistry studies can yield considerable information about the water chemistry of the paleoenvironment. Geochemical applications of ostracod valves are discussed in Chapter 7.

1.8.1.2. Qualitative Analyses

Qualitative observations of ostracods are as important as quantitative data for paleoenvironmental reconstruction. Ostracods have well-known environmental controls on their distribution (e.g., Neale, 1988; Athersuch et al., 1989) and the ecological affinities of many Ponto-Caspian and Mediterranean genera and species are at least somewhat known and documented.

Salinity is a major factor controlling ostracod distribution and ostracods are commonly categorized into marine, brackish and fresh water species (Athersuch et al., 1989). Therefore, ostracods are very good proxies for qualitative paleosalinity reconstructions, which is why they were chosen for this research. Salinity range preferences and tolerances are known for many ostracod species (Neale, 1988). Some ostracods are stenohaline, meaning they favor a very narrow salinity range, while other euryhaline species can tolerate a broad range of salinities. Boomer et al. (2010) cautions that Ponto-Caspian ostracod autecology is not fully known. Precise paleoenvironmental reconstructions (i.e., quantitative salinity interpretations) cannot yet be made. Other controls on ostracod distribution are depth, substrate, dissolved oxygen levels

temperature, pH, food availability and the stability of these conditions (Athersuch et al., 1989; Frenzel and Boomer, 2005).

Substrate is a very important factor controlling ostracod distribution. Different species prefer different substrates. Some ostracods prefer to live on or within the sediment. Within this sediment-dwelling group, some prefer softer clay and mud while some prefer sand. Many ostracods, such as the smooth-valved *Sclerochilus gewemuelleri* are phytal, meaning they live on or around marine plants (Athersuch et al., 1989).

Dissolved oxygen levels can influence the distribution of ostracods. Different species or groups of related species can have different tolerances. Some groups such as the Order Platycopida adapt well to reduced-oxygen environments and occurrences of these might indicate this type of paleoenvironment (Whatley, 1990; Boomer et al., 2003, 2005).

Ecological interpretations of a fossil assemblage can therefore be made based on what we observe of the same or closely related species living in modern environments. This is most easily done for Quaternary and late Neogene assemblages because many of the species or closely related species are still living today (Boomer et al., 2003).

1.9. Early Work on Black Sea Ostracods

A significant amount of research has been done on Black Sea and Ponto-Caspian ostracods in the last century and a half. Dubowsky (1939), Livental (1929, 1938), Schweyer (1949), Agalarova et al. (1961) and Shornikov (1964, 1966, 1969) are among the main contributors to some of the earliest data on Ponto-Caspian ostracods. The original taxonomic descriptions of these ostracods, including information on their

ecological affinities and distribution around the Ponto-Caspian basins, done by these authors are relied heavily upon in this thesis and by all researchers of Black Sea ostracods.

CHAPTER 2

METHODS

2.1. Data Acquisition

2.1.1. Geophysical Data

Multibeam images (Fig. 1.4) of the southwestern Black Sea shelf were collected in 2005 during the MAR05 research cruise of the RV *Koca Piri Reis* using a Kongsberg EM-3000 multibeam echosounder. Mosaics of bathymetry and backscatter images arising from this survey have been published by Flood et al. (2009). Approximately 1918 line-kilometres of Huntec deep-tow boomer profiles (vertical resolution 15 to 30 cm) were also collected along the 200 m apart multibeam tracks.

2.1.2. Cores

During the MAR05 cruise several piston and gravity cores were also collected from the southwestern Black Sea shelf. Two of these cores collected from closely spaced sites are used in this project: piston core MAR05-50P and gravity core MAR05-51G (Fig. 2.1). The core sites are located to the northwest of the Bosphorus Strait, on the eastern levee of a saline underflow channel (Fig. 2.1; Fig. 1.4; Flood et al., 2009). Cores MAR05-50P and MAR05-51G penetrated the seabed ~310 m apart. The location of core MAR05-50P adjacent to the main saline inflow channel is shown on a multibeam image (Fig. 1.4) and a Huntec DTS seismic reflection profile (Fig. 2.2) collected during the same cruise (Flood et al., 2009). Table 2.1 gives the penetration depths (lengths), locations, and water depths for these two cores.
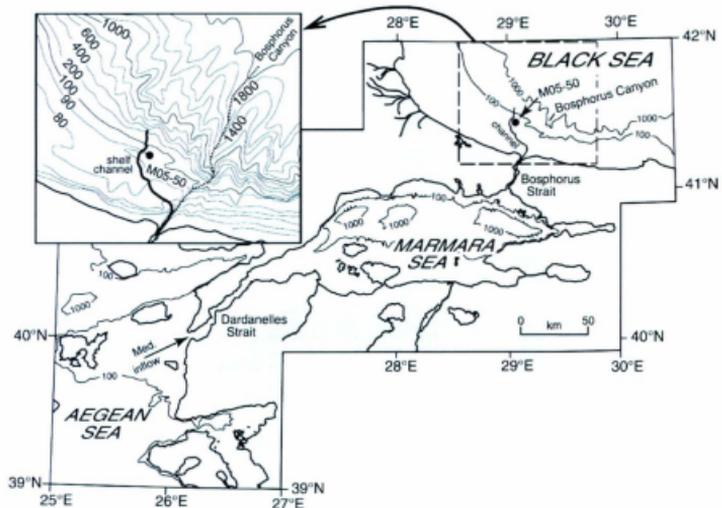
Figure 2.1. Regional map of the Black Sea study area showing the location of cores MAR05-50P and MAR05-51G (labeled here together as MAR05-50) north of the Bosphorus exit into the Black Sea and to the left of a saline inflow channel. Isobaths are in meters (modified from Flood et al., 2009).
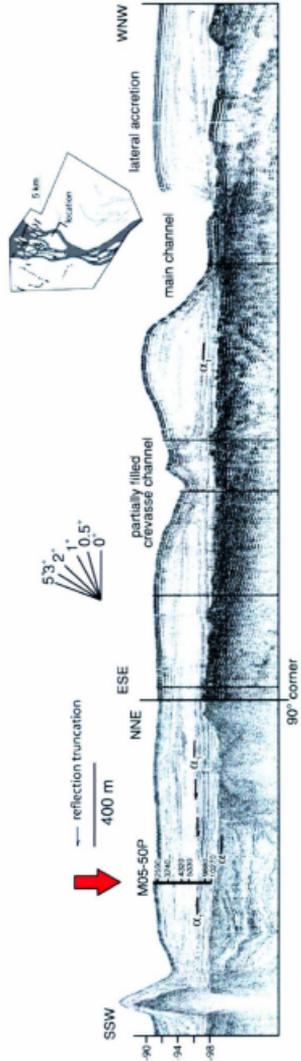
Figure 2.2. Huntec DTS seismic reflection profile showing the location of core MAR05-50P in relation to the –8.5 m deep first-order saline underflow channel (inset). Water depths are shown to the left in meters. Sub-bottom depths use the same vertical scale in these near-surface sediments. Reflection surface α_1 is interpreted to separate pre-channel deposits from levee and overbank deposits (from Flood et al., 2009). Regional unconformity α is also shown however it was not penetrated by core MAR05-50P.

30

Table 2.1. Lengths (depth below seabed), locations and water depth for cores MAR05-50P and MAR05-51G. Latitude and longitude were obtained with the GPS of the RV *Koca Piri Reis*.

Core	Length (cm)	Latitude	Longituge	Water Depth (m)
MAR05-50P	737 cm	41°29.634'N	29°04.445'E	91
MAR05-51G	157 cm	41°29.471'N	29°04.393'E	91

2.2. Composite Core Construction

Core top loss is a common occurrence during the piston coring operation, which occurs when the free-fall wire is inadvertently kept slightly longer than the distance between the tip of the trigger weight and the tip of the piston corer. Under such circumstances, the piston corer starts to penetrate into the sediment, but the piston remains at the tip of the corer preventing sediment entry into the liners until the free-fall wire is taut. Only after the free-fall wire is taut, the corer starts recovering sediments as it penetrates deeper into the seabed. On the basis of visual core descriptions and carbon and sulfur elemental and isotopic data fellow M.Sc. student Anna Linegar estimated an approximately 50 cm core top loss for core MAR05-50P relative to core MAR05-51G (Linegar, 2012). In order to compensate for this missing section, the top 50 cm of core MAR05-51G was added to the top of core MAR05-50P. Thus, 0 cm depth in core MAR05-50P is 50 cm depth in the composite core which is hereafter referred to as core MAR05-50. Core illustrations and description are given in Chapter 3.

2.3. Sediment Sample Processing

Approximately 20–25 cm^3 of sediment were taken from both cores MAR05-50P and MAR05-51G at 10 cm intervals for a total of 89 samples. Samples from MAR05-50P were numbered 0, 10, 20…730. Samples from MAR05-51G were numbered 10G, 20G, 30G…150G. There is no sample 0G because this material had already been removed from the top of the core by Turkish Customs for inspection.

The samples were first oven-dried at ~25 ºC and the dry weights were recorded. The average sample weight after drying was ~32 g. They were then put into small plastic

containers and treated with ~70 ml of 1% sodium hexametaphosphate (Calgon) and left for several days, gently shaken occasionally to disaggregate the sediments.

Next, each sample was wet-sieved using tap-water and a 63 µm sieve. The > 63 µm fractions were collected from the sieve and dried in an oven at ~25 ˚C. Once dried each > 63 µm fraction was passed through a stack of 4 sieves: 355 µm, 180 µm, 125 µm and 63 µm. The reason for this was simply to separate the sample into smaller, more manageable portions for subsequent hand-picking of the ostracod shells. The material which remained in the bottom 63 µm sieve (i.e., the > 63 µm fraction) was not examined and was returned immediately to a glass vial and stored.

A small enough sieve size must be used to collect juveniles and also adults of smaller species. Furthermore, some fragile species may only be present as fragments which will bias the assemblage if not collected. A sieve size of 125 µm is regarded as adequate (Boomer et al., 2003).

2.4. Ostracod Collection

Each sample was examined under a stereographic microscope by the author. Ostracod valves were hand-picked using a very small paint brush (size 000) wetted with water. There was no limit on the number of valves picked; all the valves that could be found in a given sample were collected. Fragments were also collected. However, fragments that were less than ~30% of the original valve, or fragments inadequate for identification, were not picked. In the case of *Candona schweyeri* (SCHORNIKOV, 1964), smaller fragments were collected so as to ensure the species was not under-represented because it has thinner walls than other species and is more prone to breaking.

All instar stages (i.e., adults and juveniles) of the ostracods were also picked. Although in some cases they are impossible to confidently identify, all juveniles found were collected.

2.5. Ostracod Identification

The ostracod valves are well-preserved throughout the cores. Because no internal soft-part preservation was observed, the ostracods were identified based on gross morphology of the valves (see Chapter 4, Plate 1 for guide to morphology). Shell shape and size, surface ornamentation and types of marginal pore canals are unique characteristics which are key to identifying ostracod taxa. Examination of valve morphology was done mainly under the stereographic microscope. Transmitted light microscopy was also used to observe characteristics not discernible with the stereographic microscope, mainly marginal pore canals. Reference materials used for identification included Schweyer (1949), Schornikov (1964, 1966), Bonaduce et al. (1975), Olteanu (1978), Athersuch et al. (1989), Stancheva (1989), Boomer et al. (1996, 2005, 2010), Horne et al. (2002) and Opreanu (2008). Considerable assistance in making identifications was provided by Dr. David Horne (Queen Mary University, United Kingdom) and Dr. Marius Stoica (University of Bucharest, Romania), during visits to their laboratories and by electronic correspondence.

2.5.1. Issues with Ostracod Identification

It is often difficult to confidently identify ostracod species, especially when working only with fossil valves lacking internal parts. Many ostracod genera contain numerous species which look very similar to one another. The genus *Xestoleberis* is a good example of this. Athersuch et al. (1989) remarked that this genus has a world-wide

distribution and its many species are often confused because their smooth carapaces look very similar. For this reason, it is not always possible to make identifications to species level.

Another significant problem arises due to the lack of taxonomic consistency in the literature. In many cases the original descriptions of species preceded microphotography and instead feature hand-drawn illustrations. These drawings may be unclear or they may be inaccurate or the illustrator may have exaggerated certain aspects of the morphology to make them clear. For these reasons, there can be uncertainty that a specimen being examined today is exactly the same as what the original author described. This problem is compounded when the original material has been lost making visual comparison impossible.

A second reason taxonomic discrepancies occur is due to intra-specific variation. Small variations in the shape or ornamentation of a carapace may be mistakenly used to describe a separate species. Similarly, if a species is wide-spread it might have been described as a new species by an author who was unaware that the species had already been described in another region. *Palmoconcha agilis* (RUGGIERI, 1967) and *Palmoconcha guttata* (NORMAN, 1865) may be an example of this (see *Palmoconcha agilis* in Chapter 4: Taxonomy for explanation).

Similarly, regional variations in names, or naming preferences of researchers, further complicate the taxonomy. For example, the same species may be known by different names in North America and Europe. A taxonomic harmony is greatly needed and some members of the ostracodology community are currently working to achieve this.

2.6. Counting Ostracods

Ostracods have nine growth stages: 8 juvenile stages and one adult stage (Athersuch et al., 1989). Thus, one individual ostracod may contribute up to 18 valves to the sediment over its lifetime. It is impossible then to really know how many individuals are actually represented in a sample because it will usually contain disarticulated valves as well as articulated carapaces and probably various juvenile stages. In this study one valve (i.e., half of a full carapace) is counted as 1. A full carapace is counted as 2. This simple counting method is a generally accepted practice (Boomer et al., 2003).

2.7. Environmental Assessments for Individual Species and Assemblages

The ecological affinities of the ostracods present in this study are mostly well-known and documented. This information was obtained from numerous sources. The main resource texts used include Puri et al. (1964), Schornikov (1964, 1966, 1969), Bonaduce et al. (1975), Athersuch et al. (1989), Stancheva (1989), Boomer et al. (1996, 2005, 2010) and Opreanu (2008).

In addition to the above literature, the aforementioned Drs. Horne (Queen Mary University, United Kingdom) and Stoica (University of Bucharest, Romania) also provided assistance regarding the ecological affinities of the species recovered from core MAR05-50.

2.8. Calibration of Radiocarbon Dates

A total of fourteen radiocarbon ages were obtained from core MAR05-50P and two from core MAR05-51G. These dates are presented in Chapter 3. Eight of the uncalibrated dates were originally published by Flood et al. (2009).

All dates have been calibrated to calendar years before present (cal yr BP) using the Marine09 calibration curve (Fig. 1.5) and the OxCal program maintained by the University of Oxford. The Marine09 calibration curve has a built-in reservoir correction of 405 yr. The dates were calibrated using reservoir ages suggested for the Black Sea. For dates older than 7100 ^{14}C yr a ΔR value of -125 yr BP equaling a 280 yr reservoir age was used, as suggested by Soulet et al. (2011). For ^{14}C dates younger than 7100 yr, a ΔR value of 10 yr BP was used to make the reservoir correction 415 yr, as suggested by Siani et al. (2000). Other authors have since used a 300 yr reservoir correction for dates older than 7100 ^{14}C dates as also described in Soulet et al. (2011). This small difference (i.e., 20 years) in reservoir correction would not have a significant effect on the calibrated radiocarbon dates. For a full explanation of reservoir corrections see Soulet et al. (2011).

2.8.1. Age Profile Construction

The original micropaleontological and sedimentological data were converted from the depth domain into age domain using the software Ager and Timer. First, the program Ager assigned an age to each sample depth based on linear interpolation (and extrapolation) between calibrated radiocarbon dates obtained from carbonate fossils in the core. The program Timer then used the output of the Ager program to create a time series over equal increments as specified by the user. In this study, a 100-year increment was used in the depth to age conversions. The ostracod data were recalculated at every 100 year time-step. The conversions from the depth domain to the age domain were done by supervisor Dr. Ali Aksu. The results are discussed in Chapters 4 and 5.

2.9. Statistical Methods

2.9.1. CONISS Cluster Analysis

Cluster analysis is a statistical technique which arranges objects (in this case, species) into two or more groups (called clusters) based on variables (R-mode) or samples (Q-mode). The purpose is to delineate groups which are more "similar, or related in some way (i.e., common physical, chemical and/or biological properties) to each other than to those in other clusters. This technique has become useful in taxonomy because it removes the element of subjectivity (Davis, 1973).

Cluster analysis starts with a data matrix, where variables and samples are placed in rows and columns. This data matrix is analysed and a table is constructed where variables are both rows and columns and the numbers in the table are measures of similarity or differences between the two values of the respective variables (in this case, species; Davis, 1973). This table is known as the similarities matrix and lists the similarities between variables as distances. There are various options in the determination of the similarities matrix, such as squared Euclidian distance option, Gower similarity coefficient option, Manhattan distance option, etc. In this thesis, the Euclidian distance is used in the determination of the similarities matrix.

After the distances between variables have been found, the next step in the cluster analysis is to divide the variables into groups based on the above calculated distances. Again, a number of options are available to do this, such as the flat method, hierarchical clustering method, and so on. In this thesis, the hierarchical clustering method is used to divide the variables into groups.

The results of the clustering technique are best presented using a dendrogram (or binary tree). The variables are represented as nodes in the dendrogram and the branches

illustrate when the cluster method joins subgroups containing that variable. The length of the branch indicates the distance (or measure of similarities) between the subgroups when they are joined (Davis, 1973). Different methods exist for computing the distance (or measure of similarities) between subgroups at each step in the clustering. Single linkage (also known as the nearest neighbor) computes the distance between two subgroups as the minimum distance (or measure of similarities) between any two members of opposite groups. Complete linkage (also known as the furthest neighbor) computes the distance between subgroups in each step as the maximum distance between any two members of the different groups. Average linkage (also known as the centroid method) computes the distance between subgroups at each step as the average of the distances between the two subgroups. Single linkage is used in this thesis. A dendrogram that clearly differentiates groups of objects will have small distances in the far branches of the tree and large differences in the near branches.

CONISS is a Constrained Incremental Sums of Squares cluster analysis subroutine which is run within the Tilia software. The technique was described and a FORTRAN program published by Grimm (1987). The current implementation in Tilia is a C version of the program. CONISS was run on four data sets: (i) complete ostracod data in depth domain, (ii) complete ostracod data in age domain, (iii) dominant species in the depth domain with less abundant species not exceeding 5% of the sum at any level removed and (iv) dominant species in the age domain with less abundant species not exceeding 5% of the sum at any level removed. The results are discussed in Chapters 5 and 6.

2.9.2. Q- and R-Mode Factor Analysis

Q- and R-mode factor analyses were run on column-normalized data. Column normalization is a critical step because factor analysis is highly affected by the frequency distribution of the data. Dominant species will be much favored over minor and auxiliary species. To prevent this discrimination we go through a column normalization procedure (Davis, 1973). The minimum value in each column is subtracted from the values, making the smallest value zero, then these values are divided by the maximum value in each column, making the biggest value 1. The result is that all the value in the data matrix range from a maximum of 1 to a minimum of 0. Thus, there are no predominant variable or minor variables, allowing the program to extract relationships between variables and samples that otherwise may have been undetected.

After column normalizing the data factor analysis was run on the data requesting that the program initially extract factors which should account for 98 % of the total variance, leaving 2 % as random (Fig. 2.3). Moving to the right in Figure 2.3, the variance values drop and Catell's scree test says to drop all values after the "elbow" where the values begin to drop-off (Catell, 1966). Finally, the five most significant factors were extracted which account for 82.8 % of the total variance. A rotation, in this case orthogonal, of the retained factors generally follows this selection step (Abdi, 2003). In this case Varimax rotation was used.

Factor analysis first produces a correlation coefficient matrix from a complex data set. The program then uses this correlation coefficient matrix to extract a small number of hypothetical samples (Q-mode) or hypothetical variables (R-mode) that explains a large proportion of the total variance in the data set. The program used was written by Klovan (1971). It performs both Q- and R-mode factor analyses during the same run.
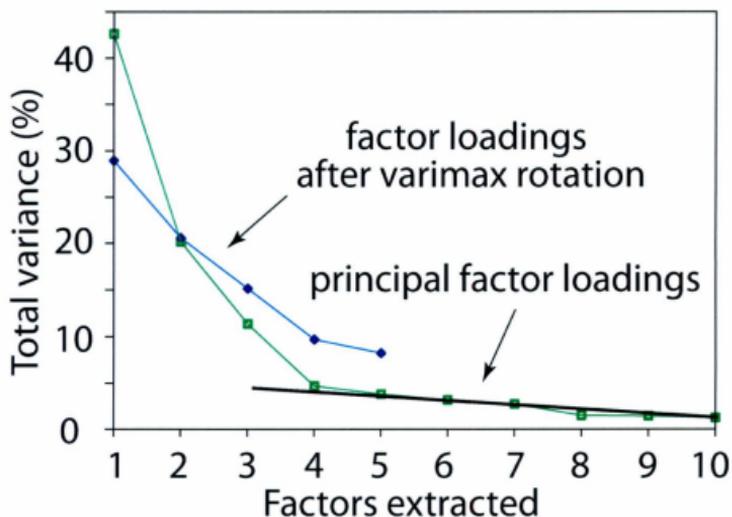
Figure 2.3. Plot showing the original factors accounting for 98 % of the total variance extracted from the depth domain data (green line) and the remaining 5 factors considered most significant (blue line) after applying Catell's scree test (thick black line).

The number of hypothetical samples, hypothetical variables as well as the amount of variance to be explained by the factors is controlled by the operator. The factor analysis results are presented in Chapters 5 and 6.

CHAPTER 3

STRATIGRAPHY AND AGE MODEL

3.1. Core Description

Cores MAR05-50P and MAR05-51G recovered a succession of late-Quaternary sediments on the eastern bank of a submarine channel north of the Bosphorus exit (Fig. 1.4; Fig. 2.2). The original core descriptions were done by supervisor Dr. Ali Aksu and were published in Flood et al. (2009). The composite core (constructed by adding the top 50 cm of MAR05-51G to the top of MAR05-50P) is 787 cm long (Fig. 3.1). Three lithostratigraphic units are defined.

In the composite core MAR05-50 the sediment is mainly silt with a mean grain size of 5.5 φ at the bottom of the core and 6.5 φ at the top. There is upward fining until ~500 cm and then slight coarsening upwards. Unit 3 extends from the base of the composite core to a depth of 695 cm (645 cm in MAR05-50P) the sediment is interbedded silty mud and graded beds of coarse silt to mainly very fine sand (Fig. 3.1; Flood et al., 2009). The brackish water bivalve *Dreissena* is abundant in some of the graded beds. Flood et al. (2009) interpreted this part of the core as a post-Younger Dryas transgressive sequence. These beds are similar to the laminated sediments below reflection surface α₁ in MAR02-45 described in Evans (2004) and Hiscott et al. (2007) which are interpreted to be storm-influenced shallow water deposits (Evans, 2004).

At 695 cm depth in the composite core there is a local unconformity referred to as the α₁ reflector (Fig. 3.1). This surface was interpreted by Flood et al. (2009) to have existed as a seabed omission surface until the beginning of levee growth in the submarine
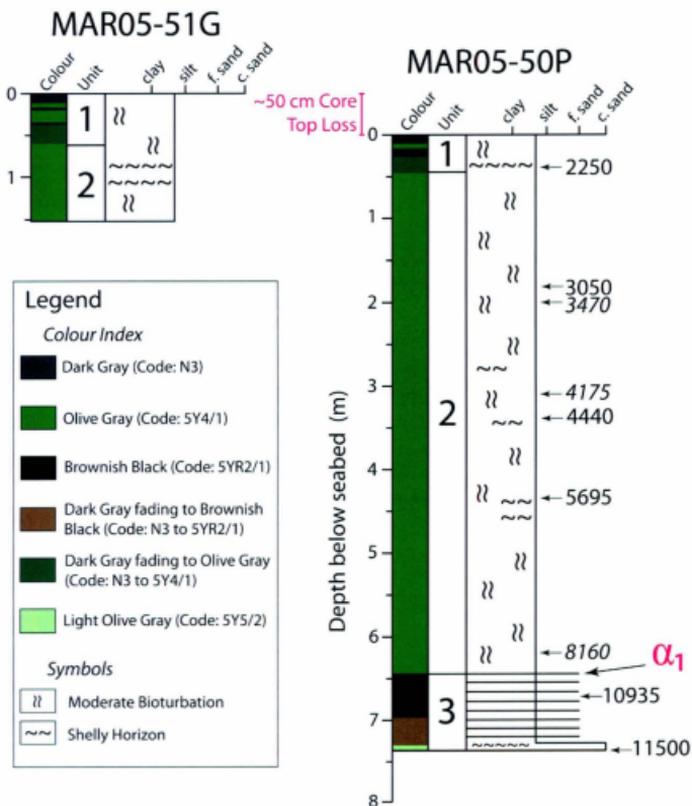
Figure 3.1. Illustrations of cores MAR05-50p and MAR05-51G (Linegar 2012). The top 50 cm of core MAR05-51G is added to the top of core MAR05-50P to create a composite core herein referred to as MAR05-50. Numbers to the right of the column indicate calibrated dates used to construct the age model. The dates in italics are previously unpublished (from Linegar, 2012).

channel north of the Bosphorus exit. The authors stated that development of this erosional surface might have been done under an early vigorous Rim Current prior to additional scouring beneath the earliest saline inflow.

Unit 2 begins above the unconformity α_1 (695 cm composite depth) there is sharp facies change to moderately bioturbated silty mud ($\leq$ 10% sand) with scattered marine mollusc shells above a composite depth of 513 cm. Flood et al. (2009) interpreted these sediments as a levee succession. The first available radiocarbon date above unconformity α_1 is 7570 ± 40 yr BP (uncalibrated) at 675 cm depth in the composite core. Unit 1 extends from 95 cm to the top of core MAR05-50 and is different from Unit 2 on the basis that it is color banded. Bioturbation is only moderate in core MAR0-50 and not interpreted to be a major factor affecting ostracod distribution.

3.2. Radiocarbon Dates

A total of fourteen radiocarbon dates were obtained from these two cores, two from core MAR05-51G and twelve from MAR05-50P. These radiocarbon dates were calibrated to calendar years (cal yr BP) using methods described in Chapter 2. Table 3.1 lists all the raw and calibrated radiocarbon dates. With the exception of 550, 620 and 625 cm (raw depths), these dates were previously published in Flood et al. (2009).

3.3. Age Model

Nine of the fourteen radiocarbon dates from cores MAR05-50P and MAR05-51G were used to construct an age model for composite core MAR05-50 (Table 3.2; Fig. 3.2). The date at the top of the core is assumed to be zero. The dates at 50, 695 and 696 cm were extrapolated and/or interpolated using constant sedimentation rates between dated

Table 3.1. All radiocarbon dates obtained from cores MAR05-50P and MAR05-51G. The material dated, the original radiocarbon dates and the calibrated dates are given. The sample depths shaded in grey indicate dates which were not used in the age model. The depths given are relative to the individual cores. For depths in the composite core MAR05-50 add 50 cm to depths in core MAR05-50P.

Core	Raw Depth (cm)	Dated Material	^{14}C Date (yr BP)	Mean cal yr BP	Median cal yr BP	Lab #
MAR05-50P	44	Bivalve fragments	2590 ± 90	2250 ± 120	2250	TO 13095
MAR05-51G	145	Bivalve fragments	3280 ± 60	3105 ± 90	3105	TO 13101
MAR05-50P	180	*Mytilus galloprovincialis*	3240 ± 50	3050 ± 80	3050	TO 13096
MAR05-50P	200	*Mytilus galloprovincialis*	3590 ± 15	3470 ± 40	3470	UCIAMS-96128
MAR05-50P	279	*Mytilus galloprovincialis*	3250 ± 70	3065 ± 100	3065	TO 13097
MAR05-50P	310	*Mytilus galloprovincialis*	4130 ± 20	4175 ± 45	4175	UCIAMS-96127
MAR05-50P	340	*Mytilus galloprovincialis*	4320 ± 60	4440 ± 90	4440	TO 13098
MAR05-50P	435	*Mytilus galloprovincialis*	5330 ± 70	5695 ± 80	5685	TO 13099
MAR05-50P	550	Foraminifera/Ostracods	7710 ± 40	8300 ± 50	8305	BETA305920
MAR05-50P	620	Foraminifera/Ostracods	8540 ± 50	9335 ± 65	9340	BETA305921
MAR05-50P	625	Foraminifera/Ostracods	7570 ± 40	8160 ± 60	8160	BETA307981
MAR05-50P	670	*Dreissena polymorpha*	9880 ± 110	10935 ± 150	10950	TO 13100
MAR05-50P	737	*Dreissena* spp. - pristine	10270 ± 90	11500 ± 175	11490	TO 12915
MAR05-50P	737	Bivalve fragments - worn	32190 ± 280	35390 ± 450	35255	TO 12734

Table 3.2. The age model for composite core MAR05-50.

Depth (cm)	Age (cal yr BP)
0	0
50	1956
94	2250
230	3050
250	3470
360	4175
390	4440
485	5695
675	8160
695	8419
696	10733
720	10935
787	11500
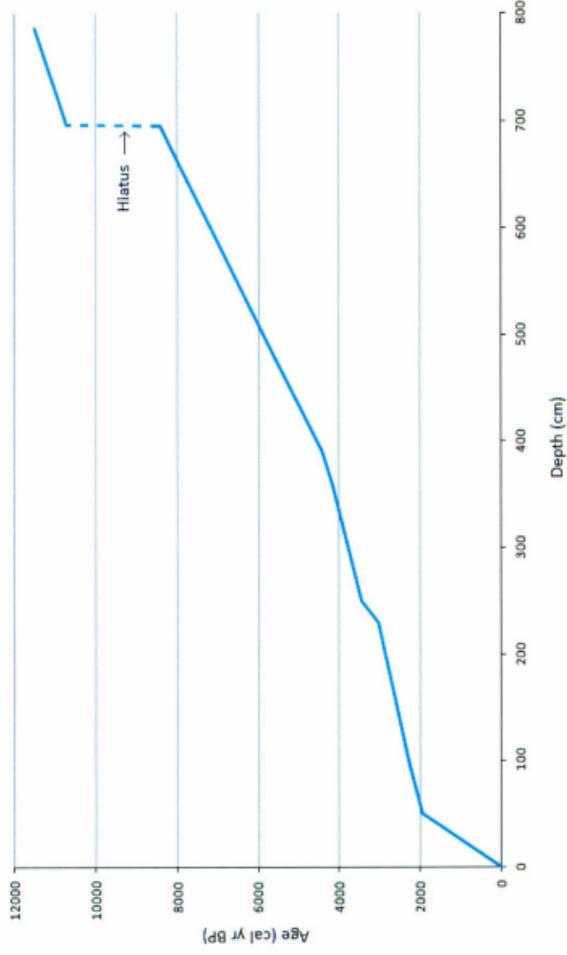
Figure 3.2. Graphic age model for composite core MAR05-50. The dotted line indicates the hiatus from ~8500 to 10600 cal yr BP which is represented by the α₁ unconformity.

intervals. Unconformity α_1 occurs between 695 and 696 cm (Fig. 3.1).

3.3.1. Dates Not Included in the Age Model

Two dates were obtained from 737 cm depth. One sample contained pristine *Dreissena* shells and gave an age of 11500 ± 175 cal yr BP (Table 3.1). The other sample contained some small pristine bivalves mixed in with numerous worn, pitted bivalve fragments. This sample gave an age of 35390 ± 450 cal yr BP. Because the latter sample appeared to be much older and contained reworked shells this date was disregarded in the final age model.

Two newly obtained dates from 550 and 620 cm raw depths were also left out of the age model. Sediments at these depths lacked any large pristine shells suitable for dating. All of the pristine ostracods and foraminifera were collected from the > 63 μm fraction of the ~ 25 cm^3 sample but were not abundant enough to fulfill the weight requirement of the dating laboratory. To obtain the desired sample size the author needed to collect additional shell fragments which were pitted and worn. These two dates ended up being older than a date obtained from pristine foraminifera at 625 cm raw depth. Thus these dates were deemed unreliable and not included in the age model.

The date from 279 cm raw depth turned out to be only 14 years older than the date from 180 cm raw depth. To determine if this date was reliable two more shells from 200 and 310 cm raw depths were sent for dating. These new dates were consistent with other dates from the core but not with the earlier date from 279 cm raw depth. Therefore this date was judged to be inaccurate and was not included in the age model.

The composite core was constructed using only the top 50 cm from core MAR05-

51G. The date from 145 cm raw depth is from core MAR05-51G and thus not included in the final age model. It also seems too old relative to the other dates but there might have been some compression of sediments in the gravity core to explain this disparity.

3.4. Sedimentation Rates

Sedimentation rates at the core site over the last 11500 cal years were calculated based on the radiocarbon dates used in the age model. The average sedimentation rate for the whole of core MAR05-50 was 70 cm ka^{-1}. Below unconformity α_1 the sedimentation rate was 120 cm ka^{-1}. The dates above unconformity α_1 show a decrease to 80 cm ka^{-1} until 4440 cal yr BP. Major et al. (2002) also noted a decrease in sedimentation rate at 8000 cal yr BP in cores from the northwestern Black Sea.

After 4440 cal yr BP the rate increased again to 110 cm ka^{-1} until 4175 cal yr BP and then 130 cm ka^{-1} until 3470 cal yr BP. It slowed down again to 50 cm ka^{-1} between 3470 and 3050 cal yr BP. The highest rate of sedimentation occurred between 3050 and 2250 cal yr BP when it increased to a relatively very high rate of 0.68 cm yr^{-1}.

The base of core MAR05-50 is dated at 11500 cal yr BP and it is 787 cm long. Assuming the date at the top of the core is 0 cal yr BP, each centimeter of sediment represents an average of 14.6 years. The core was sampled every 10 cm giving an average temporal resolution of ~ 146 years.

3.4.1. Onset of Marine Inflow into the Southwestern Black Sea Shelf

According to Major et al. (2006), strontium isotope values from carbonate shells in northwestern Black Sea cores reflect a connection with the global ocean starting at ~9150 cal yr BP (recalibrated from 8400 ^{14}C ka BP and their 9430 cal yr BP) and marks

the beginning of sedimentation on the Black Sea continental shelf. The earlier date proposed by Ryan et al. (1997) of 7570 cal yr BP is now given as the time when salinities became suitable for the colonization of the shelf area by fauna with marine affinities and not the date of the marine incursion itself (Major et al., 2006). The assessment of Major et al. (2006) is predicated on the notion that the Black Sea shelves were subaerially exposed until 9150 cal yr BP. This has been challenged by Hiscott et al. (2007) and others (e.g., Aksu et al., 1999, 2002a; Giosan et al., 2009; Mudie et al., 2007, Yanko-Hombach, 2007; Yanko-Hombach et al., 2007) who provided evidence for inundation of the shelves by at least ~ 10000 cal yr BP or earlier with no subsequent regression from then until present. Sediments from 9150 cal yr BP are "missing" from core MAR05-50 because of the hiatus represented by unconformity α_1 which spans ~8500–10600 cal yr BP.

CHAPTER 4

TAXONOMY

4.1. Ostracod Species Found

A total of 45 ostracod species were recovered from the samples from cores MAR05-50P and MAR05-51G. Five specimens have only been identified to genus level. Four have been identified using the abbreviation "sp. aff" (species *affinis*) which means the identity of the species is unknown but strongly resembles another species. There are also three "unknown species" which could not be identified by the author. A full systematic taxonomy and SEM plates follows in section 4.2. Below is a full list of all species identified from both cores in alphabetical order:

Amnicythere caspia (LIVENTAL, 1930 *nomen nudum*)

Amnicythere cymbula (LIVENTAL, 1929)

Amnicythere olivia (LIVENTAL, 1938)

Amnicythere pediformis (SCHORNIKOV, 1966)

Amnicythere propinqua (LIVENTAL, 1929)

Amnicythere quinquetuberculata (SCHWEYER, 1949)

Amnicythere striatocostata (SCHWEYER, 1949)

Amnicythere subcaspia (LIVENTAL, 1929)

Amnicythere volgensis (NEGADAEV, 1957)

Buntonia subulata rectangularis RUGGIERI, 1954

Bythocythere sp. SARS, 1866

Callistocythere diffusa (MÜLLER, 1894)

Candona schweyeri SCHORNIKOV, 1964

Carinocythereis carinata (ROEMER, 1838)

Caspiella acronasuta (LIVENTAL, 1929)

Costa edwardsi (ROEMER, 1838)

Cuneocythere semipunctata (BRADY, 1868)

Cytheroma variabilis MÜLLER, 1894

Cytheromorpha sp. aff. *fuscata* (BRADY, 1869)

Cytheropteron sp. aff. *inornatum* BRADY & ROBERTSON, 1872

Euxinocythere (*Maetocythere*) *lopatici* (SCHORNIKOV, 1964)

Euxinocythere bacuana (LIVENTAL, 1938)

Euxinocythere sp. aff. *relicta* (SCHORNIKOV, 1964)

Hemicytherura sp. ELOFSON, 1941

Hiltermannicythere rubra (MÜLLER, 1894)

Leptocythere devexa SHORNIKOV, 1966

Leptocythere multipunctata (SEGUENZA, 1884)

Leptocythere sp. 1 SARS, 1925

Loxoconcha immodulata STEPANAITYS, 1958

Loxoconcha lepida STEPANAITYS, 1962

Loxoconcha littoralis MÜLLER, 1894

Loxoconcha spp. juveniles*

Loxoconcha sublepida STANCHEVA, 1989

Palmoconcha agilis (RUGGIERI, 1967)

Paracypris polita SARS, 1866

Paradoxostoma simile MÜLLER, 1894

Pontocythere sp. DUBOWSKY, 1939

Pterygocythereis jonesii (BAIRD, 1850)

Sclerochilus gewemuelleri DUBOWSKY, 1939

Semicytherura sp. WAGNER, 1957

Tyrrhenocythere amnicola donetziensis (DUBOWSKY, 1926)

Unknown sp. 1

Unknown sp. 2

Unknown sp. 3

Xestoleberis sp. aff. *cornelii* CARAION, 1963

 *The author was unable to distinguish between the juveniles of *Loxoconcha lepida* and *Loxoconcha sublepida*. Therefore this category consists of all the juveniles of these two species.

4.2. Systematic Taxonomy

 For a guide to ostracod morphological features see section 4.2.1, Plate 1 (also see Athersuch et al., 1989 and Horne et al., 2002). The sample depths from each individual core at which each species was found is given. For each species, the morphological characteristics are described as well as the ecological affinity and geographical distribution if known. A list of synonyms is included for each species. In a few cases, the details for the original citation are omitted because the original publications could not be obtained through the inter-library loans service at Memorial University of Newfoundland.

Amnicythere caspia (LIVENTAL, 1930 *nomen nudum*)

Plate 2, Fig. 1.

1930 *Cythere caspia*; Livental, details unknown.

1961 *Leptocythere caspia* Livental; Agalarova et al., p. 108, pl. 63, figs 4–6.

2010 *Amnicythere caspia*? (Livental *nomen nudum*); Boomer et al., p. 128, pl. 1, fig. 15.

Found in: 580, 630–650 cm depth in core MAR05-50P.

Morphology: Small species (450–550 μm). Subovate elongate carapace. Valves are smooth with a c-shaped rib on the posterior-lateral surface which is parallel with the posterior margin. Anterior and posterior margins compressed.

Distribution and ecology: A Ponto-Caspian species. Boomer et al. (2010) found this species in Late Glacial sediments from the western Black Sea.

Amnicythere cymbula (LIVENTAL, 1929)

Plate 2, Figs 2–3.

1929 *Leptocythere cymbula* n. sp.; Livental, p. 21, pl. 1, fig. 25.

1966 *Leptocythere cymbula* (Livental); Schornikov, p. 35, fig. 3.

1989 *Amnicythere cymbula* (Livental); Stancheva, p. 23, pl. 2, fig. 3.

1996 *Leptocythere cymbula* Livental; Boomer et al., p. 81, fig. 4A–H.

2008 *Amnicythere cymbula* (Livental); Opreanu, p. 59, fig. 3.

Found in: 520, 610–650, 690, 700 cm depth in core MAR05-50P.

Morphology: Small to medium species (450–500 μm). Subreniform elongate carapace. Valves almost smooth to finely pitted. Some valves possess a small "ridge" on the lateral surface of the posterior-ventral margin which may extend slightly along the ventral

55

margin. Anterior and posterior margins compressed. Marginal pore canals simple or bifurcated.

Distribution and ecology: Schornikov (1966) found this species living in the Dniester River, Don Delta and Caspian Sea. Boomer et al. (1996) found this bottom-dwelling species in the Aral Sea in water less than 27 m deep and with a salinity range of 8-10 psu. Opreanu (2008) remarks this species is found today in lagoons and estuaries in the Ponto-Caspian region. Stancheva (1989) found this species in Middle-Upper Pleistocene sediments in the western Black Sea.

Remarks: Stancheva (1989) gives a length of 600–675 μm for this species. The specimens found in this study are smaller and may be A-1 instars.

Amnicythere olivia (LIVENTAL, 1938)

Plate 2, Figs 4–5.

1938 *Cythere olivia*; Livental, p. 62, pl. 1, figs 27–29.

1961 *Leptocythere olivina* Livental; Agalarova et al., p. 84, p. 50, fig. 1a,b, pl. 51, figs 1–3a,b, pl. 57, figs 4, 5a,b.

1962 *Leptocythere olivina* Livental; Mandelstam et al., p. 194, pl. 30, figs 9, 10.

2008 *Amnicythere olivina* (Livental); Opreanu, p. 59, fig. 5.

2010 *Amnicythere olivia* (Livental); Boomer et al., p. 128, pl. 2, figs 4–6, 9.

Found in: 340, 390, 490–570, 590–730 cm depth in core MAR05-50P.

Morphology: Medium species (500–600 μm). Subquadrate carapace. Conspicuously pitted with deep fossae. Dorsal margin straight. Anterior and posterior margins tapered. Posterior margin tapered with two distinct depressions which may be pitted or smooth.

Distribution and ecology: Boomer et al. (2010) found this species in Late Glacial sediments in the western Black Sea. Opreanu (2008) also found this species as fossils in late Quaternary sediments on the Romanian coast of the Black Sea.

Remarks: Livental originally described *Cythere olivia* in 1938 from the Baku region on the Caspian coast (Boomer et al., 2010). Agalarova et al. (1961) describe *Leptocythere olivina* and refers to Livental (1938) as a synonym. Therefore, the spelling *olivina* is probably a spelling error. See Boomer et al. (2010) for a full explanation.

Amnicythere pediformis (SCHORNIKOV, 1966)

Plate 2, Figs 6–7.

1966 *Leptocythere pediformis* sp. n.; Schornikov, p.33, pl. 2, figs 1–13.

1969 *Leptocythere pediformis* Schornikov; Schornikov, p. 183, pl. 10, fig. 2.

2010 *Amnicythere pediformis* (Schornikov); Boomer et al., p. 128, pl. 1, fig. 13.

Found in: 540, 550, 600–640, 660, 690 cm depth in core MAR05-50P.

Morphology: Small species (400–450 μm). Dorsal margin straight. Ventral margin slightly sinuous. Evenly ornamented with fine punctae which fine slightly toward all margins, especially the anterior. Posterior and anterior margins compressed.

Distribution and ecology: Boomer et al. (2010) found this species in Late Glacial sediments in the western Black Sea. They remarked that this species is also found in contemporaneous sediments of the Caspian Sea. Schornikov (1966) also found this species only as a fossil in the Azov-Black Sea basin.

Amnicythere propinqua (LIVENTAL 1929)

Plate 2, Figs 8–9.

1929 *Cythere propinqua*; Livental, p. 20, pl. 1, figs 21–24.

2010 *Amnicythere propinqua* (Livental); Boomer et al., p. 129, pl. 1, fig. 14.

Found in: 070 cm depth in core MAR05-50P; 110 cm depth in core MAR05-51G.

Morphology: Medium species (550–600 μm). Carapace elongate, narrow and smooth with no ornamentation. Rounded anteriorly and posteriorly. Ventral margin slightly sinuous. Height of valve almost uniform but posterior margin slightly tapered.

Distribution and ecology: This species is living today in the Caspian Sea, Aral Sea, Black Sea and Azov Sea. Boomer et al. (2010) recorded this species in Quaternary deposits of the western Black Sea.

Amnicythere quinquetuberculata (SCHWEYER, 1949)

Plate 2, Figs 10–11.

1949 *Cythere quinquetuberculata* sp. n.; Schweyer, p. 27, pl. 9, figs 5, 6.

1964 *Leptocythere quinquetuberculata* (Schweyer); Schornikov, p. 1285, fig. 7.

1969 *Leptocythere quinquetuberculata* (Schweyer); Schornikov, p. 187, pl. 15, fig. 2.

1989 *Amnicythere quinquetuberculata* (Schweyer); Stancheva, p. 25, pl. 7, fig. 8.

2002 *Amnicythere quinquetuberculata* (Schweyer); Tunoğlu, pl. 3, fig. 6.

2004 *Callistocythere quinquetuberculata* (Sceyer); Evans, p. 18, pl. 1, figs 4, 5.

2008 *Amnicythere quinquetuberculata* (Schweyer); Opreanu, p. 59, fig. 4.

Found in: 340, 490–660, 680–730 cm depth in core MAR05-50P.

Morphology: Medium species (500–600 μm). Subquadrate carapace. Sexually dimorphic with the male being more elongate. Dorsal margin straight. Anterior margin

compressed. Posterior margin compressed and tapered, more so in female. Valve conspicuously ornamented with five large tubercles pitted with large shallow fossae.

Distribution and ecology: Schornikov (1964) recorded this species living in the Danube and Don deltas and the Caspian Sea. Opreanu (2008) reported this species living in a group of saline lakes near the Romanian Black Sea coast south of the Danube Delta. She also remarked that this species prefers depths less than 5 m and reduced salinities of around 5 psu. Stancheva (1989) found this species in Lower–Upper Pleistocene deposits in the western Black Sea.

Amnicythere striatocostata (SCHWEYER, 1949)

Plate 2, Figs 12–13.

1949 *Cythere striatocostata* sp. n.; Schweyer, p. 27, pl. 9, fig. 8.

1961 *Leptocythere striatocostata* (Schweyer); Agalarova et al., p. 108, pl. 63, figs 1–3a,b.

1964 *Leptocythere striatocostata* (Schweyer); Schornikov, p. 1284, pl. 6, figs 1–15.

1969 *Leptocythere striatocostata* (Schweyer); Schornikov, p. 187, pl. 14, fig. 3.

2004 *Leptocythere striatocostata* (Schweyer); Evans, p. 31, pl. 3, fig. 5.

2008 *Amnicythere striatocostata* (Schweyer); Opreanu, p. 58, fig. 1.

2010 *Amnicythere striatocostata* (Schweyer); Boomer et al., p. 125, pl. 1, fig. 10.

Found in: 530, 600, 620, 700 cm depth in core MAR05-50P.

Morphology: Carapace small (450–500 μm) and elongate. Ornamented with parallel ribs which run longitudinally from the posterior margin and fade toward the anterior. Valve is otherwise smooth and thin. Anterior margin is compressed.

Distribution and ecology: Opreanu (2008) reported this species found as a fossil in Pliocene to Recent deposits all around the Ponto-Caspian basins. This species is living today in the Caspian and Black Seas (Stancheva, 1989).

Amnicythere subcaspia (LIVENTAL, 1929)

Plate 2, Figs 14–15.

1961 *Leptocythere subcaspia* Livental; Agalarova et al., p. 102, pl. 59, figs 6a,b.

Found in: 410, 490–510, 530, 550–570, 590–600, 630–660, 690, 730 cm depth in core MAR05-50P.

Morphology: Small species (400–450 μm). Similar to *A.caspia* but less elongate. Anterior margin rounded and compressed. Posterior margin approximately two thirds the width of anterior margin. Valves smooth with a raised c-shaped "ridge" or rib which parallels the posterior margin. This ribbing may extend subtly to the posterior-lateral surface and contains smaller ribbing surrounded by the more prominent "ridge".

Distribution and ecology: Presumably a Ponto-Caspian species. Illustrated by Agalarova et al. (1961) in *Ostracoda from Pliocene and post-Pliocene deposits of Azerbaijan* [in Russian].

Remarks: The drawings in Agalarova et al. (1961) appear exaggerated.

Amnicythere volgensis (NEGADAEV, 1957)

Plate 3, Fig. 1.

2011 *Amnicythere volgensis* (Negadaev); Schornikov, p. 180, fig. 1.

Found in: 510, 610, 620, 690, 720 cm depth in core MAR05-50P.

Morphology: Medium to large species (~700 µm). Rounded anterior margin strongly compressed. Pitted with large fossae. One or two bumps or tubercles at posterior-ventral margin.

Distribution and ecology: Found as a fossil in Pleistocene and Holocene sediments of the Back Sea and still living in the Caspian Sea (Schornikov, 2011).

Buntonia subulata rectangularis RUGGIERI, 1954

Plate 3, Figs 2–3.

1969 *Buntonia subulata rectangularis* Ruggieri; Schornikov, p. 190, pl. 17, fig. 1.

2011 *Rectobuntonia rectangularis* (Ruggieri); Cabral et al., fig. 2, #7.

Found in: 70, 170, 220, 230, 290, 310, 340 cm depth in core MAR05-50P; 10, 40, 120, 130 cm depth in core MAR05-51G.

Morphology: Small to medium species (500–525 µm). Carapace ovate and inflated. Valves smooth in centre. Concentric ribbing parallel to posterior and anterior margins. Finley pitted between ribbing. Vertical muscle scar pattern can sometimes be seen.

Distribution and ecology: Cabral et al. (2011) found this species in Recent sediments on the continental shelf of western Algarve, Portugal.

Bythocythere sp. SARS, 1866

Plate 3, Figs 4–5.

1969 *Bythocythere turgida* Sars; Schornikov, p. 209, pl. 35, fig. 1 (*pars*) (non Sars, 1866).

Found in: 0, 10, 30, 40, 70, 80, 100, 110, 170, 180, 230–250, 270, 290–400, 420 cm depth in core MAR05-50P; 10, 30–50, 80, 100, 110, 130 cm depth in core MAR05-51G.

61

Morphology: Large species (750–800 µm). Subrhomboidal and strongly inflated carapace. Small caudal process above mid-height. Valves ornamented with very fine reticulation and wavy "lines" which give a wrinkled appearance. Posterior margin strongly compressed.

Distribution and ecology: Presumably marine since other species of *Bythocythere* such as *B. robinsoni*, *B. intermedia* and *B. zetlandica* are marine sublittoral species found around the coasts of Britain and northwestern Europe (Athersuch et al., 1989).

Callistocythere diffusa (MÜLLER, 1894)

Plate 3, Figs 6–7.

1894 *Cythere diffusa*; Müller, p. 354

1969 *Callistocythere diffusa* (Müller); Schornikov, p. 189, pl. 16, fig. 4.

Found in: 10, 30, 40, 60–80, 170, 270 cm depth in core MAR05-50P; 10, 60, 100, 110 cm depth in core MAR05-51G.

Morphology: Medium species (550–600 µm). Reniform carapace with the anterior margin curved downward. Heavily ornamented with irregular fossae and indentations surrounded by large, rounded muri. Posterior margin compressed.

Distribution and ecology: Marine species. Puri et al. (1964) recorded this species living in the Gulf of Naples associated with *Posidonia* and calcareous algae up to 100 m water depth. Bonaduce et al. (1975) recorded this species from the Adriatic Sea up to 119 m, mainly on medium sand. They also mention this species being found in the Tyrrhenian Sea. Schornikov (1966) found this species to be common in the Black Sea at depths of 13–70 m.

Candona schweyeri SCHORNIKOV, 1964

Plate 3, Figs 8–9.

1964 *Candona schweyeri* nom. n.; Schornikov, p. 1277, fig. 1.

1969 *Candona schweyeri*; Schornikov, p. 173, pl. 5, fig. 1.

2004 *Candona* aff. *schweyeri* Schornikov; Evans, p. 19, pl. 1, fig. 10.

2008 *Candona schweyeri* (Schornikov); Opreanu, p. 61, fig. 10.

2010 *Candona schweyeri* Schornikov; Boomer et al., p.124, pl. 1, fig. 7.

Found in: 340, 490, 510–730 cm depth in core MAR05-50P.

Morphology: Carapace large (~1 mm). Valves are smooth, elongate, evenly inflated and very thin. Generally rounded with slightly straight anterior margin and slightly concave ventral margin.

Distribution: Schornikov (1964) recorded this species living around the Danube, Dniester and Don deltas and in the Caspian Sea.

Remarks: Due to its thin fragile valves, *C. schweyeri* was often found as fragments in samples from cores MAR05-50P and MAR05-51G. It was therefore difficult to count the exact number of whole valves present.

Carinocythereis carinata (ROEMER, 1838)

Plate 3, Figs 10–15.

1838 *Cytherina carinata* sp. nov.; Roemer, p. 518, pl. 6, fig. 28.

1850 *Cythereis antiquata* sp. nov.; Baird, p. 176, pl. 20, fig. 2.

1987 *Carinocythereis carinata* (Roemer); Athersuch & Whittaker, p. 97–102.

2004 *Carinocythereis carinata* (Roemer); Evans, p. 19, pl. 2, figs 2, 3.

Found in: 0–130, 150–400, 420–480, 530–570, 670 cm depth in core MAR05-50P; 10–150 cm depth in core MAR05-51G.

Morphology: Large quadrate carapace (0.8–1 mm). Sexual dimorphism pronounced with the male being more elongate and narrow. Conspicuously ornamented with three sub-parallel longitudinal carinae which can be continuous or broken. Surface of valve is otherwise heavily to subtly tuberculate or sometimes smooth. Prominent eye tubercle. Anterior margin carinate and denticulate. Posterior margin spinose.

Distribution and ecology: Far-ranging species living in marine sublittoral waters at depths of 2–60 m. Today it is found around the British Isles, the Atlantic coast of France, the Mediterranean Sea and the Black Sea (Athersuch et al., 1989). Puri et al. (1964) recorded this species living in the Gulf of Naples associated with *Posidonia* (seagrass) and algae at water depths less than 100 m.

Caspiella acronasuta (LIVENTAL, 1929)

Plate 4, Fig. 1.

1961 *Caspiella acronasuta* (Livental); Agalarova et al., p. 41, pl. 10, figs 1–3, pl. 11, figs 1–4, pl. 12, figs 1, 2, pl. 26, fig. 6, pl. 32, fig. 2.

2005 *Caspiolla acronasuta*; Boomer et al., p. 178, pl. 1, figs 1, 4.

Found in: 730 cm depth in core MAR05-50P

Morphology: Large species (~1 mm). Smooth thick valves. Anterior margin rounded. Dorsal margin arched. Posterior margin tapered to a point. Wide inner lamella. Marginal pore canals simple and numerous.

Distribution and ecology: Typical benthic Caspian species. Boomer et al. (2005) recorded this species in Recent core tops from the southern Caspian Basin at a current water depth of 315 m. This species prefers very deep water (E. I. Schornikov, personal communication).

Remarks: There seems to be some confusion regarding the correct spelling of this genus. Boomer et al. (2010) said that *Caspiella* is the correct genus name.

Costa edwardsi (ROEMER, 1838)

Plate 4, Figs 2–3.

1838 *Cytherina edwardsi* n. sp; Roemer, p. 518, pl. 6.

1889 *Cythere runcinata* (Baird); Brady & Norman, p. 160, pl. 15, figs 24, 25, 30, 31.

1962 *Costa edwardsii* (Roemer); Ruggieri, p. 5, pl. 8, figs 1–5.

1975 *Costa edwardsi* (Roemer); Bonaduce et al., p. 51, pl. 25, figs 1–7.

Found in: 0–130, 150, 170, 180, 210–330 cm depth in core MAR05-50P; 10–150 cm depth in core MAR05-51G.

Morphology: Carapace large (800–900 μm). Conspicuously ornamented with three longitudinal carinae (costae) sloping downward but not reaching the anterior margin. Areas between carinae can be smooth but are often heavily pitted. Anterior and posterior margins are compressed and strongly denticulate and/or spinose. Sexual dimorphism is present with the male being more elongate and narrow.

Distribution and ecology: Marine sublittoral species with a preference for silty substrates. Puri et al. (1964) recorded this species living around the Island of Ischia and

other shallow areas of the Gulf of Naples. Bonaduce et al. (1988) recorded it on the Tunisian shelf between 18 and 28 m on muddy sand with scattered algal vegetation.

Cuneocythere semipunctata (BRADY, 1868)

Plate 4, Figs 4–5.

1868 *Cythere semipunctata* sp. nov.; Brady, p. 411, pl. 29, figs 33–37.

1963 *Cuneocythere semipunctata* (Brady); Van Morkhoven, p. 321.

Found in: 0, 10 cm depth in core MAR05-50P; 20, 40 cm depth in core MAR05-51G.

Morphology: Carapace small (450–600 μm) and inflated posteriorly. Posterior half of valve pitted with large rounded fosae. Anterior margin smooth, very compressed and slightly upturned. Marginal pore canals numerous and simple, sometimes in groups of four or five.

Distribution and ecology: Marine sublittoral species often found on sandy substrates. Athersuch et al. (1989) recorded this species in waters around the coast of Ireland, England and southwest France. They also remarked that it is occasionally found in association with *Laminaria* (brown algae) at the lower limit of the intertidal zone. Smith and Horne (2002) recorded this species in an estuary on the coast of Wales in salinity range of 30–35 psu. Bonaduce et al. (1975) recorded this species in the Adriatic Sea on sandy mud and silt at depths up to 194 m and always represented by only a few individuals. They remarked that it has also been found in the Bay of Naples.

Cytheroma variabilis MÜLLER, 1894

Plate 4, Figs 7–8.

1894 *Cytheroma variabilis*; Müller, p. 350, pl. 26, figs 5, 9–15.

1969 *Cytheroma variabilis* Müller; Schornikov, pl. 22, fig. 2.

Found in: 0, 10, 40, 60–80, 100, 160–180, 200–410, 500, 550, 570 cm depth in core MAR05-50P; 10, 40, 60, 80, 90, 110 cm depth in core MAR05-51G.

Morphology: Small species (~400 μm) with narrow, thin, inflated valves. Smooth and unornamented except for some widely scattered pores. Anterior margin rounded. Dorsal margin arched. Posterior margin tapered.

Distribution and ecology: Müller originally described this species from the Gulf of Naples. Puri et al. (1964) also reported this species living in the Gulf of Naples associated with *Posidonia*. Bonaduce et al. (1975) noted this species has a widely scattered distribution in the Adriatic Sea to a depth of 127 m. They remarked that it is present on all substrates but seems to prefer sandy clay and sandy silt.

***Cytheromorpha* sp. aff. *fuscata* (BRADY, 1869)**

Plate 4, Fig. 6.

1969 *Cytheromorpha fuscata* (Brady); Schornikov, p. 181, pl. 8, fig. 3.

Found in: 570 cm depth in core MAR05-50P.

Morphology: Medium species (500–600 μm). Carapace subquadrate. Valves ornamented with small rounded fossae which fine toward the anterior margin. Anterior margin compressed and curved downward.

Distribution and ecology: Recorded by Opreanu (2003/04) in Sinoe lagoon, Danube Delta area. She described this species as a brackish, littoral species found in the Baltic and the North Seas, Black and Azov Sea basin and in the Caspian Sea.

Cytheropteron **sp. aff.** *inornatum* BRADY & ROBERTSON, 1872

Plate 4, Figs 9–10.

1872 *Cytheropteron inornatum* sp. nov.; Brady & Robertson, p. 61, pl. 2, figs 1–3.

1989 *Cytheropteron inornatum* sp. nov. Brady & Robertson; Athersuch et al., p. 226, Fig. 95, pl. 8, fig. 4.

Found in: 0, 10 cm depth in core MAR05-50P; 10, 20 cm depth in core MAR05-51G.

Morphology: Carapace sub-rhomboidal and small (~400 µm). Upturned caudal process just above mid-height. Valves generally smooth with scattered punctae. Recognizable by prominent pointed ala on each valve.

Distribution and ecology: Athersuch et al. (1989) wrote that little is known of the ecology of this species. It is presumed to be marine and sublittoral.

Euxinocythere (Maetocythere) lopatici (SCHORNIKOV, 1964)

Plate 4, Figs 11–12.

1964 *Leptocythere lopatici*; Schornikov, p. 1279, pl. 2, figs 1–7, pl. 3, figs 1–11.

2008 *Euxinocythere lopatici* (Schornikov); Opreanu, p. 60, fig. 7.

2010 *Euxinocythere (Maetocythere) lopatici* (Schornikov); Boomer et al., p. 129, pl. 1, figs, 9, 12, q.v. for full synonymy.

2011 *Euxinocythere virgata* (Schneider); Scornikov, p. 180, fig. 1.

Found in: 210, 280, 300, 530, 610, 620, 640–670, 690, 720 cm depth in core MAR05-50P.

Morphology: Medium species (500–550 µm). Subquadrate carapace. Valves thick conspicuously ornamented with large rounded fossae and pits surrounded by muri, giving

a "wrinked" appearance. Transverse ridge parallel to posterior margin. Anterior and posterior margins compressed.

Distribution and ecology: Boomer et al. (2010) found this species in Late Glacial to Holocene sediments in the Black Sea. Schornikov (2011) found *E. virgata* (which the author believes to be synonymous) living in the Caspian Sea, basins of the Don River and Taganrogsky Bay (Azov Sea) and the Danube River Delta.

Euxinocythere bacuana (LIVENTAL, 1938)

Plate 4, Figs 13–14.

1969 *Leptocythere bacuana* (Livental); Schornikov, p. 187, pl. 15, fig. 3.

1989 *Euxinocythere (Euxinocythere) bacuana* (Livental); Stancheva, p. 29, pl. VII, fig. 9.

2004 *Callistocythere bacuana* (Livental); Evans, p. 26, pl. 1, fig. 3.

2005 *Callistocythere bacuana*; Boomer et al., pl. 1, fig. 8.

2008 *Amnicythere bacuana* (Livental); Opreanu, p. 60, fig. 6.

2011 *Euxinocythere bacuana* (Livental, 1938); Schornikov, p. 180, fig. 1.

Found in: 340, 510, 520, 540, 560, 590–640, 660, 670, 720, 730 cm depth in core MAR05-50P.

Morphology: Small to medium species (400–500 μm). Carapace subtrapezoidal and strongly convex. Conspicuously ornamented with large pitted tubercles in the centre of the valve and two transverse ridges - one at the posterior margin and one at the anterior margin.

Distribution and ecology: Brackish species found in Holocene deposits of the Black Sea, Caspian Sea and the Dniester River and the Don Delta. Currently living in the Black

69

and Caspian Seas (Opreanu 2008).

Euxinocythere* sp. aff. *relicta (SCHORNIKOV, 1964)

Plate 4, Fig. 15; Plate 5, Fig. 1.

1964 *Leptocythere relicta* sp. n.; Schornikov, p. 1282, fig. 4.

1969 *Leptocythere relicta* Shornikov; Schornikov, p. 184, pl. 11, fig. 1.

2011 *Euxinocythere relicta* (Schornikov); Schornikov, p. 180, fig. 1.

Found in: 340, 510, 540, 550, 580, 600–660, 690–710, 730 cm depth in core MAR05-50P.

Morphology: Small species (~400 µm). Reniform carapace. Valves generally evenly ornamented with small fossae. Posterior and anterior margins compressed.

Distribution: Schornikov (1964) first described this species from deltas flowing into the Azov and Black Seas. Schornikov (2011) found this species living in the Caspian Sea, Azov Sea and several Ukrainian estuaries in the western Black Sea and as a fossil or subfossil in the Recent sediments of the Black Sea and Aegean Sea.

***Hemicytherura* sp.** ELOFSON, 1941

Plate 5, Figs 2–3.

Found in: 220, 340 cm depth in core MAR05-50P.

Morphology: Small species (~400 µm). Carapace conspicuously ornamented with large fossae which often have secondary reticulation within. Caudal process above mid-height.

Distribution and ecology: Presumably marine, littoral, phytal species like other *Hemicytherura* species such as *H. cellulosa* and *H. hoskini* (Athersuch et al., 1989).

Hiltermannicythere rubra (MÜLLER, 1894)

Plate 5, Figs 4–6.

1894 *Cythereis rubra* sp. nov.; Müller, p. 372, pl. 28, figs 21, 26, pl. 31, figs, 2, 3.

1969 *Carinocythereis rubra* (Müller); Schornikov, p. 191, pl. 18, fig. 1.

1975 *Hiltermannicythere* aff. *H. rubra* (Müller); Bonaduce et al., p.49, pl. 28, figs 1–5.

1979 *Hiltermannicythere rubra* (Müller); Athersuch, p. 140, fig. 2 (13).

Found in: 0–120, 150–180, 200–330, 360–500, 530, 540 cm depth in core MAR05-50P; 0–150 cm depth in core MAR05-51G.

Morphology: Large species (800–850 μm). Subquadrate carapace. Tapered slightly at posterior. Posterioventral margin denticulate. Thick valves weakly ornamented with three longitudinal carinae – dorsal, median and ventral. Median carinae most prominent. Areas between carinae generally evenly pitted with large rounded fossae.

Distribution and ecology: Marine euryhaline species capable of living in salinities of 8–40 psu (Aladin, 1993). Puri et al. (1964) recorded this species living on the shallow banks around Ischia, Procida, Naples and Sorrento Peninsula associated with *Posidonia* in depths up to 100 m. Bonaduce et al. (1975) recorded this species in the Adriatic Sea. Ivanova et al. (2007) found this species in upper Holocene sediments of the Black Sea and commented that this species is thought to indicate polyhaline (18–30 psu) conditions.

Leptocythere devexa SCHORNIKOV, 1966

Plate 5, Figs 7–8.

1966 *Leptocythere devexa* sp. n.; Schornikov, p. 39, fig. 5.

1969 *Leptocythere devexa* Schornikov; Schornikov, p. 185, pl. 12, fig. 3.

Found in: 50, 70, 180, 240, 270, 300, 320, 340, 370–390 cm depth in core MAR05-50P; 100 cm depth in core MAR05-51G.

Morphology: Small species (375–400μm). Reniform carapace. Valves ornamented with numerous muri and fine punctae.

Distribution: Shallow marine species. Opreanu (2005) recorded this species in Recent sediments of the western Black Sea at an average depth of 28.5 m.

Leptocythere multipunctata (SEGUENZA, 1884)

Plate 5, Figs 9–10.

1966 *Leptocythere (Leptocythere) multipunctata multipunctata* (Seguenza); Schornikov, p. 40, fig. 6.

1969 *Leptocythere multipunctata* (Seguenza); Schornikov, p. 185, pl. 12, fig. 2.

1975 *Leptocythere multipunctata* (Seguenza); Bonaduce et al., p.33, pl. 17, figs 4–7.

Found in: 0, 10, 60–90, 130, 170, 180, 200–240, 270–440, 460, 600 cm depth in core MAR05-50P; 20, 50, 100, 110, 130, 140 cm depth in core MAR05-51G.

Morphology: Small species (450–500 μm). Reniform carapace. Valves distinctly ornamented with defined muri and fine punctae often arranged in groups of 6–10. Reticulation fines towards all margins. Posterior margin compressed.

Distribution and ecology: Schornikov (1966) found this species in the Black Sea commonly on mud at depths of 30–60 m. He comments that this species can live in interstitial water and without oxygen Schornikov (1969) recorded this species in the Azov and Black Seas and commented that its preferred salinity is >11 psu. Kılıç (2000) recorded this species on the Black Sea coast of Turkey.

72

Leptocythere **sp. 1** SARS, 1925

Found in: 130 cm depth in core MAR05-50P.

Morphology: Elongate, subquadrate carapace. Valve smooth with a rounded ridge structure on posterior-ventral surface. All margins, excluding dorsal margin, compressed.

Distribution and ecology: Unknown.

Loxoconcha immodulata STEPANAITYS, 1958

Plate 5, Figs 11–12.

1958 *Loxoconcha immodulata*; Stepanaitys, p. 19, pl. 1, fig. 18.

1969 *Loxoconcha immodulata* Stepanaitys; Schornikov, p. 201, pl. 27, fig. 2.

1996 *Loxoconcha immodulata* Stepanaitys; Boomer et al., p. 81, pl. 1, fig. 18.

2010 *Loxoconcha immodulata* Stepanaitys; Boomer et al., p. 130, pl. 2, figs 7–8, 12.

Found in: 80, 340, 490, 510–620, 640, 670–700 cm depth in core MAR05-50P.

Morphology: Small to medium species (400–500 µm). Strongly convex, trigonal carapace. Sexual dimorphism present with male being more quadrate than female. Pitted with rounded fossae which fine towards all margins. Marked eyespot.

Distribution: Boomer et al. (1996) recorded this species from the Aral Sea. They remark that it is also present in the Caspian Sea.

Loxoconcha lepida STEPANAITYS, 1962

Plate 5, Figs 13–15

1962 *Loxoconcha lepida* Stepanaitys; Mandelstam et al., p. 178, pl. 28, fig. 7.

1962 *Loxoconcha unodensa* Mandelstam; Mandelstam et al., p. 178, pl. 28, fig. 9.

1964 *Loxoconcha lepida* Stepanaitys; Schornikov, p. 1290, pl. 11, figs 1–12.

1969 *Loxoconcha lepida* Stepanaitys; Schornikov, p. 199, pl. 25, fig. 2.

2008 *Loxoconcha lepida* Stepanaitys; Opreanu, p. 61, fig. 9.

2010 *Loxoconcha lepida* Stepanaitys; Boomer et al., p. 129, pl. 2, figs 1–3.

Found in: 240, 250, 340, 370, 490, 520–540, 560, 570, 590–700, 720, 730 cm depth in core MAR05-50P.

Morphology: Medium to large species (600–650 μm). Subovate carapace. Sexual dimorphism very pronounced with the male being more elongate and oval shaped and the female having greater height and more strongly arched dorsal margin. Valves ornamented with deep pits which are larger in the centre and fine towards margins. Some valves have a small slightly upturned spine at the dorsoventral margin.

Distribution and ecology: Schornikov (1964) recorded this species living from deltas in the Azov and Black Seas. It was also found in the Caspian Sea in 30 % of samples between 5 and 125 m. Stancheva (1989) also commented this species lives today in the Black and Caspian Sea. Ivanova et al. (2007) recorded this species in lower Holocene sediments of the Black Sea and commented that this species is oligohaline (i.e., preferring a salinity range of 0.5–5 psu). Boomer et al. (2010) recorded this species as fossils in Quaternary deposits of the western Black Sea. Boomer et al. (1996) recorded this species in Holocene sediments in the Aral Sea.

Remarks: *L. lepida* and *L. unodensa* were originally described as separate species. Schornikov (1964) recognized that they were actually a male and female of *L. lepida*.

Loxoconcha littoralis MÜLLER, 1894

74

Plate 6, Figs 4–5.

1894 *Loxoconcha littoralis*; Müller, p. 346, pl. 27, fig. 9, pl. 29, figs 1–7.

1964 *Loxoconcha littoralis* Müller; Ruggieri, p. 517, figs 1, 2.

1975 *Loxoconcha littoralis* Müller; Bonaduce et al., p. 108, pl. 66, figs 8–12.

Found in: 50, 80, 390, 420, 480–580, 600–620, 670, 690–710, 730 cm depth in core MAR05-50P.

Morphology: Small species (400–450 μm). Subtrigonal to subquadrate carapace. Sexually dimorphic with male being more elongate. Valves ornamented with defined muri and rounded fossae. A prominent ridge-like structure curves up from the posteriorventral area to the marked eyespot.

Distribution and ecology: Marine species. Described as "surely stenohaline" by Ruggieri (1964). Rare in the Adriatic Sea, found along the Apulia coast on medium sand (Bonaduce et al., 1975). Puri et al. (1964) recorded this species in the Gulf of Naples associated with sponges in shallow water. It has also been recorded from the Miocene and Pliocene of the Mediterranean. Ivanova et al. (2007) figured this species is "probably mesohaline (5–18 psu) based on its occurrence in the Mediterranean".

Loxoconcha spp. juveniles
Plate 6, Figs 1–3.

Found in: 240, 270, 300, 310, 330–360, 380–400, 420, 430, 480–730 cm depth in core MAR05-50P.

Remarks: This group contains all the juveniles of both *L. lepida* and *L. sublepida*. These are so numerous and similar looking it would have been too time-consuming and

extremely difficult to attempt to separate them. Because these species are both Ponto-Caspian types, occur in most samples together and are the same genus they are considered here together.

Loxoconcha sublepida STANCHEVA, 1989

Plate 6, Figs 6–7.

1989 *Loxoconcha sublepida* sp. n.; Stancheva, p. 35, pl. 8, figs 8–10.

2002 *Loxoconcha tumida* Brady; Tunoglu, p. 9, pl. 1, fig. 11.

2005 *Loxoconcha* sp. 1; Boomer et al., pl. 1, figs 3, 6.

Found in: 210, 250, 270, 320–340, 480–730 cm depth in core MAR05-50P.

Morphology: Stancheva chose this name because of the close resemblance to *L. lepida*. Carapace is medium (500–600 µm). Valves are ovate with straight dorsal margin, sometimes slightly inclined. Ornamentation consists of pitting which is largest in the centre and decreases towards margins. Several concentric parallel ridges sometimes present in the posteriorventral area.

Distribution and ecology: Stancheva first described this species from Middle–Upper Pleistocene deposits from the western Black Sea shelf. In Upper-Pleistocene to Neoeuxinian sediments it was found in samples dominated by *L. lepida*.

Palmoconcha agilis (RUGGIERI, 1967)

Plate 6, Figs 10–14.

1967 *Loxoconcha agilis* sp. n.; Ruggieri, p. 377, figs 39–45, pl. 37, fig. 6.

1975 *Loxoconcha* aff. *L. agilis* Ruggieri; Bonaduce et al., pl. 65, figs 9–14.

2004 *Palmoconcha* aff. *guttata* (Norman); Evans, 24, pl. 4, figs 6–8 (see Remarks).

2010 *Palmoconcha agilis* (Ruggieri); Boomer et al., p. 130, pl. 2, fig. 11.

Found in: 0–330, 360, 370, 390–490, 510–580, 600, 620–660, 680–700, 720 cm depth in core MAR05-50P; 10–150 cm depth in core MAR05-51G.

Morphology: Carapace medium (500–600 μm). Inflated, ovate valves with a prominent marginal rim which is flattened posteriorly. Caudal process above mid-height. Valves smooth to finely pitted. Sexual dimorphism present with male being more elongate.

Distribution and ecology: Bonaduce et al. (1975) recorded this species (as *Loxoconcha* aff. *L. agilis*) on sandy and silty mud in the Adriatic Sea. This species is abundant today on clays around the shorelines of the Black Sea at depths of 10–100 m (Schornikov, 1967). Boomer et al. (2010) found this species in recent sediments of the western Black Sea and commented that "the species forms part of the 'Mediterranean' fauna...which has become established in the post-connection period".

Remarks: *P.agilis* is remarkably similar to *P.guttata* which is found in the North Sea and around the Atlantic coasts of Europe (Athersuch et al., 1989; Penny, 1993). Ruggieri described *P.agilis* from the eastern Mediterranean. It is possible that they are the same species. Comparison of internal parts is necessary to be certain.

Paracypris polita SARS, 1866

Plate 6, Fig. 15; Plate 7, Fig. 1.

1866 *Paracypris polita* sp. n.; Sars, p. 12.

1969 *Paracypris polita* Sars; Schornikov, p. 171, pl. 3, fig. 3.

Found in: 0–40, 60, 120, 230, 270, 310 cm depth in core MAR05-50P; 10, 20, 40–100, 130, 150 cm depth in core MAR05-51G.

Morphology: Carapace smooth and large (1–1.3 mm). Anterior margin rounded. Dorsal margin arched. Posterior margin tapered to a point. Ventral margin gently concave at about mid-length. Marginal pore canals conspicuously branching. Distinct vertical scar pattern.

Distribution and ecology: This marine species has been recorded from southern Norway, the Skagerak (strait between Norway and southwestern Sweden), north and southwest Britain in littoral environments up to 70 m (Athersuch et al.. 1989). Found in the Bay of Naples off Capri at 70 m depth (Brady & Norman, 1889).

Paradoxostoma simile MÜLLER, 1894

Plate 7, Fig. 2.

1894 *Paradoxostoma simile*; Müller, p. 318, pl. 22, fig. 30, pl. 23, figs 2, 25, 27, 32.

1969 *Paradoxostoma simile* Müller; Schornikov, pl. 41, fig. 3.

Found in: 340, 350, 380, 390 cm depth in core MAR05-50P.

Morphology: Medium carapace (650–700 µm). Subrhomboidal valves are very thin and smooth. Anterior margin narrow and rounded. Caudal process well above mid-height.

Distribution and ecology: Puri et al. (1964) recorded this species living in the Gulf of Naples associated with *Posidonia* and calcareous algae at depths less than 100 m. Bonaduce et al. (1975) found this species living in the Adriatic Sea. Athersuch et al. (1989) refers to this species in passing as being Mediterranean.

78

Pontocythere sp. DUBOWSKY, 1939

Plate 7, Fig. 3.

Found in: 10, 70 cm depth in core MAR05-50P; 10 cm depth in core MAR05-51G.

Morphology: Small species (~450 µm). Carapace elongate and reniform. Valves thin and smooth with widely scattered pores. Anterior margin finely denticulate.

Distribution and ecology: This species of the genus *Pontocythere* is unknown. Other species of this genus are marine. *P.rubra* and *P.turbida* are found in the Mediterranean and *P.elongata* is found around the coasts of Britain and northwestern Europe (Athersuch et al., 1989).

Pterygocythereis jonesii (BAIRD, 1850)

Plate 7, Figs 4–5.

1850 *Cythereis jonesii* sp. nov.; Baird, p. 175, pl. 20, fig. 1.

1975 *Pterygocythereis jonesii* (Baird); Bonaduce et al., p. 54, pl. 29, figs 1–11.

1989 *Pterygocythereis jonesii* (Baird); Athersuch et al., p. 146, pl. 4, fig. 6.

 2011 *Pterygocythereis jonesi* (Baird); Cabral et al., p. 40, fig. 2, #9.

Found in: 0–90, 110–180, 200–330, 530, 560 cm depth in core MAR05-50P; 10–150 cm depth in core MAR05-51G.

Morphology: Large species (~1 mm). Carapace quadrate and conspicuously ornamented with prominent spinose alae. Anterior, dorsal and posterior margins spinose. Valves otherwise smooth. Prominent eye tubercle.

Distribution and ecology: A common marine, sublittoral species found in the Mediterranean and Black Seas. Bonaduce et al. (1975) recorded this species on medium

and fine sand and sandy silt and mud in the Adriatic Sea from shallow water till the maximum collection depth, noting the highest concentrations were between 80 and 170 m. Penny (1993) recorded this species in the North Sea (salinity 34-35 psu) abundant at depths >80 m on fine sandy mud.

Sclerochilus gewemuelleri DUBOWSKY, 1939

Plate 7, Fig. 6.

1939 *Sclerochilus gewemuelleri* nom. nov. var.; Dubowsky, p. 4, p. 65, figs 1, 2.

1969 *Sclerochilus gewemuelleri*; Schornikov p. 210, pl. 36, fig. 1.

1987 *Sclerochilus gewemuelleri* Dubowsky; Athersuch & Horne, p. 209, fig. 8A–J.

 Found in: 290, 340, 350, 370, 390, 400 cm depth in core MAR05-50P.

Morphology: Small to medium species (450–650 µm). Reniform carapace. Valves thin and smooth. All margins smooth and rounded. Ventral margin strongly sinuous and concave just before mid-length. Weak hinge.

Distribution and ecology: Marine sublittoral, occasionally littoral, species found around the British Isles, the Mediterranean and the Black Sea (Athersuch et al., 1989). Van Morkhoven (1962) remarks that the genera belonging to the subfamily *Paradoxostominae* (including *Sclerchilus*) are mainly phytal. Their smooth, elongate carapaces seem suitable for moving around amongst marine plants. Whittaker (1972) recorded this species on the south coast of England living on sublittoral algae in salinities of 26–35 psu.

Semicytherura sp. WAGNER, 1957

Plate 7, Fig. 7.

Found in: 70, 280 cm depth in core MAR05-50P.

Morphology: Small species (~350 μm). Valves thin and weakly ornamented with very faint muri and punctae. Caudal process at mid-height. Dorsal margin arched. Ventral margin almost straight.

Distribution and ecology: Species of the genus *Semicytherura* are mainly phytal, marine, littoral and often found associated with algae.

Tyrrhenocythere amnicola donetziensis (Dubowsky, 1926)

Plate 7, Figs 8–12.

1969 *Tyrrhenocythere amnicola donetziensis* Dubowsky; Schornikov, p. 194, pl. 21, fig. 1.

1996 *Tyrrhenocythere donetziensis* (Dubowsky); Boomer et al., p. 78, fig. 2A–B, fig. 3A–H., q. v. for full synonymy.

Found in: 40, 70, 80, 150, 180, 270, 280, 300–320, 340, 360–390, 480–730 cm depth in core MAR05-50P; 20, 100, 130 cm depth in core MAR05-51G.

Morphology: Large species (800–900 μm). Carapace is rounded, subtrigonal and inflated. Sexual dimorphism is present with the male being more elongate. Marginal pore canals are conspicuously branching. Valves are very finely pitted and sometimes possess a slightly upturned caudal process. Prominent muscle scar pattern.

Distribution and ecology: This species lives in the Black, Aral and Caspian Seas (Boomer et al., 1996). It also lives in the Azov Sea (Stancheva, 1989). Schornikov (2011) found this species living in the Caspian Sea, basins of the Don River and the

Danube Delta. Schornikov (2011) also found it as a fossil in the Aral Sea, Black Sea and Aegean Sea. He commented that this species is capable of living in fresh water.

Remarks: This species exhibits a great deal of intra-specific morphological variation. A caudal process is present on some valves. Ventral margins are sinuous to varying degrees. This variation caused significant difficulty for identification. Schornikov (1969) is incorrect in not using parentheses for "Dubowsky" because the genus *Tyrrhenocythere* was not described until the 1950s (D. Horne, personal communication).

Unknown sp. 1

Plate 7, Fig. 13.

Found in: 60, 510, 520, 580, 620, 690, 720 cm depth in core MAR05-50P; 130 cm depth in core MAR05-51G.

Morphology: Medium species (500– 600 μm). Inflated, rounded, subtrigonal carapace. Valves smooth and ornamented only with widely scattered pores.

Distribution and ecology: Unknown.

Unknown sp. 2

Found in: 730 cm depth in core MAR05-50P.

Morphology: Medium (~600 μm). Elongate carapace. Valves smooth and unornamented. Small bump or ridge at posterior-ventral margin.

Distribution and ecology: Unknown.

Unknown sp. 3

Plate 7, Fig. 14.

Found in: 90 cm depth in core MAR05-50P.

Morphology: Small (~400 µm). Subquadrate carapace. Valves ornamented with large rounded fossae which are finer and shallower in the centre of the valave and get larger towards the margins. Anterior and posterior margins thick and strongly compressed.

Distribution and ecology: Unknown.

***Xestoleberis* sp. aff. *cornelii* CARAION, 1963**

Plate 7, Fig. 15.

1963 *Xestoleberis cornelii*; p. 325–329, pl. 15, fig. 3.

Found in: 10, 40, 70, 90, 120, 200, 210, 240, 280–460, 480, 500, 560, 610, 640, 660, 670 cm depth in core MAR05-50P; 80, 100, 130 cm depth in core MAR05-51G.

Morphology: Medium species (600–700 µm). Carapace rounded, subtrigonal and inflated. Dorsal margin strongly convex. Ventral margin sinuous to straight. Valves thin, smooth and ornamented only with widely scattered normal pores.

Distribution and ecology: This genus has a world-wide distribution with many similar-looking species. Most species are marine and inhabit algae in shallow water but brackish species are also known (Athersuch et al., 1989).

4.2.1. SEM Plates

Plates 1–7 contain scanning electron microscope (SEM) images of virtually every type of ostracod recovered from cores MAR05-50P and MAR05-51G. Plate 1 is intended as a guide to some key ostracod valve characteristics. All scale bars are 100 µm.
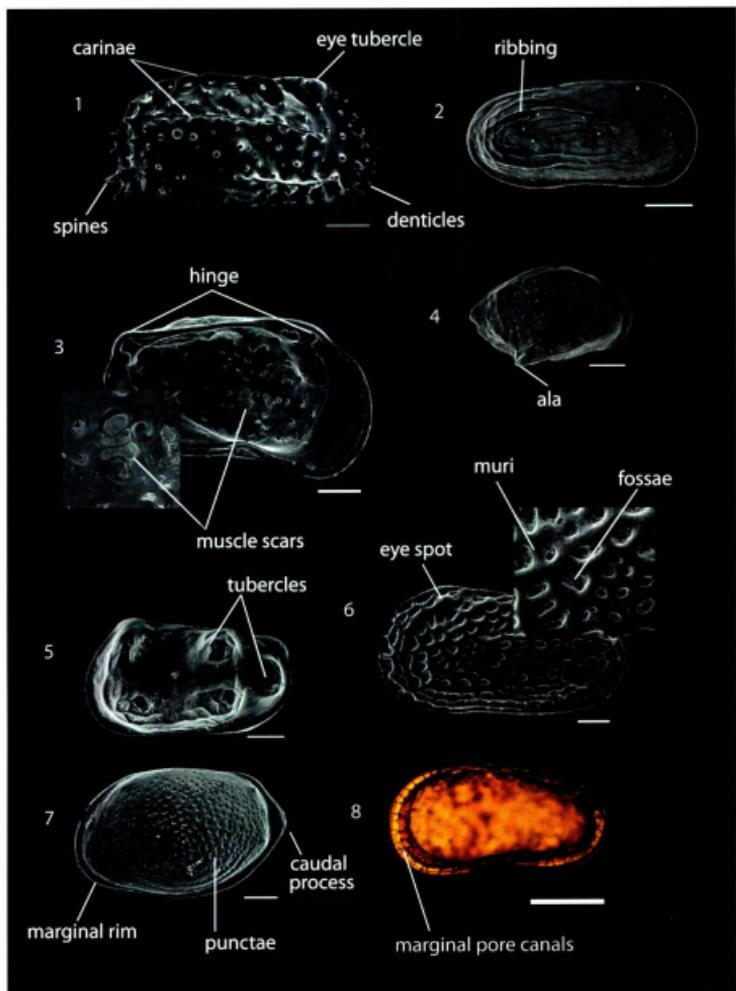
PLATE 1

Explanation of Plate 1

Fig.1 – *Carinocythereis carinata*

       Eye tubercle: A slight elevation of the carapace to cover the eye.

       Carina: A longitudinal ridge on the valve.

       Denticle: A small spine-like projection on the valve.

       Spine: A long pointed projection on the valve.

Fig. 2 – *Amnicythere striatocostata*

       Ribbing: Raised, mainly longitudinal, "lines" on the valve. There may be only one or several concentric ribs.

Fig. 3 – C*allistocythere diffusa*

       Hinge: Dorsal feature; interlocking grooves and sockets join the two valves together to form a carapace. Hinge type is useful for taxonomy.

       Muscle scars: Scars left from where the muscles of the living ostracod were attached to the valve. Muscle scar patterns are distinct and thus useful for taxonomy.

Fig. 4 – *Cytheropteron* sp. aff*. inornatum*

       Ala: A pointed, wing-like projection.

Fig. 5 – *Amnicythere quinquetuberculata*

       Tubercle: A raised, rounded protuberance on the valve surface.

Fig. 6 – *Hiltermannicythere rubra*

       Fossae (*pl.*): Relatively large depressions or pits; sometimes reticulated.

       Muri (*pl.*): Wall-like structures surrounding the fossae.

       Eye spot: A "spot" on the anteriodorsal area of the valve accommodating the eye.

Fig. 7 – *Palmoconcha agilis*

Marginal rim: The outermost area or edge of the valve.

Punctae (*pl.*): Small pits on the valve.

Caudal process: A projection at the posterior of the valve.

Fig. 8 – *Amnicythere cymbula* (in transmitted light)

Marginal pore canals: Nerve-bearing canals. These have a distinct character (i.e., few, many, straight, curved, simple, bifurcated, branching, etc.) and are useful for identification.
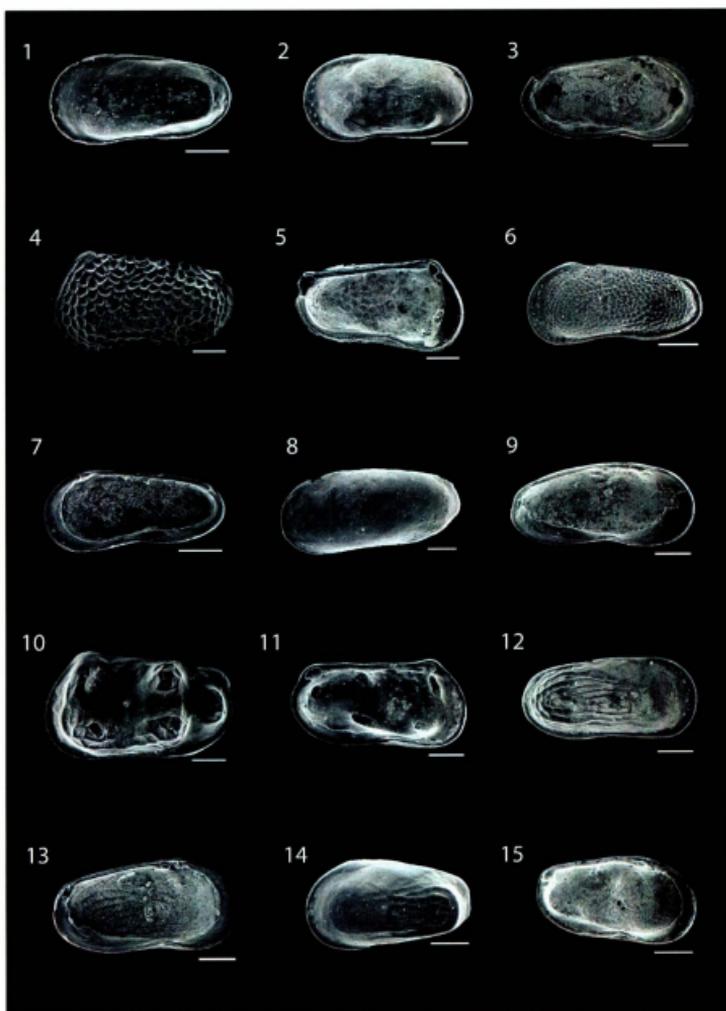
PLATE 2

Explanation of Plate 2

Fig. 1 – *Amnicythere caspia*, left valve, external.

Fig. 2 – *Amnicythere cymbula*, left valve, external.

Fig. 3 – *Amnicythere cymbula*, left valve, internal.

Fig. 4 – *Amnicythere olivia*, left valve, external.

Fig. 5 – *Amnicythere olivia*, left valve, internal.

Fig. 6 – *Amnicythere pediformis*, left valve, external.

Fig. 7 – *Amnicythere pediformis*, right valve, internal.

Fig. 8 – *Amnicythere propinqua*, left valve, external

Fig. 9 – *Amnicythere propinqua*, left valve, internal.

Fig. 10 – *Amnicythere quinquetuberculata*, female, left valve, external.

Fig. 11 – *Amnicythere quinquetuberculata*, male, left valve, internal.

Fig. 12 – *Amnicythere striatocostata*, right valve, external.

Fig. 13 – *Amnicythere striatocostata*, left valve, internal.

Fig. 14 – *Amnicythere subcaspia*, left valve, external.

Fig. 15 – *Amnicythere subcaspia*, left valve, internal.
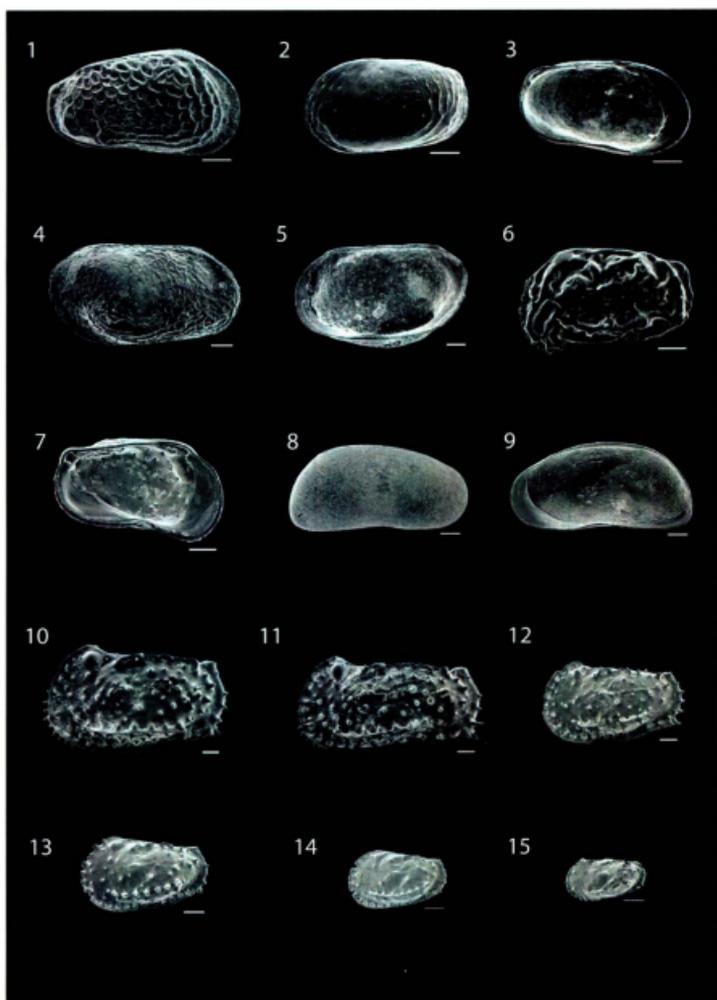
PLATE 3

Explanation of Plate 3

Fig. 1 – *Amnicythere volgensis*, right valve, external.

Fig. 2 – *Buntonia subulata rectangularis*, left valve, external.

Fig. 3 – *Buntonia subulata rectangularis*, left valve, internal.

Fig. 4 – *Bythocythere* sp., right valve, external.

Fig. 5 – *Bythocythere* sp., right valve, internal.

Fig. 6 – *Callistocythere diffusa*, left valve, external.

Fig. 7 – *Callistocythere diffusa*, left valve, internal.

Fig. 8 – *Candona schweyeri*, right valve, external.

Fig. 9 – *Candona schweyeri*, right valve, internal.

Fig. 10 – *Carinocythereis carinata*, female, left valve, external.

Fig. 11 – *Carinocythereis carinata*, male, left valve, external.

Fig. 12 – *Carinocythereis carinata*, juvenile (A-1), left valve, external.

Fig. 13 – *Carinocythereis carinata*, juvenile (A-2), left valve, external.

Fig. 14 – *Carinocythereis carinata*, juvenile (A-3), left valve, external.

Fig. 15 – *Carinocythereis carinata*, juvenile (A-4), left valve, external.
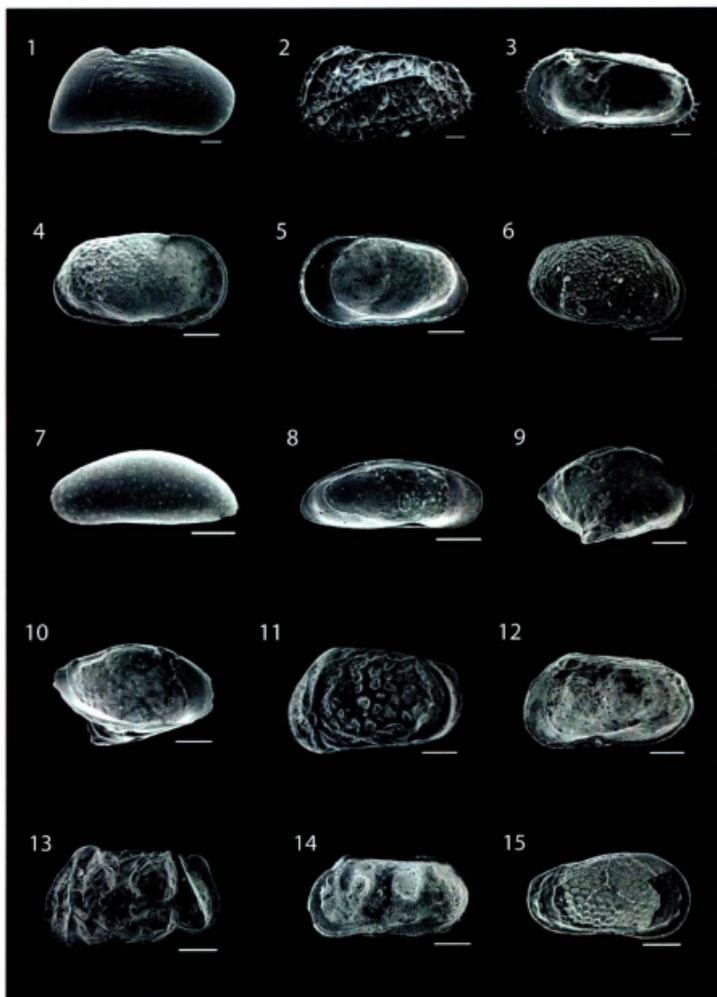
PLATE 4

Explanation of Plate 4

Fig. 1 – *Caspiella acronasuta*, right valve, external.

Fig. 2 – *Costa edwardsi*, female, left valve, external.

Fig. 3 – *Costa edwardsi*, male, right valve, internal.

Fig. 4 – *Cuneocythere semipunctata*, right valve, external.

Fig. 5 – *Cuneocythere semipunctata*, right valve, internal.

Fig. 6 – *Cytheromorpha* sp. aff. *fuscata*, female, right valve, external.

Fig. 7 – *Cytheroma variabilis*, left valve, external.

Fig. 8 – *Cytheroma variabilis*, left valve, internal.

Fig. 9 – *Cytheropteron* sp., right valve, external.

Fig. 10 – *Cytheropteron* sp., left valve, internal.

Fig. 11 – *Euxinocythere* (*Maetocythere*) *lopatici*, left valve, external.

Fig. 12 – *Euxinocythere* (*Maetocythere*) *lopatici*, right valve, internal.

Fig. 13 – *Euxincythere bacuana*, female, left valve, external.

Fig. 14 – *Euxincythere bacuana*, right valve, external.

Fig. 15 – *Euxincythere* sp. aff. *relicta*, right valve, external.

PLATE 5

93
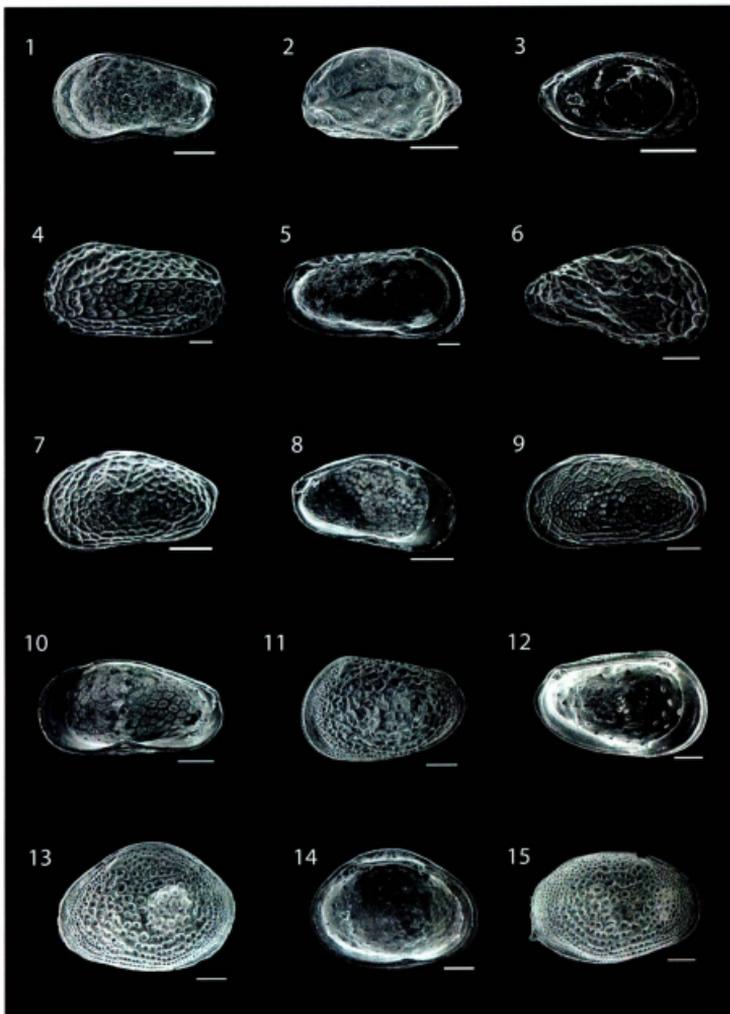
Explanation of Plate 5

Fig. 1 – *Euxincythere* sp. aff. *relicta*, right valve, internal.

Fig. 2 – *Hemicytherura* sp., left valve, external.

Fig. 3 – *Hemicytherura* sp., left valve, internal.

Fig. 4 – *Hiltermannicythere rubra*, left valve, external.

Fig. 5 – *Hiltermannicythere rubra*, left valve, internal.

Fig. 6 – *Hiltermannicythere rubra*, right valve, external, deformed.

Fig. 7 – *Leptocythere devexa*, left valve, external.

Fig. 8 – *Leptocythere devexa*, left valve, internal.

Fig. 9 – *Leptocythere multipunctata*, left valve, external.

Fig. 10 – *Leptocythere multipunctata*, right valve, internal.

Fig. 11 – *Loxoconcha immodulata*, left valve, external.

Fig. 12 – *Loxoconcha immodulata*, left valve, internal.

Fig. 13 – *Loxoconcha lepida*, female, left valve, external.

Fig. 14 – *Loxoconcha lepida*, female, left valve, internal.

Fig. 15 – *Loxoconcha lepida*, male, right valve, external.
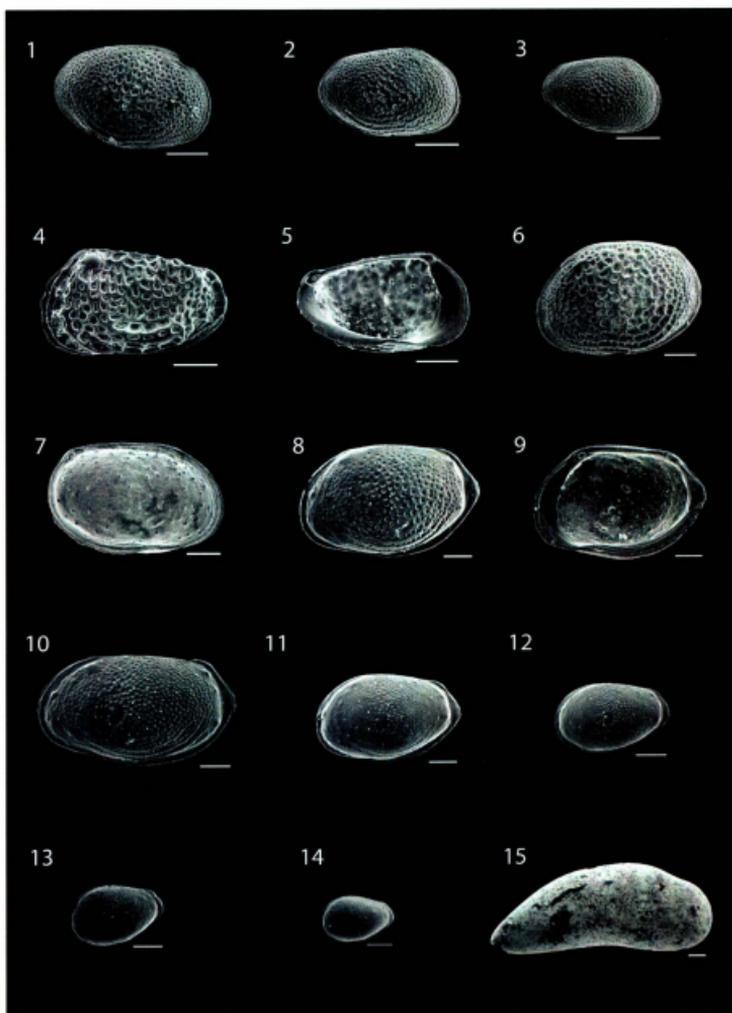
PLATE 6

Explanation of Plate 6

Fig. 1 – *Loxoconcha* spp. juvenile, possibly A-2, right valve, external.

Fig. 2 – *Loxoconcha* spp. juvenile, possibly A-3, right valve, external.

Fig. 3 – *Loxoconcha* spp. juvenile, possibly A-4, right valve, external.

Fig. 4 – *Loxoconcha littoralis*, female, left valve, external.

Fig. 5 – *Loxoconcha littoralis*, female, left valve, internal.

Fig. 6 – *Loxoconcha sublepida*, left valve, external.

Fig. 7 – *Loxoconcha sublepida*, left valve, internal.

Fig. 8 – *Palmoconcha agilis*, female, left valve, external.

Fig. 9 – *Palmoconcha agilis*, female, right valve, internal.

Fig. 10 – *Palmoconcha agilis*, male, left valve, external.

Fig. 11 – *Palmoconcha agilis*, juvenile (A-1), left valve, external.

Fig. 12 – *Palmoconcha agilis*, juvenile (A-2), left valve, external.

Fig. 13 – *Palmoconcha agilis*, juvenile (A-3), left valve, external.

Fig. 14 – *Palmoconcha agilis*, juvenile (A-4), left valve, external.

Fig. 15 – *Paracypris polita*, right valve, external.
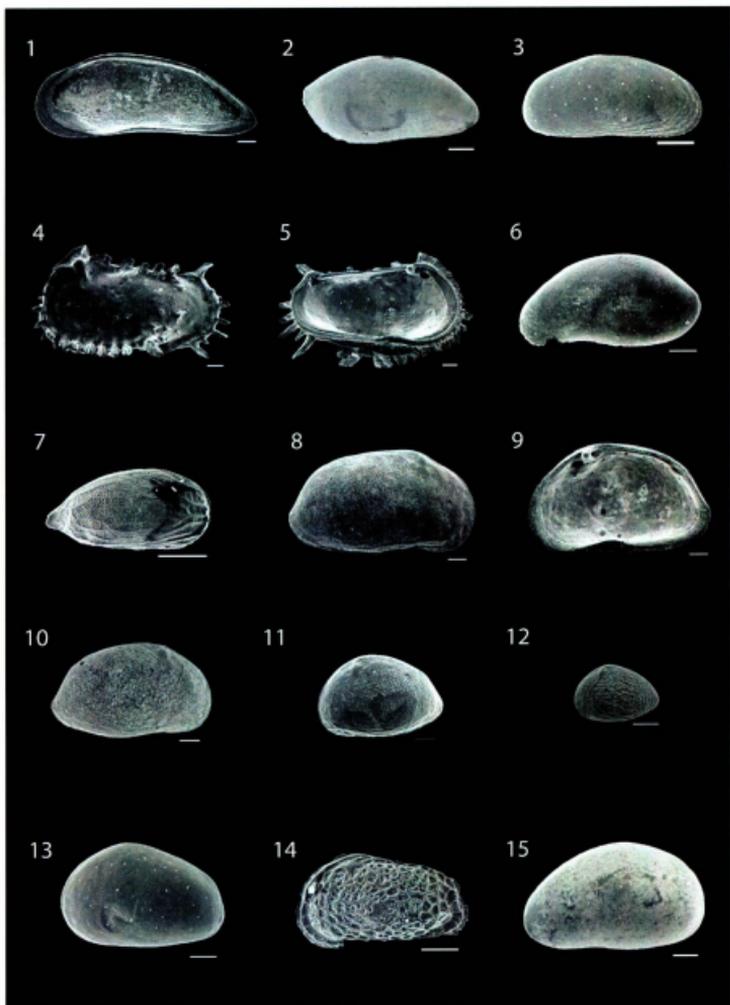
PLATE 7

Explanation of Plate 7

Fig. 1 – *Paracypris polita*, right valve, internal.

Fig. 2 – *Paradoxostoma simile*, right valve, external.

Fig. 3 – *Pontocythere* sp., right valve, external.

Fig. 4 – *Pterygocythereis jonesii*, left valve, external.

Fig. 5 – *Pterygocythereis jonesii*, left valve, internal.

Fig. 6 – *Sclerochilus gewemuelleri*, left valve, external.

Fig. 7 – *Semicytherura* sp., probably juvenile (A-1), right valve, external.

Fig. 8 – *Tyrrhenocythere amnicola donetziensis*, male, right valve, external.

Fig. 9 – *Tyrrhenocythere amnicola donetziensis*, female, right valve, external.

Fig. 10 – *Tyrrhenocythere amnicola donetziensis*, juvenile (A-1), right valve, external.

Fig. 11 – *Tyrrhenocythere amnicola donetziensis*, juvenile (A-2), left valve, external.

Fig. 12 – *Tyrrhenocythere amnicola donetziensis*, juvenile (A-4), left valve, external.

Fig. 13 – Unknown sp. 1, left valve, external.

Fig. 14 – Unknown sp. 3, left valve, external.

Fig. 15 – *Xestoleberis* sp. aff. *cornelii*, left valve, external.

CHAPTER 5

RESULTS

The results in this chapter are presented with respect to depth in composite core MAR05-50. In later chapters these results are discussed with respect to calendar years BP. The original data are given in Appendix A.

Distinct changes are evident in the ostracod assemblages of core MAR05-50 (Fig. 5.1). From the base of the core at 780 cm depth to 630 cm depth in the core the assemblage is dominated by ostracods commonly found in the present-day brackish waters of the Ponto-Caspian basins (e.g., Schornikov, 1969; Opreanu, 2008; Boomer et al., 2010). From 620 cm to 540 cm depth in the core there is an interval characterized by occurrences of more or less equal proportions of Ponto-Caspian species and species which are commonly found in the more saline waters of the Mediterranean Sea (Fig. 5.1; e.g., Athersuch et al., 1989; Bonaduce et al., 1975). At 530 cm depth in the core the assemblage becomes essentially fully Mediterranean and remains so to the top of the core. For the purposes of further discussion these three distinct assemblages will herein be referred to as the "brackish", "transitional" and "marine" assemblages or sections respectively.

5.1. General Sample Description

In addition to abundant ostracods, the samples from core MAR05-50 also contain the remains of various other calcareous organisms. Benthic foraminifera, bivalves and gastropods are common throughout the core. The abundances of these calcareous remains fluctuates a lot with no noticeable trend. Some samples have essentially
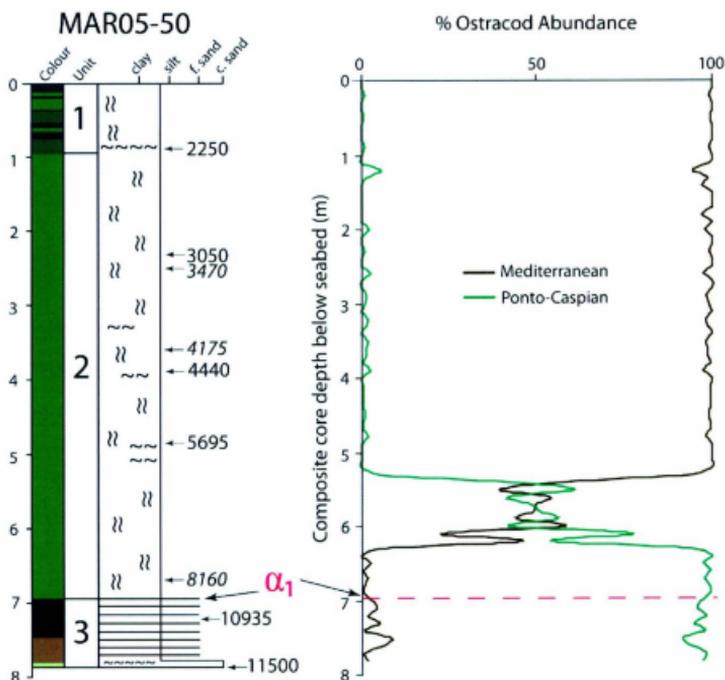
Figure 5.1. A graph of ostracod % abundance of Mediterranean vs. Ponto-Caspian species as it changes with depth alongside an illustration of composite core MAR05-50. The % abundance graph clearly shows a turnover from a Ponto-Caspian (brackish) to a Mediterranean (marine) ostracod assemblage beginning at 620 cm depth in composite core MAR05-50 and becoming essentially fully marine from 540 cm upward. The level of unconformity surface α₁ is shown. Vertical wavy lines indicate moderate bioturbation. Horizontal wavy lines indicate shelly horizons. See Chapter 3 for core unit descriptions. (core log modified from Linegar, 2012).

none of these while some of the samples are full of large shells and shell fragments. In the lowest ~80 cm as well as 370–390 cm and 510 cm depth in core MAR05-50 shells from gastropods and bivalves are particularly abundant.

5.2. Ostracod Abundance in Core MAR05-50

Ostracods are very abundant and well-preserved throughout core MAR05-50 (Fig. 5.2). Throughout the core small amounts of pyrite are precipitated on or inside the valves. The lowest concentration is 0.2 valves per gram of dry sediment and the highest concentration is 60.8 valves per gram of dry sediment. The average ostracod concentration in the core is 7.7 valves per gram of dry sediment (Fig. 5.2). The brackish assemblage of the core (780–630 cm) has an average concentration of 5.0 valves per gram of dry sediment. The transitional assemblage (620–540 cm) has an average concentration of 4.5 valves per gram. The marine assemblage (530–0 cm) has an average concentration of 8.9 valves per gram (Fig. 5.2).

5.3. Ostracod Diversity

The core shows a high species diversity overall with a total of 45 individual ostracod species being found (Fig. 5.2). The average number of individual species found in each sample throughout the entire core MAR05-50 is 10.3. The pattern of diversity fluctuations generally matches the pattern of concentration fluctuations (Fig. 5.2).

In the brackish assemblage the average number of species is 12.6. The highest diversity in this assemblage occurs at 670 cm with 18 species represented. The lowest diversity is at 760 cm with only 8 species found (Fig. 5.1).

The transitional assemblage has a similar average diversity to the brackish
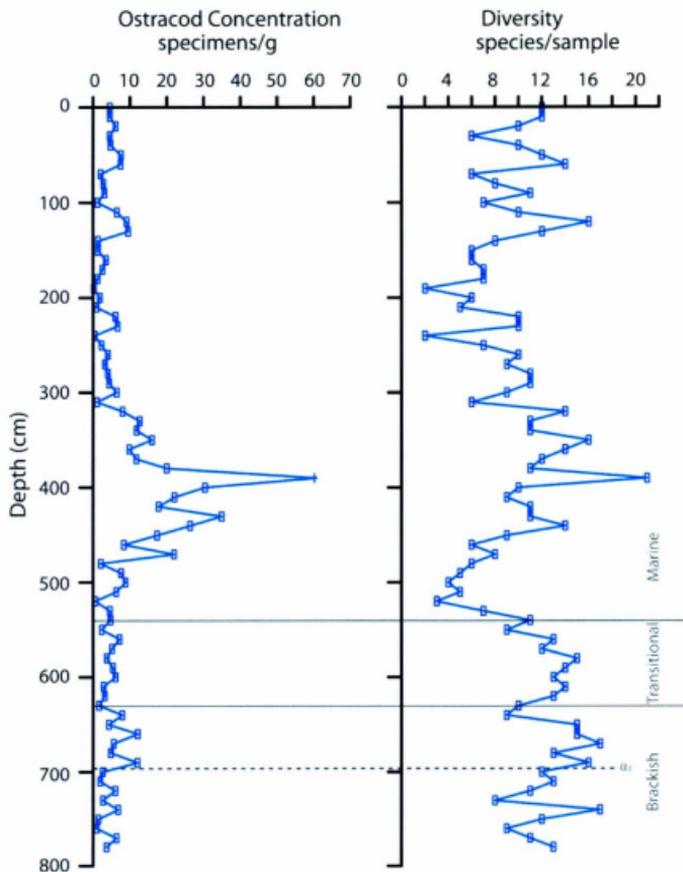
Figure 5.2. Ostracod concentration (valves per gram of dry sediment) and diversity (number of species) fluctuate throughout core MAR05-50. The graph shows a trend of diversity and concentration generally increasing and decreasing together. Both show a general increase around 4 m depth with a maximum spike at 390 cm depth.

assemblage with an average of 12.7 species in each sample. In this interval where Ponto-Caspian and Mediterranean species co-occur, the diversity initially increases slightly from 13 species to a maximum of 15 species at 580 cm. Then the diversity gradually declines upwards to 11 species by 540 cm depth, the end of the transitional section (Fig. 5.2).

The onset of the marine assemblage at 530 cm is characterized by low species diversity (Fig. 5.2). Until 450 cm depth in the core the average number of species per sample is 5.9 and almost always includes *Palmoconcha agilis*, *Carinocythereis carinata*, *Hiltermannicythere rubra* and *Xestoleberis* sp. aff. *cornelii*. Directly following this interval upcore, the diversity nearly doubles and reaches a maximum of 21 species at 390 cm depth in the core (Fig. 5.1). This is also the maximum diversity for the entire core. This sample at 390 cm also shows the highest concentration. Nine of the 21 species found in this sample are Ponto-Caspian types. However, considering the high numbers of the marine ostracod valves, the sample is considered to be 97.7 % marine.

After reaching a maximum diversity at 390 cm depth in the core the number of species decreases upcore, fluctuating between 2 and 16 species. The minimum diversity for the entire core occurs at both 240 and 190 cm depth in the core.

5.4. Whole Carapaces versus Valves

Workers often use this information to comment on the changing energy of the environment or possible *post-mortem* reworking within a sequence (Boomer et al., 2003). For example, an increase in the number of broken or disarticulated valves might indicate a higher energy environment.

However, the information that is gained from counting whole carapaces versus

disarticulated valves is limited and must be treated with caution. Ostracod valves and hinges are fragile and can easily be broken during processing and picking. This frailty is largely a function of the carapace morphology of individual species. Therefore, the final state of the valves is not necessarily a true reflection of the *in situ* state of the valves before sample processing (De Deckker, 2002). Boomer et al. (2003) indicated that carapace to valve ratios should really only be used to compare changes within a species or closely related taxa within the a sequence.

In the case of core MAR05-50 disarticulated valves constitute an average of 96 % of all samples. The highest occurrence of intact carapaces is at 480 cm depth with 90 % valves and 10 % carapaces.

5.5. Valve Coloration

Color changes are noticeable moving upward in core MAR05-50. In the lower brackish section of the core the adult specimens of *Loxoconcha sublepida* are mainly opaque chalky white to translucent white or clear in appearance. The adult specimens of *Loxoconcha lepida* are mainly grey and very chalky looking. The opaque chalky appearance is caused by dissolution of the calcite valve when deposited in eutrophic, organic rich sediment and subsequent pyrite formation on the valve which may later become oxidized to H_2SO_4 resulting in slight to total dissolution (De Deckker, 2002). The *Loxoconcha* juveniles are usually opaque white or translucent but are not chalky in appearance. It is very apparent that the valves of *Tyrrhenocythere amnicola donetziensis* are almost always very dark grey, sometimes translucent and sometimes very chalky grey to white and opaque.

Beginning around 470 cm depth in the core there are higher numbers of grey colored ostracod valves. Valves become grey or brown when in contact with anoxic sediments (De Deckker, 2002). Then, at 340 cm depth in the core there seems to be fewer grey valves again; here most valves are opaque white and a few are translucent white in appearance. In the transitional assemblage the Mediterranean species *Loxoconcha littoralis* is mainly translucent clear to translucent white and *T. amnicola donetziensis* is grey and often chalky as is found in the brackish assemblage. In the marine section of core MAR05-50 the valves are mainly opaque translucent white. Occasionally a few orange or brownish colored valves also occur. Most notably these colored valves are often the Mediterranean species *Costa edwardsi* and *Carinocythereis carinata*.

5.6. Upcore Changes in Ostracod Assemblages

There is a major turnover in ostracod assemblages in core MAR05-50 (Fig. 5.1). In this section upcore changes involving key ostracod species are described in detail. Key species are considered to be those which are consistently abundant, occur in most samples and are represented by both adults and several stages of juveniles (see below). They can therefore be assumed to have lived and died at the core site, as opposed to having been reworked or transported to the site, and are therefore reliable for reconstructing ecological changes in the study area (see Chapter 6).

5.6.1. Population Age Diagrams

Population age diagrams (Fig. 5.3a, b) are useful when using ostracods to interpret paleoenvironments (Boomer et al., 2003; De Deckker, 2002). Ostracods have nine growth stages (Athersuch et al., 1989). The adult is known as stage A. The penultimate
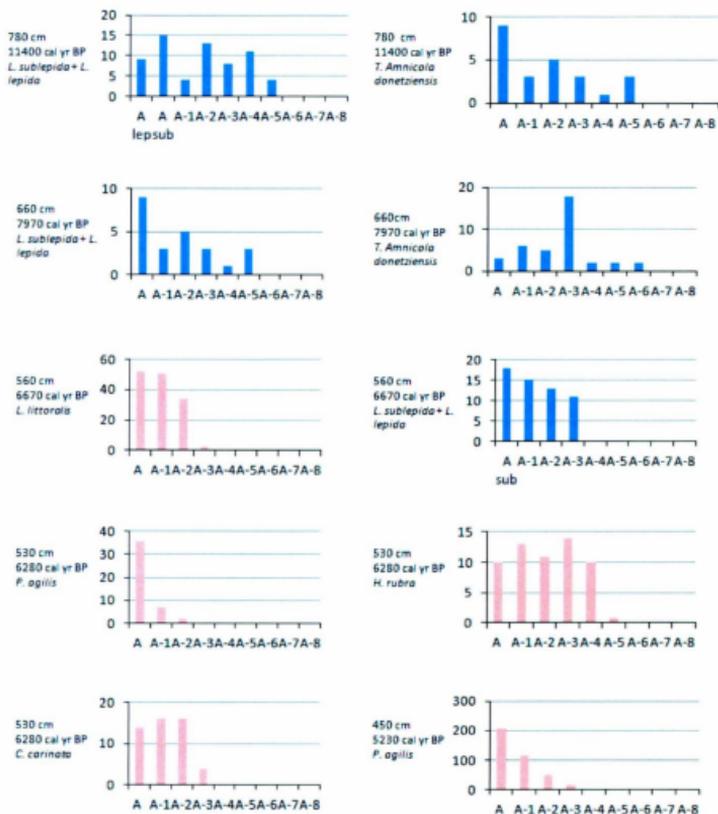
Figure 5.3a. Population age diagrams for key species from irregularly spaced depths throughout core MAR05-50. The presence of adults (A) and various juveniles (A-1 to A-6) confirms an autochthonous assemblage on which an environmental interpretation can be based. Blue bars indicate brackish species and pink indicate marine species. Note: The population age diagrams for *L. lepida* + *L. sublepida* show two separate A stages ("sub" and "lep"). These species were counted in the same diagram because their juveniles could not be distinguished.

106
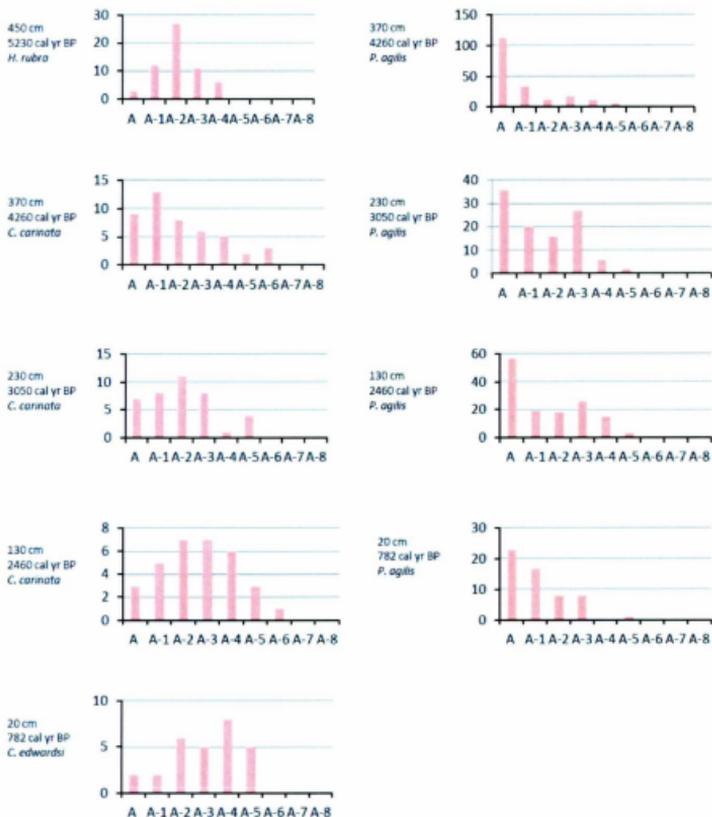
Figure 5.3b. Population age diagrams continued. These diagrams clearly show that these species were well represented by both adults and various juvenile stages and are therefore autochthonous and can be used for paleoenvironmental interpretation.

instar stage is known as A-1 (read as "A minus 1") and so on to A-8. By plotting how many valves of a particular species are present, from A down to the smallest juveniles an assessment of the type of environment can be made (Boomer et al., 2003).

An ostracod population which contains adults and all instar stages down to the earliest juveniles (smaller than A-4) can be said to represent a low-energy autochthonous assemblage (Boomer et al., 2003). If the smaller juveniles are missing, then the assemblage can be said to be a moderate-energy autochthonous assemblage because the tiniest valves have been removed by water currents. An assemblage which contains only adults and the largest juveniles (A-1 and A-2 possibly) is considered to be a high-energy autochthonous assemblage because strong water currents carried away the medium and small juvenile valves (Boomer et al., 2003).

Finally, an assemblage of juveniles without adults is probably not autochthonous. These small valves may have been transported to the area by moving water. Another alternative is that something, such as a sudden environmental change, prevented the juveniles from reaching adulthood (De Deckker, 2002). The population age diagrams for core MAR05-50 show that the autochthonous assemblage changed from brackish species to marine species going upward in the core. The presence of various stages of juveniles in most samples probably indicates a low to moderate energy system.

5.6.2. Brackish (Ponto-Caspian) Assemblage (780–630 cm)

The samples from 780–630 cm depth in core MAR05-50 contain on average 96.9 % specimens commonly found in brackish waters of the Ponto-Caspian basins (Fig. 5.1; e.g., Schornikov, 1969; Opreanu, 2008; Boomer et al., 2010). The brackish assemblage is

clearly dominated by *L. sublepida* and *L. lepida* (Fig. 5.4). In this interval, valves of *L. sublepida and L. lepida* together make up an average of 63.5 % of each sample, with a maximum abundance of 81.5 % at 660 cm. From 620 cm to 540 cm depth in the core this average drops to 33.3 % as *L. sublepida and L. lepida* co-exist with the Mediterranean species *Loxoconcha littoralis* (Fig. 5.4). In the brackish section of core MAR05-50 *L. littoralis* occurs in only 9 out of the 16 samples and has an average abundance of less than 2 %.

Other significant species in the lower, brackish assemblage are *Tyrrhenocythere amnicola donetziensis* (averaging 11.2 % of each sample), *Amnicythere olivia* (5.4 %), *Candona schweyeri* (4.9 %) and *Amnicythere quinquetuberculata* (4.3 %; Fig. 5.4). Other species commonly appearing in the brackish assemblage but in low abundances are *Amnicythere bacuana*, *Amnicythere pediformis, Amnicythere subcaspia*, *Amnicythere striatocostata*, *Amnicythere cymbula*, *Euxinocythere relicta*, and *Loxoconcha immodulata*. These species appear somewhat sporadically and when present typically account for less than 2 % of a given sample. The marine species *Palmoconcha agilis* is present at most depths in the brackish section but in extremely low abundances, typically only one or two valves.

5.6.3. Ostracod Variation Below and Above Unconformity α₁

The unconformity α₁ occurs at a core depth of 695 cm in composite core MAR05-50 (Fig. 5.1). It spans from ~10700 to 8400 cal yr BP (see Chapter 3). This unconformity occurs within the brackish section of core MAR05-50 (Fig. 5.1). The changes in the ostracod assemblage before and after this ~2300 year hiatus are not very

109
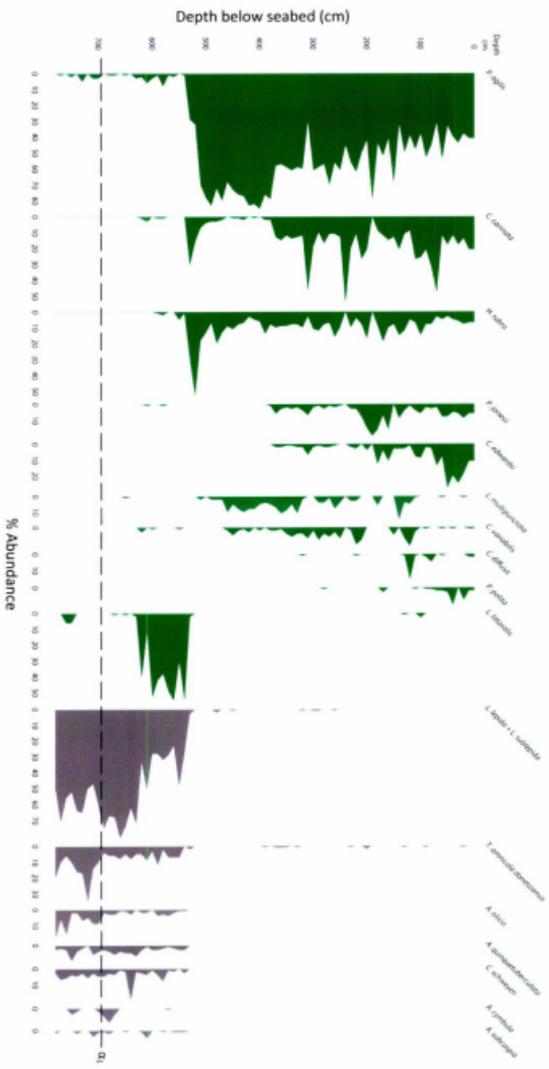
Figure 5.4. Percent abundances (for key Mediterranean (green) and Ponto-Caspian (grey) ostracod species illustrate the upcore species changes in core MAR05-50.

noticeable in core MAR05-50 but some changes do occur. For example, *L. sublepida* and *L. lepida* together increase from 55.6 to 70.0 % from 730–700 cm depth (200 years preceding the hiatus, see Chapter 4) to 690–670 cm depth in the core (250 years after the hiatus; Fig. 5.4). Other changes over the same interval involve *T. amnicola donetziensis* which decreases from 18.9 to 5.6 % and *A. olivia* which decreases from 7.4 to 2.6 % in abundance (Fig. 5.4). The average number of species present at 730–700 cm depth is 11.0 and increases to 15.3 for 690–670 cm depth. The concentration also increases from 3.3 to 7.4 valves per gram of dry sediment when comparing the same intervals (Fig. 5.2).

5.6.4. Transitional Assemblage (620–540 cm)

Between 620 cm and 540 cm depth in core MAR05-50 there is an interval where brackish and marine ostracod species co-occur (Fig. 5.1; Fig. 5.4). From the base of the core to 630 cm depth, the ostracods have brackish water affinities and the assemblage is dominated by *L. sublepida* and *L. lepida*. There is a major change in the assemblage at 620 cm depth in the core. At this depth the Mediterranean species *L. littoralis* abruptly becomes the most abundant species. Its valves constitute 40.6 % of the sample at this depth (Fig. 5.4). This is a dramatic increase from the sample directly below at 630 cm depth in which this species comprises only 1.7 % of the specimens in that sample. *L. littoralis* maintains an average of 41.6 % abundance in the transitional assemblage from 620 cm to 540 cm depth in the core, making it the dominant species in this assemblage.

Brackish water species remain abundant in the transitional section (Fig. 5.4). *L. sublepida* and *L. lepida*, which had been the dominant species in the brackish assemblage, become the second most abundant species in the transitional assemblage with an average

abundance of 33.3 % (Fig. 5.4). Likewise, *T. amnicola donetziensis*, which had been the second most abundant species in the brackish section, is still present in the transitional assemblage but its average abundance decreases from 11.2 to 5.8 %, now making it the third most abundant species.

During this interval where brackish and marine species co-occur, the number of brackish species is still greater than the number of marine species. However, given the high number of specimens of the Mediterranean species *L. littoralis*, the average ratio of marine to brackish specimens is calculated to be 60:40 in the transitional section.

In the earliest stages of the transitional section the Mediterranean species *Carinocythereis carinata*, *Hiltermannicythere rubra* and *Cytheroma variabilis* first appear in significant numbers in the southwestern Black Sea study area. The marine species *Palmoconcha agilis*, which is also present in the brackish section, increases from 1.3 to 2.7 % average abundance in the transitional assemblage.

5.6.5. Marine (Mediterranean) Assemblage (530–0 cm)

At 530 cm depth in core MAR05-50 another striking change occurs in the ostracod assemblage (Fig. 5.1; Fig. 5.3). The Mediterranean species *L. littoralis* decreases dramatically from 55.4 % abundance at 540 cm depth to only 2.5 % at 530 cm depth (Fig. 5.4). At the same sample depths the Ponto-Caspian species *L. sublepida* and *L. lepida* together decreases from 28.4 to a mere 3.1 %.

All of the Ponto-Caspian species are replaced immediately and unequivocally by the Mediterranean ostracods *P. agilis*, *H. rubra*, and *C. carinata* together constituting 89.4 % of the sample from 530 cm depth in core MAR05-50 (Fig. 5.4). Together with

112

other marine ostracods, these marine species dominate the ostracod assemblage from that point upward to the top of the core. In this section of core MAR05-50 the samples consist on average of 99.2 % valves from marine species (Fig. 5.1).

   L. littoralis all but disappeared in the marine assemblage, occurring only a few times represented by a valve or two (Fig. 5.4). *L. sublepida* and *L. lepida* do occur often in the marine assemblage but in extremely low abundances (< 1 % of the sample) and mainly below a depth of 250 cm (Fig. 5.4). *T. amnicola donetziensis* also occurs in the marine assemblage in abundances typically 1 % or less and most frequently between the depths 440 cm and 320 cm (Fig. 5.4).

   By far, the most abundant species in the entire marine assemblage is the Mediterranean species *P. agilis* (Fig. 5.4). Valves of this species make up an average of 56.6 % of each sample in this section of core MAR05-50. *P. agilis* is also the most frequently occurring species throughout the entire core. It was found in 83 of the original 89 samples albeit in extremely low abundances in the brackish section.

   The other significant species present in the marine assemblage of core MAR05-50 are *C. carinata*, *H. rubra*, *C. edwardsi* and *P. jonesii*. Notable changes occur within this section involving the relative abundances of these species.

5.6.6. Notable Upward Changes in Key Marine Species

   C. carinata does not occur in core MAR05-50 until the transitional section begins at 620 cm depth, except for one juvenile valve at 720 cm depth in the core (Fig. 5.4). Within the transitional section, from 620 cm to 580 cm depth, *C. carinata* appears in low abundances (average 1.1 %). It then disappears and does not appear again until 530 cm

113

depth when the marine assemblage begins to dominate. At 530 cm depth in the core *C. carinata* suddenly becomes very abundant making up 31.1 % of that sample. It then gradually decreases to 1.8 % by 380 cm depth. At 370 cm depth it increases again and maintains an average of 13.1 % abundance until 310 cm depth when its abundance spikes to 47.7 %. Thereafter, its abundance fluctuates significantly and the average abundance is 19.4% until the top of core MAR05-50 (Fig. 5.4).

H. rubra does not appear in core MAR05-50 before the transitional section except for one deformed valve (Plate 5, Fig. 6) from 780 cm depth. In the transitional section it occurs between 590 cm and 540 cm depth with maximum abundance at 550 cm of 5.4 %. When the marine section begins at 530 cm depth *H. rubra* increases immediately to 29.8 % (Fig. 5.4). *H. rubra* continues to be a significant marine species, constituting an average of 10.2 % of the marine assemblage until the top of core MAR05-50.

P. jonesii is represented by a single valve in two samples at 610 and 580 cm depth within the transitional assemblage. Apart from this, *P. jonesii* and *C. edwardsi* both begin to occur from 380 cm upward and thereafter have average abundances of 5.4 and 5.8 % respectively (Fig. 5.4). There are considerable fluctuations in these abundances but overall they increase going upward in the core. For example, *C. edwardsi* reaches a maximum abundance of 27.7 % at 50 cm and yet in several samples in the marine section it does not appear at all. *C. edwardsi* is more abundant towards the top of the core. Considering only the top 70 cm its abundance is 16.8 %. *P. jonesii* does not deviate from its average abundance as much as *C. edwardsi* but it also generally increases in the uppermost part of core MAR05-50.

Other marine species frequently appearing in core MAR05-50 are *Paracypris*

polita, *Leptocythere multipunctata*, *Callistocythere diffusa*, *Cytheroma variabilis*, *Bythocythere* sp. and *Xestoleberis* sp. aff. *cornelii* (Fig. 5.4). *X.* sp. aff. *cornelii* appears frequently but sporadically throughout core MAR05-50 between 720 cm and 60 cm depth and consistently appears between 510 cm and 330 cm depth with a maximum of 5.5 % abundance at 490 cm depth in the core.

5.7. Statistical Results

Cluster analysis and factor analysis were run on the ostracod data in both depth and age (calendar years) domains. In this chapter only the results involving data in the depth domain (with less abundant species not exceeding 5% of the sum at any level removed) are presented. In Chapter 6 the data is interpreted with respect to calendar years.

5.7.1. Cluster Analysis

Figure 5.5 shows the results of CONISS run only on dominant species in the depth domain with less abundant species not exceeding 5% of the sum at any level removed. The CONISS dendrogram clearly shows several well-defined clusters. The interpretation of the clusters results is discussed in Chapter 6.

5.7.2. Factor Analysis

5.7.2.1. R-factor Analysis

Factor analysis first produced a correlation coefficient matrix (Table 5.1). In the correlation coefficient matrix the value at the intersection of a row and column gives the degree of correlation between the two species, 0.99 being a strong correlation, zero
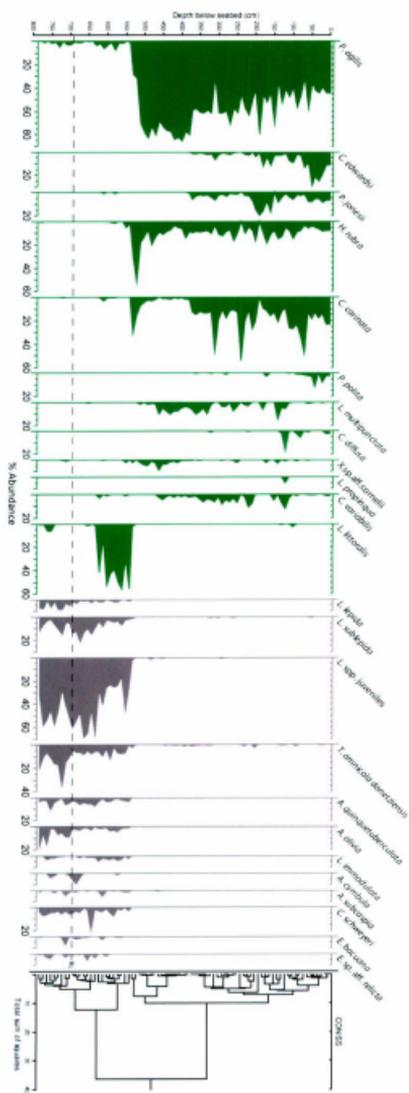
Figure 5.5. % abundance of Mediterranean (green) and Ponto-Caspian (grey) ostracod species with the CONISS dendrogram (clusters) to the right.

116

Table 5.1. The correlation-coefficient matrix produced by R-mode factor analysis shows the correlation or relatedness of 25 of the main species in core MAR05-50.   A closer the correlation coefficient is to 0.99, the stronger the correlation between the species. Inversely, the closer the correlation coefficient is to -0.99, the more negative the correlation between two species. The closer the correlation coefficient is to 0, both positive and negative correlations become weaker.

	P. agilis	C. carinata	H. rurba	P. jonesii	C. edwardsi	P. polita	L. multipunctata	X. diffusa	X. sp. aff. cornelii	C. variabilis	A. propinqua	L. littoralis	Pontocythere sp.	L. lepida	L. sublepida	L. spp. juveniles	T. amnicola donetziensis	A. quinquetuberculata	A. olivia	A. immodulata	A. cymbula	A. subcaspia	C. schweyeri	A. bacuana	E. sp. M. relita
P. agilis	**0.99**	0.24	0.59	0.16	0.09	0.04	0.33	0.09	0.41	0.37	-0.14	-0.41	0.01	0.52	0.68	0.76	-0.68	0.71	0.55	0.58	-0.34	0.46	0.44	0.44	0.44
C. carinata	0.24	**0.99**	0.4	0.51	0.49	0.28	-0.09	0.35	-0.13	0.27	-0.1	-0.26	0	-0.35	-0.44	-0.5	-0.43	-0.47	-0.37	-0.38	-0.22	-0.31	-0.45	-0.28	-0.29
H. rurba	0.59	0.4	**0.99**	0.32	0.13	0.08	0.26	0.07	0.43	0.17	-0.09	-0.3	-0.03	-0.43	0.53	-0.6	-0.51	-0.56	-0.55	-0.4	-0.33	-0.56	-0.36	-0.36	-0.36
P. jonesii	0.16	0.51	0.32	**0.99**	0.34	-0.05	0.13	-0.17	0.06	-0.07	-0.2	-0.2	0.23	-0.26	-0.29	-0.17	-0.23	-0.14	-0.17	-0.23	-0.21	-0.21	-0.21	-0.21	-0.21
C. edwardsi	0.09	0.49	0.13	0.6	**0.99**	0.45	-0.14	0.15	-0.22	-0.06	-0.06	-0.17	-0.22	-0.28	-0.29	-0.17	-0.23	-0.14	-0.28	-0.18	-0.28	-0.18	-0.28	-0.18	-0.18
P. polita	0.04	0.28	0.08	0.04	0.45	**0.99**	0.04	0.23	-0.08	-0.12	-0.03	-0.1	0	-0.13	-0.17	-0.19	-0.16	-0.17	-0.14	-0.15	-0.08	-0.11	-0.17	-0.11	-0.11
L. multipunctata	0.33	-0.09	0.26	-0.05	-0.14	0.04	**0.99**	0.12	0.83	0.2	0.18	0.13	0.11	0.18	0.34	0.34	-0.34	0.35	0.28	0.3	-0.17	0.21	0.35	-0.22	-0.22
X. diffusa	0.09	0.35	0.07	0.13	0.15	0.23	0.12	**0.99**	0.12	0.69	0.45	0.08	-0.01	0.06	-0.05	0.07	0.05	0.17	0	0.15	0.31	0.2	0.13	-0.1	-0.1
X. sp. aff. cornelii	0.41	-0.13	0.43	-0.17	-0.22	-0.08	0.2	0.12	**0.99**	0.07	0.07	0.04	-0.21	-0.21	-0.21	-0.2	-0.22	-0.16	0.25	0.15	-0.03	-0.04	-0.24	-0.12	-0.14
C. variabilis	0.37	0.27	0.17	0.06	-0.06	-0.12	0.31	0.03	0.06	**0.99**	0.06	0.07	0.32	-0.3	-0.26	-0.27	-0.17	-0.18	-0.32	-0.23	-0.18	-0.2	-0.2	-0.2	-0.2
A. propinqua	-0.14	-0.1	-0.09	-0.07	-0.06	-0.03	-0.07	-0.07	0.99	0.04	**0.99**	0.01	0.04	0.01	0.07	0.07	0.15	0.01	0.16	0.03	0.21	0.13	-0.04	0.34	0.34
L. littoralis	-0.41	-0.26	-0.3	-0.2	-0.17	-0.11	0.22	-0.09	0.12	0.11	-0.04	**0.99**	-0.04	0.07	0.16	0.23	0.2	0.18	0.65	0	0.15	0.31	0.2	0.13	0.13
Pontocythere sp.	0.01	0	-0.03	-0.02	-0.01	0	0.11	0.01	0.04	0.06	0.01	0.06	**0.99**	0.07	0.06	-0.06	0.03	-0.05	-0.07	-0.05	-0.05	-0.05	-0.05	-0.05	-0.05
L. lepida	-0.52	-0.35	-0.43	-0.26	-0.22	-0.13	0.27	-0.12	0.21	0.25	0.04	0.07	0.06	**0.99**	0.54	0.61	0.78	0.42	0.49	0.2	0.31	0.35	0.61	0.26	0.3
L. sublepida	-0.68	-0.44	-0.53	-0.34	-0.28	-0.17	0.34	-0.15	-0.21	-0.32	-0.01	0.16	0.07	0.54	**0.99**	0.72	0.64	0.66	0.44	0.35	0.23	0.37	0.6	0.55	0.6
L. spp. juveniles	-0.76	-0.5	-0.6	-0.38	-0.31	-0.19	0.38	-0.17	-0.24	-0.34	0.07	0.23	-0.06	0.61	0.72	**0.99**	0.7	0.82	0.64	0.53	0.46	0.49	0.77	0.45	0.56
T. amnicola donetziensis	-0.68	-0.43	-0.51	-0.33	-0.28	-0.16	-0.34	-0.15	-0.2	-0.32	0.07	0.2	0.03	0.78	0.64	0.74	**0.99**	0.67	0.57	0.4	0.32	0.54	0.62	0.39	0.45
A. quinquetuberculata	-0.71	-0.47	-0.56	-0.36	-0.29	-0.17	-0.35	-0.16	-0.22	0.1	0.5	0.24	-0.07	0.42	0.66	0.82	0.67	**0.99**	0.51	0.48	0.3	0.58	0.56	0.34	0.45
A. olivia	-0.55	-0.37	-0.45	-0.28	-0.24	-0.14	-0.28	-0.12	0.16	-0.26	0.01	0.16	-0.06	0.49	0.44	0.64	0.57	0.49	**0.99**	0.46	0.21	0.37	0.72	0.21	0.49
A. immodulata	-0.58	-0.38	-0.47	-0.29	-0.24	-0.15	-0.28	-0.13	0.25	-0.27	0.05	0.53	0.43	0.48	0.46	**0.99**	0.27	0.12	0.56	0.57	0.33	0.38	0.39	0.38	0.41
A. cymbula	-0.34	-0.22	-0.08	-0.17	-0.13	-0.08	-0.07	-0.07	-0.13	-0.17	-0.03	0	-0.03	0.31	0.23	0.46	0.32	0.3	0.21	0.27	**0.99**	0.12	0.43	0.27	0.45
A. subcaspia	-0.44	-0.31	-0.44	-0.38	-0.11	-0.11	0.21	0.15	0.05	0.37	0.49	0.54	0.58	0.37	0.12	0.2	**0.99**	0.18	0.13	0.34	0.45	0.55	0.34	0.45	0.45
C. schweyeri	-0.69	-0.45	-0.56	-0.34	-0.28	-0.17	-0.35	-0.15	-0.24	-0.32	0.13	0.6	0.6	0.77	0.62	0.56	0.72	0.56	0.43	0.18	0.38	0.13	**0.99**	0.41	0.49
A. bacuana	-0.44	-0.28	-0.36	-0.21	-0.18	-0.11	-0.22	-0.1	-0.14	-0.23	-0.04	0.2	-0.05	0.26	0.55	0.45	0.39	0.34	0.21	0.37	0.13	0.41	**0.99**	0.45
E. sp. aff. relicta	-0.44	-0.29	-0.36	-0.21	-0.18	-0.11	-0.22	-0.1	-0.14	-0.2	-0.04	0.13	-0.05	0.3	0.56	0.55	0.52	0.49	0.41	0.45	0.45	0.34	0.45	0.05	**0.99**

117

indicating no relationship and -0.99 indicating a strong negative correlation. R-mode factor analysis extracted five factors, R-factor 1 to R-factor 5, which account for 83.1 % of the total variance in the sequence (Fig. 5.6).

R-factor 1 accounts for 32.3 % of the total variance. This factor is mainly controlled by the Mediterranean ostracod species *P. agilis*. *L. multipunctata* and *X.* sp. aff. *cornelii* are also significant. There are minor contributions from *H. rubra* and *C. variablis*. There are minor negative correlations with *P. jonesii* and *C. edwardsi* (Fig. 5.6).

R-factor 2 accounts for 22.2 % of the total variance. This factor is controlled mainly by the Ponto-Caspian species *L. sublepida* and *L. lepida* in addition to *T. amnicola donetziensis*, *A. quinquetuberculata* and *A. olivia*. *C. schweyeri* and *A. subcaspia* are minor contributors to this factor (Fig. 5.6).

R-factor 3 accounts for 17.8 % of the total variance. This factor is controlled by the Mediterranean species *P. agilis*, *C. carinata*, *P. jonesii* and *C. edwardsi* with minor contributions from *H. rubra* and *P. polita*. There is a nearly (statistically) significant correlation with *L. multipunctata* (Fig. 5.6).

R-factor 4 accounts for 6.1 % of the total variance. This factor is controlled by the Mediterranean species *L. littoralis*, the dominant species in the transitional section of core MAR05-50, and the Ponto-Caspian species *L.immodulata*. This factor has many very minor contributions, mainly from Ponto-Caspian species but also from the Mediterranean Species as well (Fig. 5.6).

R-factor 5, which accounts for 4.7 % of the total variance, is another factor with contributions from the Mediterranean species. This factor is controlled by *L.*
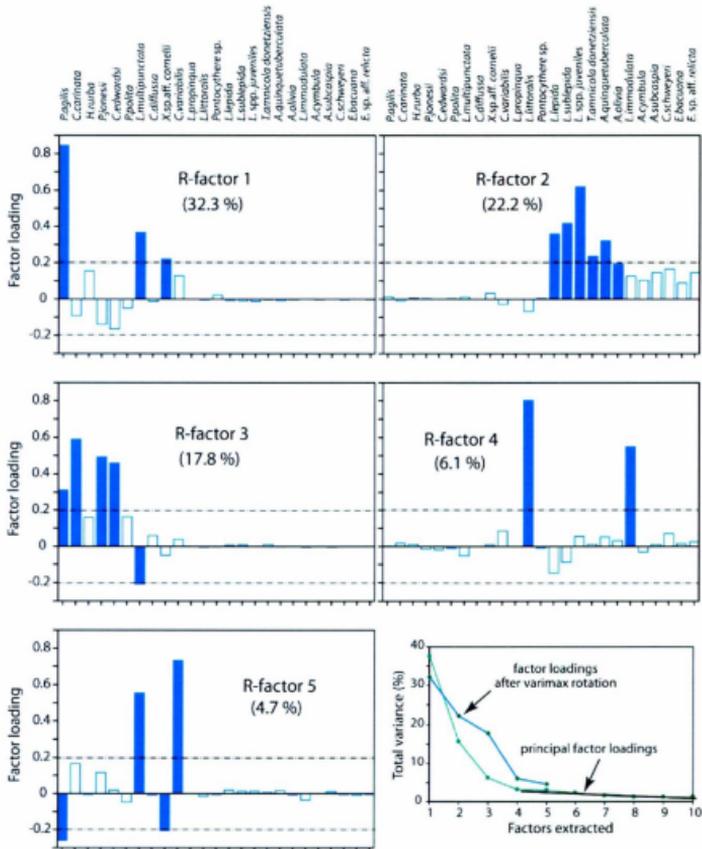
Figure 5.6. R-factors 1–5 showing the significant species (factor loadings). Factors exceeding 0.2 are significant (solid blue). Minor factors (blue outline) are also shown. The graph (bottom, right) shows the factor loadings before and after Varimax rotaion and a thick black line indicates Catells' scree test which eliminates the least significant factors.

multipunctata and *C. variablis* with a minor contribution from *C. carinata* and a negative correlation with *P. agilis* and *X.* sp. aff. *cornelii* (Fig. 5.6).

5.7.2.2. Q-factor Analysis

These R-factors can be plotted down-core just as the abundance of any single species can be plotted down-core (Fig. 5.7). These plots are called Q-factors. Q-factors 1–5 are the plots of R-factors 1–5 respectively. These plots show where in the core these assemblages, or factors, are occurring.

Starting at the base of core MAR05-50, Q-factor 2 (Ponto-Caspian species) dominates the lower, brackish section of the core, comprising almost 100 % of the assemblage to a depth of ~620 cm. Above 620 cm depth in the core Q-factor 4 (mixed Mediterranean and Ponto-Caspian species) sharply increases and dominates the assemblage at ~80 % abundance until a depth of ~520 cm (Fig. 5.7). Above 520 cm depth in the core Q-factor 1 (Mediterranean species) sharply increases and dominates the lower marine section of core MAR05-50 with an average abundance of ~70 %. Above ~380 cm depth in the core the general abundance trend of Q-factor 1 is oscillating but generally decreasing until the top of core MAR05-50. Above 380 cm depth in the core Q-factor 3 (Mediterranean species) begins to increase and has an increasing trend directly disproportionate to Q-factor 1 to the top of the core. Q-factor 5 (Mediterranean species), which only accounts for 4.7 % of the total variance, is more erratic but does noticeably fall to an abundance of 0 % above ~100 cm depth in the core. From 100 cm depth to the top of the core Q-factor 3 dominates the sequence.
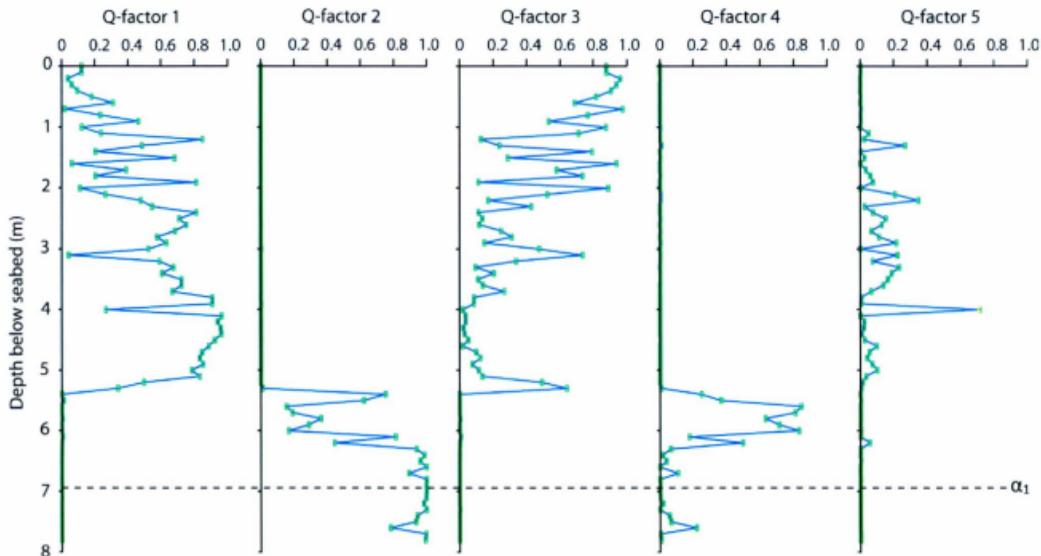
Figure 5.7. Q-factors 1-5 are the down-core plots of R-factors 1–5 respectively. The Q-factor results match the observed results that there are clearly three separate "sections" in core MAR05-50. R-factors 1, 3, and 5 occur in the upper, marine section of the core. R-factor 2 dominates the lower, brackish section and R-factor 4 dominates the transitional section of the core.

CHAPTER 6

INTERPRETATION

In the ostracod data recovered from core MAR05-50 there is a distinct faunal turnover from a brackish to a marine assemblage beginning at 7450 cal yr BP (Fig. 5.1). The suddenness of this turnover, occurring in ~146 years, and its magnitude strongly suggest that it must have been driven by ecological changes which took place at the core site on the southwestern Black Sea shelf during the Holocene, specifically associated with changes in salinity driven by a systematic reconnection to the Mediterranean Sea. The high faunal diversity excludes changes in oxygen availability as a cause of this turnover.

In this chapter the results presented in Chapter 5 are discussed in calendar years. Table 6.1 lists sample depths in the composite core MAR05-50 and the corresponding ages in calendar years (see Chapter 2).

6.1. Bio-zones

In paleoecological microfossil studies it is common to divide the sedimentary sequence into faunal or floral assemblage "zones". These are sections of the sequence that are distinctively characterized by particular assemblages of species and are divided by distinct changes that are observed in those assemblages. Zones can be determined visually by the researcher, but the process can also be done easily by numerical (statistical) analysis. Statistical analysis is most useful because it basically eliminates the element of subjectivity and can detect relationships within the data that a researcher might not perceive. The basic principles of numerical analysis as used in this thesis were established by Gordon & Birks (1972) and Birks & Gordon (1985).

Table 6.1. Sample depths from core MAR05-50 with corresponding ages (cal yr BP) as determined by the software Ager. The shaded area indicates the transitional section (assemblage) of the core. Above this is the marine section and below is the brackish section. The hiatus denoted by the unconformity α_1 is shown as a red line between 690 and 700 cm depth in the core.

Depth (cm)	Cal ^{14}C ka BP	Depth (cm)	Cal ^{14}C ka BP	Depth (cm)	Cal ^{14}C ka BP
0	0	270	3600	540	6410
10	391	280	3660	550	6540
20	782	290	3730	560	6670
30	1170	300	3790	570	6800
40	1570	310	3860	580	6930
50	1960	320	3920	590	7060
60	2020	330	3980	600	7190
70	2090	340	4050	610	7320
80	2160	350	4110	620	7450
90	2220	360	4180	630	7580
100	2290	370	4260	640	7710
110	2340	380	4350	650	7840
120	2400	390	4440	660	7970
130	2460	400	4570	670	8100
140	2520	410	4700	680	8230
150	2580	420	4840	690	8350
160	2640	430	4970	700	10800
170	2700	440	5100	710	10900
180	2760	450	5230	720	10900
190	2820	460	5370	730	11000
200	2870	470	5500	740	11100
210	2930	480	5630	750	11200
220	2990	490	5760	760	11300
230	3050	500	5890	770	11400
240	3260	510	6020	780	11400
250	3470	520	6150		
260	3530	530	6280		

In this chapter Figure 5.5 (species % abundance) is re-drawn to present the ostracod data with respect to calendar years (Fig. 6.1). Based on the CONISS cluster results, Figure 6.1 can be divided into 6 "bio-zones" where marked changes in the ostracod assemblage reflect ecological changes which took place at the MAR05-50 core site over the past ~11400 years. Table 6.2 briefly summarizes the bio-zones.

6.1.2. Bio-zone 1 (11400–10700 cal yr BP)

Bio-zone 1 is part of the lower, brackish assemblage which occurs from the base of core MAR05-50 dated from 11400 cal yr BP to 10700 cal yr BP. The most abundant species over this time interval are *L. sublepida* and *L. lepida*, *T. amnicola donetziensis*, *C. schweyeri*, *A. quinquetuberculata* (Fig. 6.1). These species and other less abundant ones such as *A. bacuana*, *A. pediformis* and *A. cymbula* are currently found living in the Caspian Sea which has a salinity range of 1–13 psu. *C. schweyeri* prefers salinities of up to 8 psu (Aladin, 1993) and *A. quinquetuberculata* prefers salinities of up to 5 psu (Opreanu, 2008). *L. lepida* is also found living in deltas around the Azov Sea where the maximum water depth is 14 m and salinity is very low, certainly far less than 10 psu at the coast. *A. cymbula* is found today in lagoons and estuaries in the Ponto-Caspian basins (Opreanu, 2008).

Bio-zone 1 is interpreted to represent a low salinity environment; probably less than 10 psu based on the above species and possibly as low as 5–8 psu based on the upper salinity preferences of *C. schweyeri*, *A. quinquetuberculata* and *L. lepida* (see Taxonomy). There were marine species (*e.g.*, *P. aglis* and *L. littoralis*) present in this interval but the low salinity strictly limited their distribution and thus their abundances

124
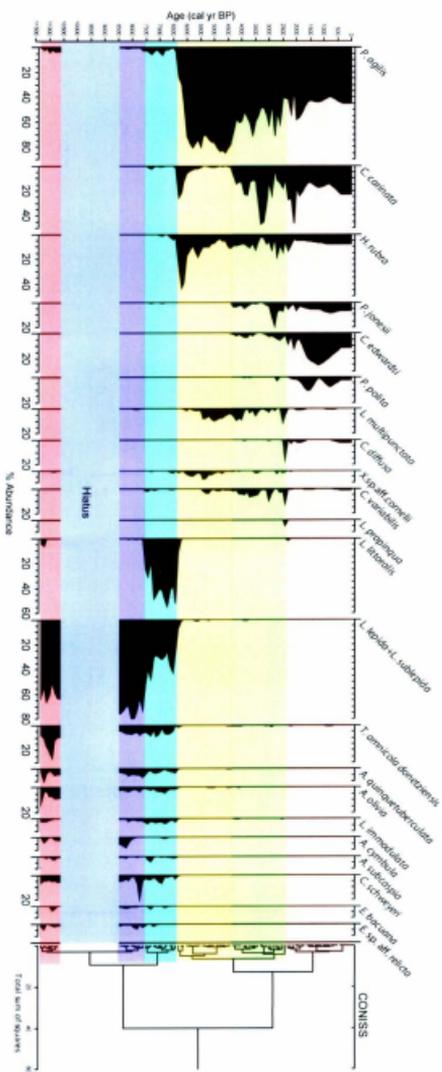
Figure 6.1. CONISS cluster results show that core MAR05-50 can be divided into 6 bio-zones based on distinct assemblages of key ostracod species. Going upward in the sequence these bio-zones reflect step-by-step ecological changes in the Black Sea driven by gradual salinization after a post-glacial reconnection to the Mediterranean Sea.

Table 6.2. Outline of Bio-zones 1–6 giving the main ostracod species and ecological significance of each bio-zone.

Bio-zone # Age (cal yr BP)	Main Ostracod Species	Ecological Significance
Bio-zone 1 11400–10700 cal yr BP	*L. sublepida, L. lepida, T. amnicola donetziensis, A. quinquetuberculata, A. olivia, C. schweyeri*	Low salinity, possibly 5–8 psu but not fresh water
Bio-zone 2 8400–7580 cal yr BP	*L. sublepida, L. lepida, T. amnicola donetziensis, A. quinquetuberculata, A. olivia, C. schweyeri*	Remains brackish, possibly slight salinity increase possibly related to processes which re-initiated sedimentation after the hiatus (i.e., inflow of Mediterranean water)
Bio-zone 3 7450–6410 cal yr BP	*L. littoralis, L. lepida, T. amnicola donetziensis, A. quinquetuberculata, A. olivia, C. schweyeri*	Post-reconnection transitional phase, rising salinity suitable for brackish and marine ostracods, possibly up to
Bio-zone 4 6280–4350 cal yr BP	*P. agilis, C. carinata, H. rubra, L. multipunctata, C. variablis*	Salinity increased allowing new Mediterranean species to dominate
Bio-zone 5 4300–2350 cal yr BP	*P. agilis, C. carinata, H. rubra, L. multipunctata, C. variablis, P. jonesii, C. edwardsi*	Introduction of two new Mediterranean sublittoral species, possible sea level rise, salinity perhaps ≥25 psu
Bio-zone 6 2300 cal yr BP–Present	*P. agilis, C. carinata, H. rubra, P. jonesii, C. edwardsi, P. polita*	New Mediterranean species *P. polita*, salinity similar to today

are extremely low (Fig. 5.4; Fig. 6.1). The energy regime of the environment is interpreted to be low-moderate based on the high abundance of juvenile stages in the samples (Fig. 5.3).

6.1.3. Bio-zone 2 (8400–7580 cal yr BP)

Bio-zone 2 begins above the α_1 unconformity surface at ~8400 cal yr BP (see Chapter 3; Table 3.2) and extends to 7580 cal yr BP (Fig. 6.1). There are not many distinctive changes in the Bio-zone 2 ostracod assemblage relative to Bio-zone 1 that existed before the hiatus. *L. lepida* together with *L. sublepida* together increase in abundance and *T. Amnicola* and *A. olivia* decrease in abundance (see Chapter 5). Increases in concentration (3.2 to 7.4 valves per gram) and diversity (11 to 15 species) both occur in the first 250 years after the hiatus. These changes might have been simply random fluctuations which can be seen throughout the core and not necessarily related to processes which formed unconformity α_1 (see Chapter 3; Flood et al., 2009).

The data suggest that during the Bio-zone 2 interval a brackish environment persisted on the southwestern Black Sea shelf suitable for ostracods which favor brackish waters. The changes in ostracod abundances from Bio-zone 1 to Bio-zone 2 might be related to processes which re-initiated sedimentation after the hiatus at ~8400 cal yr BP. This low salinity environment persisted in the area of the core site until 7450 cal yr BP.

6.1.4. Bio-zone 3 (7450–6410 cal yr BP)

Bio-zone 3 marks a major change in the ostracod assemblage (Fig. 6.1). This interval encompasses the transitional assemblage from the first significant occurrence of marine ostracods (*L. littoralis*) at 7450 cal yr BP to the end of the co-occurrence of

127

marine and brackish species at 6410 cal yr BP (Fig. 6.1). The change in the assemblage at 7450 cal yr BP happens rather abruptly, in geological terms, considering that it occurs within 10 cm core depth which represents ~ 146 years (see Chapter 3). If the species *L. littoralis* is truly stenohaline, as described by Ruggieri (1964), then it stands to reason that when the water reached precise conditions favored by *L. littoralis* this species was able to rapidly expand its population from only a one or two specimens per sample in Bio-zones 1 and 2 to making up ~40 % of Bio-zone 3.

The sudden appearance and rapid proliferation of *L. littoralis*, suggests that bio-zone 3 places the persistent reconnection to the Mediterranean Sea (via the Bosphorus Strait) at or sometime before 7450 cal yr BP and that the salinity rose quickly (in ~146 years) to a level suitable for *L. littoralis*. Ivanova et al. (2007) regards this species as preferring salinities up to 18 psu so this might be an upper limit for the salinity range sometime during or near the end of the Bio-zone 3 interval at 6410 cal yr BP.

However, during this interval the brackish species *Loxoconcha sublepida*, *Loxoconcha lepida* and *Tyrrhenocythere amnicola donetziensis* were still able to sustain their existence for another ~1000 years, until 6410 cal yr BP. The coexistence of brackish and marine species during this interval suggests that salinities were rising but still in a range suitable for both marine and brackish ostracods tolerant of increasing salinities.

6.1.4.1. Significance of *Loxoconcha littoralis*

Other marine ostracods, namely *P. agilis*, were present in the brackish interval along with *L. littoralis* (Fig. 6.1). When the opportunity (i.e., a more saline environment)

128

developed *L. littoralis* was the first of the marine species to take advantage and aggressively colonize the area. It is possible that the salinity at that time was in the exact range suitable for *L. littoralis* to thrive. However, that particular salinity range was only sustained for ~1000 years after which time it became unsuitable for *L. littoralis* and other Mediterranean species were able to take advantage of its waning dominance.

Another possibility is that *L. littoralis* is simply an aggressive and opportunistic species and was simply the fastest to move in and take advantage of the lack of competition from other marine species. Other species such as *P. agilis* took longer to establish themselves but eventually dominated the area, out-competing *L. littoralis*.

6.1.4.2. Cohabitation or Bioturbation?

During the transitional interval the Mediterranean species *L. littoralis* co-existed with the lingering brackish species for ~1000 years (Fig.6.1). This supports the idea that the reconnection with the Mediterranean involved steps in a protracted process. But is it possible that bioturbation simply mixed these species together and they were not actually *living* at core site MAR05-50 together? The author argues that the observed trends are not a result of bioturbation and that these species truly were living together. The boundary between *L. littoralis* and the later marine species, especially *P. agilis* is very sharp (Fig. 6.1). If bioturbation was mixing sediment over thicknesses of >10 cm there would be more overlap between these species. In addition, *L. littoralis* was already present in the brackish assemblage so it was not simply introduced into the marine assemblage and bioturbated downward. *L. littoralis* and the brackish species are consistently represented in the transitional assemblage as many adults and various

129

juveniles, which is further evidence that they were living and dying there. Based on visual observation, bioturbation is only moderate in core MAR05-50 and is not interpreted to be a major factor in the distribution of ostracod valves throughout the core. Nowhere else in the core is there a "blur" or overlap that mixes species with dramatically different environmental preferences.

6.1.5. Bio-zone 4 (6280–4350 cal yr BP)

Bio-zone 4 begins at 6280 cal yr BP and marks the time when the brackish assemblage was essentially completely overtaken by the marine species immigrating in through the Bosphorus Strait (Fig. 6.1). The pioneering *L. littoralis* was rapidly replaced at this time by new Mediterranean species and the ostracod assemblage in core MAR05-50 became essentially fully comprised of marine species until present (Fig. 5.1).

The first ostracods to dominate the new marine assemblage in bio-zone 4 were *P. agilis*, *C. carinata* and *H. rubra* (Fig. 6.1). These species are found living today around the Mediterranean and adjoining seas where the salinities are 37–39 psu. *P. agilis* is found in the Adriatic Sea (Bonaduce et al., 1975) and it is abundant today around the shallow (10–100 m) shoreline of the Black Sea (Schornikov, 1967). *C. carinata* can be found today all around the Atlantic Ocean and Mediterranean Sea and prefers depths of ~60–80 m (Keen, 1982; Athersuch et al., 1989). *H. rubra* lives on the shallow banks around Ischia, Procida, Naples and the Sorrento Peninsula in depths up to 100 m (Puri et al., 1964).

Bio-zone 4 is defined as an "early marine" stage. This is called the *early* marine stage because it is the beginning of increasingly saline bottom water in the southwestern

130

Black Sea shelf due to steady Mediterranean inflow with water depths probably around 80 m or less. Salinity had risen to a point where it was unfavorable for brackish Ponto-Caspian species and they soon all but disappeared. During this interval, the Mediterranean ostracods began to diversify and flourish.

At ~4440 cal yr BP there is a tremendous spike in the number of valves and the number of species (Fig. 5.2). While almost half of the 21 species are brackish, the sheer number of marine valves (especially *P. agilis*) makes the sample at this age/depth 97.7 % marine specimens. *P. agilis* makes up 75 % of the sample at this level. The reason for this spike in abundance and diversity is not clear. It could simply be a time when conditions at the core site were favorable for all of these species, particularly *P. agilis*. It might be that at this time bottom water conditions were optimal for *P. agilis* whose population was consequently exploding, creating the abundance spike.

6.1.6. Bio-zone 5 (4350–2350 cal yr BP)

Bio-zone 5 is defined as a "mid-marine" stage marked by a further increase in salinity indicated by the introduction of two new marine species (Fig. 6.1). At 4350 cal yr BP *C. edwardsi* and *P. jonesii* both appear for the first time in core MAR05-50 and continue on as two of the more common species in the marine assemblage. *P. jonesii* prefers salinities of 26–35 psu (Neale, 1988) so the core site on the southwestern Black Sea shelf might have been close to or in that salinity range during this interval. *C. edwardsi* and *P. jonesii* are both sublittoral species (Athersuch et al., 1989.) and *P. jonesii* commonly occurs in water well over 80–100 m deep (Bonaduce et al., 1975; Penny, 1993).

131

6.1.7. Bio-zone 6 (~2350 cal yr BP–Present)

Bio-zone 6 is defined as "late marine" because this stage started only about 2300 years ago (Fig. 6.1). By this time the bottom water salinity was probably very similar to modern values (see also Soulet et al., 2010). This bio-zone is defined by a decline in the marine species *P. agilis* and *H. rubra* common to Bio-zones 4 and 5. *P. agilis* has an average abundance of 63.1 % in Bio-zones 4 and 5 and in Bio-zone 6 it decreases to just 42.6 %. There is also a major decline in *L. multipunctata*, *X.* sp. aff. *cornelii* and *C. variablis* whose abundances all drop well below 1 % in Bio-zone 6. Bio-zone 5 ostracods *P. jonesii* and *C. edwardsi* become more abundant and *P. polita* notably becomes a much more commonly occurring species in this late marine bio-zone (Fig. 6.1).

6.2. R-mode Factor Analysis

In Chapter 5 Q- and R-mode factor analysis results were presented using ostracod data in the depth domain. Q-mode analysis seeks to discover similarity between samples, whereas R-mode analysis reveals similar behavior of variables (in this case the various species). In this chapter, Q- and R- mode factor results are presented again, but with respect to calendar years. The statistical analysis of 25 key species in 92 samples produced 5 R-factors after Varimax rotation accounting for 82.8 % of the total variance (Fig 6.2).

R-factors 1 accounts for 28.9 % of the total variance and is mainly controlled by Mediterranean species *P. agilis*, *L. multipunctata* and *X.* sp. aff. *cornelii* with a minor contribution from *H. rubra* (Fig 6.2).

R-factor 2 accounts for 20.6 % of the total variance and its main controlling
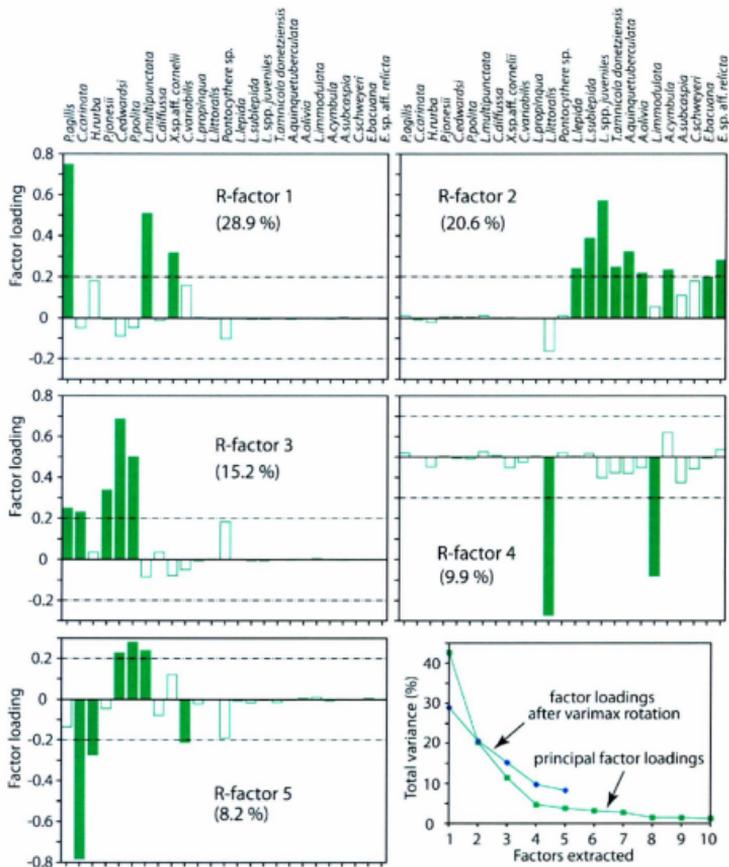
Figure 6.2. R-mode factor analysis extracted 5 factors from the age (cal yr BP) data after Varimax rotation (bottom right). Factors (species) more than ±0.2 are considered statistically significant (solid green). Minor contributing factors are also shown (outlined green).

133

species are the Ponto-Caspian species *L. lepida*, *L. sublepida*, *T. amnicola donetziensis*, *A. quinquetuberculata*, *A. olivia*, *A. cymbula*, *A. bacuana* and *E.* sp. aff. *relicta* (Fig 6.2).

R-factor 3 accounts for 15.2 % of the total variance and is mainly controlled by *C. edwardsi*, *P. polita*, *P. jonesii*. *P. agilis* and *C. carinata* are also significant species in this factor (Fig 6.2).

R-factor 4 accounts for 9.9 % of the total variance and is mainly controlled by the Mediterranean species *L. littoralis* which dominates the transitional assemblage. According to the analysis *L. immodulata* is also a significant contributor. This is a surprising result because *L. immodulata* is a very minor species in core MAR05-50 with an average transitional section abundance of 2.8 %. R-factor 4 also has numerous minor factor loadings, mainly from brackish ostracod species (Fig 6.2).

R-factor 5 accounts for 8.2 % of the total variance and is mainly controlled by the occurrence of *C. carinata*, *H. rubra* and *C. variabilis* with a negative correlation with *C. edwardsi*, *P. polita* and *L. multipunctata* (Fig 6.2).

6.3. Q-mode Factor Analysis and Relationship to Bio-zones 1–6

The downcore plots of the Q-factors clearly show 3 divisions: lower, middle and upper areas of the Q-factor graphs, corresponding to earlier observations of brackish, transitional and marine sections respectively in core MAR05-50 (Fig. 6.3; Fig. 5.4; Fig. 5.1). The Q-factors are described in the order they occur moving upward from the base of core MAR05-50, and thus forward in time from ~11400 cal yr BP. Q-factor 2 is the dominant factor from the base of core MAR05-50 at ~11400 cal yr BP to ~7400 cal yr BP (Fig. 6.3). Between ~7400 cal yr BP and ~6400 cal yr BP this factor shows a sharp stepwise decrease reaching 0 factor loadings at ~6400 cal yr BP. It is
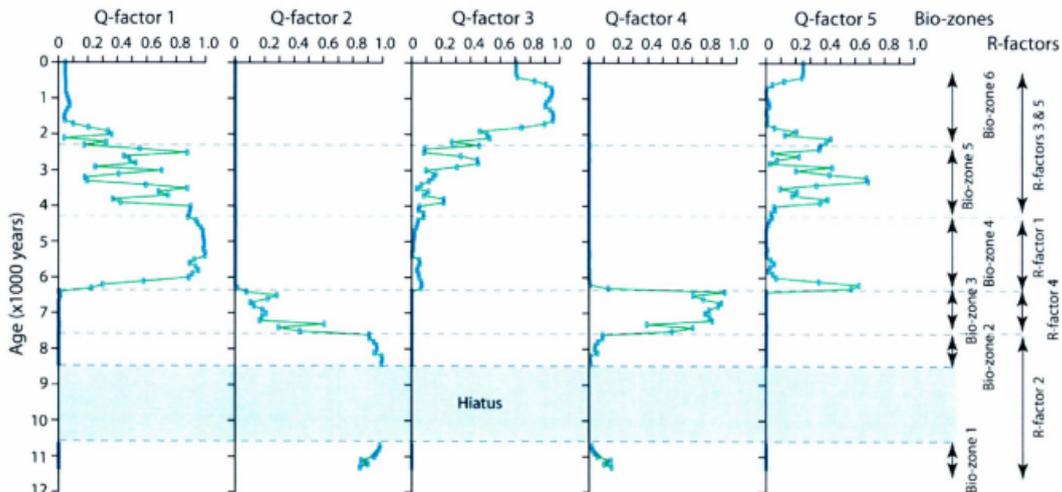
Figure 6.3. Q-factors 1–5 show the down-core distribution of R-factors 1–5 respectively. The Q-factor plots clearly show that the R-factors are distinctly distributed in lower, middle and upper parts of core MAR05-50. On the right, the location of Bio-zones 1–5 in the core are shown alongside the R-factor assemblages which control each bio-zone.

absent in the upper 6400 years of the core. Q-factor 2 clearly correlates to the lower brackish section of core MAR05-50 (Fig. 6.3). Therefore, the R-factor 2 assemblage is the main component of the earliest Bio-zones 1 and 2 (Fig. 6.1).

Q-factor 4 has fluctuating but very low factor loadings on samples from ~11400 cal yr BP to ~7400 cal yr BP. Then Q-factor 4 becomes the dominant factor with >80 % loading from ~7400 cal yr BP to ~6400 cal yr BP. The sharp decline at ~6400 cal yr BP is nearly perfectly matched with the sharp increase at this time of Q-factor 5 (see below), broadly matched with the reciprocal increase in Q-factor 1. Q-factor 4 is absent from ~6400 cal yr BP to the top of core MAR05-50. Q-factor 4 clearly correlates to the transitional section of core MAR05-50 (Fig. 6.3). Therefore the R-factor 4 assemblage which is controlled by *L. littoralis* is the main component of Bio-zone 3 (Fig. 6.1).

Q-factors 1, 3 and 5 (and the corresponding R-factors) all correlate with some part or parts of the marine section of core MAR05-50 which includes the Bio-zones 4–6 (Fig. 6.3; Fig. 6.1). Q-factor 1 is absent from the base of the core at ~11400 cal yr BP to ~6400 cal yr BP (Fig. 6.3). It becomes the dominant factor from ~6400 cal yr BP to ~4000 cal yr BP. The transition at ~6400 cal yr BP is remarkably abrupt. Between ~4000 cal yr BP and ~1500 cal yr BP, Q-factor 1 exhibits fluctuating but gradually decreasing factor loadings in the samples. It is less than 10 % in the upper ~1500 years of core MAR05-50. Q-factor 1 clearly denotes the earliest marine stage and Bio-zone 4. *P. agilis* is the main factor in the temporally associated R-factor 1. There is a clear similarity even between the trend of Q-factor 1 (Fig. 6.3) and the abundance trend for *P. agilis* (Fig. 6.1). R-factor 1 therefore is the main component of Bio-zone 4, the "early marine" stage.

Q-factor 3 is absent from the base of the core to ~6400 cal yr BP (Fig. 6.3). It

becomes the dominant factor in the upper ~2000 years of the MAR05-50 record and displays a nearly perfectly reciprocal relationship with Q-factor 1. This is particularly true in the upper ~2000 years of the record. Q-factor 3 follows a similar trend/shape to the abundance plots of *P. jonesii*, *C. edwardsi* and *P. polita* (Fig. 6.1) which are the main contributors in R-factor 3. Therefore, the R-factor 3 assemblage is a component of Bio-zone 5. Because *P. polita* is a statistically significant contributor to R-factor 3 (i.e., it has a high loading on that factor), and this species does not become significant until Bio-zone 6 (Fig. 6.1), the importance of R-factor 3 also extends into Bio-zone 6.

Q-factor 5 is absent from the base of core MAR05-50 at ~11400 cal yr BP to ~6400 cal yr BP. Between ~6400 cal yr BP and the top of the core, this factor exhibits large amplitude fluctuations which are roughly reciprocal with those observed in Q-factor 1, but appear to be weakly correlated with Q-factor 3. Q-factor 5 and R-factor 5 are more cryptic than the four preceding factors. Q-factor 5 (Fig. 6.3) very closely resembles the abundance trend for *C. carinata* (Fig. 6.1) which is the main controlling species on R-factor 5. Therefore, R-factor 5 might be a part of all three marine Bio-zones 4–6. In Chapter 5 the statistical results for the depth data are given. In those results R-factor 5 is much different than R-factor 5 results presented here in the age domain. This discrepancy is discussed further in Chapter 7.

CHAPTER 7

DISCUSSION

7.1. Timing of Two-way Flow and Increasing Salinity in the Black Sea

The ostracod data described in Chapters 5 and 6 showed that the post-glacial reconnection between the Black Sea and the Mediterranean Sea occurred at or before 7450 cal yr BP. Based on the work of others (e.g., Major et al., 2006; Hiscott et al., 2007; Marret et al., 2009; Flood et al., 2009) the actual timing of the first Mediterranean inflow was earlier than suggested by the ostracod turnover in core MAR05-50. On the basis of the strontium isotopic signal in dated mollusc shells, Major et al. (2006) suggested that Mediterranean water first entered the Black Sea in significant amounts as early as 9150 cal yr BP. This date is the revised timing of the catastrophic flooding of the Black Sea that was first proposed by Ryan et al. (1997). It was interpreted by others (Hiscott et al., 2007; Marret et al., 2009) to be the timing of a short pulse of Mediterranean water inflow due to a temporary weakening of Black Sea outflow and not the beginning of persistent two-way flow across the Bosphorus Strait.

The sediments from cores MAR05-50 above the unconformity α_1 provide evidence for the timing of post-glacial Mediterranean inflow into the Black Sea. If the sediments deposited above unconformity α_1 coincide with Mediterranean water inflow as suggested by Flood et al. (2009), then the inflow must have begun at least as early as 8160 cal yr BP, because this is the first available date above unconformity α_1 at 675 cm depth in core MAR05-50 (Fig. 3.1; Table 3.1). This date is from 695 cm depth in the core, ~20 cm above unconformity α_1; thus, the first persistent inflow must have started

138

sometime earlier to build ~20 cm of levee succession. The chronostratigraphy of core MAR05-50 (see Chapter 3) would suggest that ~290 years would be needed to deposit ~20 cm of sediment thickness, putting the timing of first persistent inflow at no later than ~8450 cal yr BP, and possibly earlier if the inflow began during the hiatus at unconformity α_1.

In core MAR02-45, raised ~70 km west-northwest of core site MAR05-50, the start of sulfate reduction signifying a good input of saline water into the Black Sea occurs at 8520 cal yr BP (age recalibrated from Hiscott et al., 2007, unpublished data). Accordingly, it seems likely that the persistent inflow had begun sometime between 8520 and 8450 cal yr BP. Based on dinocyst data Hiscott et al. (2007) suggested that after the initiation of persistent Mediterranean inflow, and the associated establishment of two-way exchanges across the Bosphorus Strait, the salinity increased to >10–12 psu. This salinity level would still have been tolerable for the brackish water ostracods in Bio-zone 2.

7.1.2. Salinization Lag

The above evidence suggests that there is a lag of at least 1000 years between the beginning of persistent marine inflow into the Black Sea at ~8500 cal yr BP and the aggressive colonization of the area by the first Mediterranean ostracod *L. littoralis* at 7450 cal yr BP. This lag is interpreted as the time needed for enough Mediterranean water to enter the Black Sea to raise the salinity to a level suitable for marine ostracods. This is in agreement with Major et al. (2006) who moved the date of the initial incursion back to ~9150 cal yr BP, and who reinterpreted the date of ~7570 cal yr BP (Ryan et al., 1997) to mark the point when the salinity became suitable for Mediterranean molluscan

fauna to begin colonizing the Black Sea. In this study, this lag is interpreted as evidence that the post-glacial reconnection of the Black Sea to the Mediterranean Sea and subsequent salinization of Black Sea bottom water was a progressive and gradual process. This does not rule out a catastrophic initial reconnection, because modelling by Soulet et al. (2010) showed that even a very rapid rise in the level of the Black Sea from ~-90 m to ~-40 m due to the addition of ~28000 km^3 of 38 psu Mediterranean water would only increase the average salinity of the Black Sea by ~2 psu.

7.2. Correlation with Geochemical Data from Core MAR05-50

A concurrent geochemical study was done on the sediments from core MAR05-50 by fellow M.Sc. candidate (A. Linegar, *Paleoenvironmental History of the Southwestern Black Sea: and Elemental and Stable Isotopic Study*, 2012). The results showed that organic carbon from the base of the core to unconformity α_1 (Bio-zone 1 in this study) is isotopically light (~-27 ‰) indicating its source was predominantly terrestrial or lacustrine (Fig.7.1). Above unconformity α_1 the organic carbon signal becomes increasingly marine (Fig. 7.1) and an increase in sulfate reduction suggests that by ~6300 cal yr BP a sustained two-way flow had been well established (A. Linegar, personal communication). This is in agreement with this study, which documents the first fully marine Bio-zone 4 after ~6300 cal yr (Fig. 6.1; Table 6.2), consistent with a strong and persistent input of marine water by this time.

7.3. Relation to Previous Black Sea Studies

The ostracod data conflict with the hypotheses of Ryan et al. (1997, 2003) and Major et al. (2002, 2006). The location of core site MAR05-50 is currently at ~-91 m

140
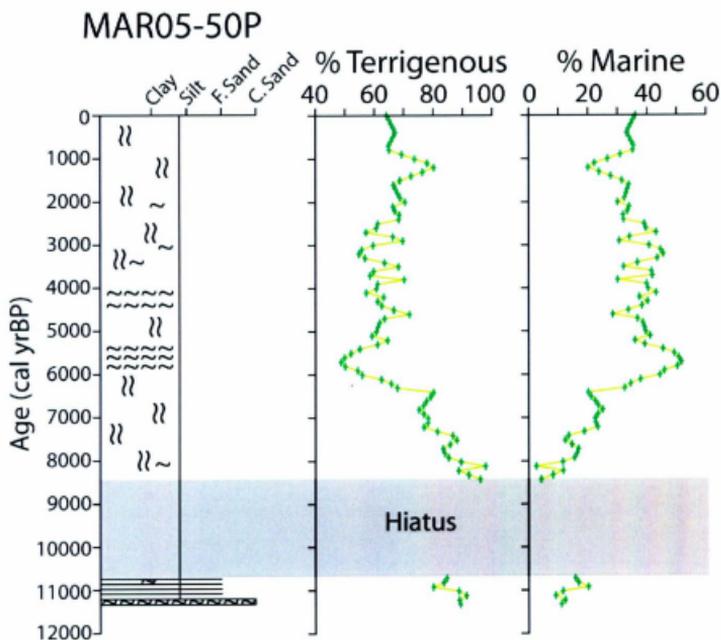
Figure 7.1. An illustration of composite core MAR05-50 next to plots of organic carbon sources shows that prior to the hiatus the source of organic carbon was >80 % terrestrial. At the start of re-deposition following the hiatus at ~8400 cal yr BP the source of organic carbon became increasingly marine indicating the onset of Mediterranean inflow (modified from Linegar, 2012).

below sea level, and the α_1 unconformity lies at an elevation of ~-97 m (Figs 2.2, 3.1). Clearly the ostracod data suggest that the core site was submerged by at least a few meters of water by ~11400 cal yr BP for the ostracods to be living there and that there could not ever have been a drawdown of the water level to ~-95 m below the current sea level since that time, as proposed by the Flood Hypothesis (Ryan et al., 2003). Such a drawdown would have effectively placed the core site at the paleo-shoreline. Hiscott et al. (2007) suggested that the water depth could not have been shallower than ~-55 m during this time based on early Holocene deposits which indicated accumulation below storm wave base. On the modern shelf, accumulation is prevented by wave agitation in water depths less than 50–60 m (Hiscott and Aksu, 2002). Similarly, Yanko-Hombach (2007) and Ivanova et al. (2007) agree that the water level in the Black Sea never dropped below -40 m after ~11000 cal yr BP. These water levels would have been suitable for the ostracod species living at core site MAR05-50 from ~11400 cal yr BP. Unconformity α_1 occurs at a depth of 695 cm in the brackish section of core MAR05-50. This unconformity is widely traceable in Holocene deposits of the southwestern Black Sea shelf and is also present in core MAR02-45 (Flood et al., 2009), suggesting that core site MAR05-50 was connected to the open Black Sea and not an isolated pond at an elevation above a regressed "lake".

Furthermore, the ostracod species found in core MAR05-50 clearly show that conditions in the Black Sea from ~11400 to 7580 cal yr BP were brackish and not freshwater as previously proposed by Ryan et al. (1997) and, for the older part of this time interval, by Soulet et al. (2010), before a gradual reconnection to the Mediterranean Sea. Brackish conditions in the early Holocene Black Sea have also been shown by a

142

number of previous authors. Marret et al. (2009) concluded from dinocyst data from core MAR02-45 that the salinity of the pre-reconnection Black Sea was between 7 and 12 psu until ~7700 cal yr BP and gradually became more saline over ~1500 years. Although Soulet et al. (2010) criticized that conclusion stating that the dinocysts used to estimate this salinity actually are known to have a wider salinity tolerance, Mudie et al. (2007) also concluded the early Holocene Black Sea fluctuated between 5 and 15 psu based on dinocyst data and a study of the process lengths of the dinocyst *Lingulodinium machaerophorum*. Mertens et al. (2012) confirms these estimates.

After the reconnection, the salinity values might have been around 13–15 psu during Bio-zone 3 (Mertens et al., 2012). These salinity suggestions would seem tolerable for both marine and brackish water ostracods which were found together in core MAR05-50 in the transitional assemblage and Bio-zone 3 (Chapters 5 and 6). The MAR05-50 site is immediately adjacent to the site of saline inflow through the Bosphorus Strait, so it would seem reasonable to assume that the bottom waters after reconnection were more saline than ~15 psu, even more conducive to marine ostracods.

After the transitional Bio-zone 3, the start of the first marine bio-zone at 6280 cal yr BP (Fig 6.1; Table 6.1) more or less coincides with weakening of Black Sea outflow at ~6400 cal ka BP proposed by Hiscott et al. (2002) letting in more marine water to raise the salinity and provide easier access for the Mediterranean ostracods because the floor of the Bosphorus Strait would have been continuously bathed with Mediterranean water and juveniles ostracods would have been more effectively transported by stronger northward-flowing bottom waters. This timing also coincides with the maximum input of organic carbon from marine sources indicating a well-established reconnection (Fig. 7.1).

In addition to the salinization lag proposed by Major et al. (2006), a lag of ~900 years was also observed by Soulet et al. (2011), although they believe that the Mediterranean waters entered the Black Sea without any preceding Black Sea outflow. Whatever the mechanism, Soulet et al. (2010, 2011) agree with a slow salinization as do Lane-Serff et al. (1997) who conclude that complete salinization would have taken ~5000 years, largely prolonged by the high river input into the Black Sea during the early Holocene. This is in agreement with the ostracod data from core MAR05-50 which showed that salinity conditions reached near modern levels in Bio-zone 6 starting at ~2300 cal yr BP, which is ~5000 years after the faunal turnover is observed at 7450 cal yr BP.

The results of this study are also similar to the findings of Giunta et al. (2007) who noted three "ecozones" in sediment cores from the western Black Sea. These authors similarly showed a gradual increase in salinity in the Black Sea after ~7600 cal yr BP. Based on changes in the calcareous nannoplankton E. huxley and B. bigelowii they interpreted a salinity of less than 11 psu prior to ~7600 cal yr BP and 17 psu after this time until ~3100 cal yr BP which is in agreement with salinity values given for these intervals by Hiscott et al. (2007), Mudie et al. (2007) and Marret et al. (2009). In addition, the authors state that the colonization of the Black Sea at ~3100 cal yr BP by E. huxley marks the onset of salinity conditions similar to those observed today which the ostracod data supports. Giunta et al. (2007) also noted that lithological boundaries always preceded the biostratigraphic boundaries "probably because colonization of the new habitat by calcareous nannoplankton is gradual" which is also in line with this study and the revised Flood Hypothesis (Major et al., 2006).

144

7.3.1. Comparison of Ostracod Date from Cores MAR05-50 and MAR02-45

Core MAR02-45 was taken from the southwestern Black Sea shelf during a cruise of the RV *Koca Piri Reis* in 2002. This core site is ~70 km from the core site of MAR05-50 (Fig. 7.2). The ostracod data from this core are published as a Master of Science research report completed at the University College London (Evans, 2004) and briefly summarized in Hiscott et al. (2007). The fundamental similarities and differences between these two cores are described below.

7.3.1.1. Timing and Nature of Faunal Turnover in cores MAR02-45 and MAR05-50

The most notable similarity between these two cores is that core MAR02-45 also shows an analogous turnover from a brackish to marine ostracod assemblage at approximately the same time as core MAR05-50 (Fig. 7.3). The turnover in core MAR02-45 begins at ~7600 cal yr BP which is ~150 years earlier than the turnover in core MAR05-50, and is fully changed over to a marine assemblage by 6400 cal yr BP. In core MAR02-45 the ratio of marine to brackish specimens increases steadily until eventually the samples become essentially fully made up of marine species in ~800 years. This is different from the turnover in core MAR05-50 in which the ratio of brackish to marine specimens fluctuates irregularly for ~1000 years until the marine species finally dominate (Fig. 7.3).

Obvious questions are: Why does the transition begin ~150 years earlier at core site MAR02-45 when it is farther from the Bosphorus Strait? And why is the transition more rapid and steady at core site MAR02-45?

There are a few simple points that can explain this small time difference. First,
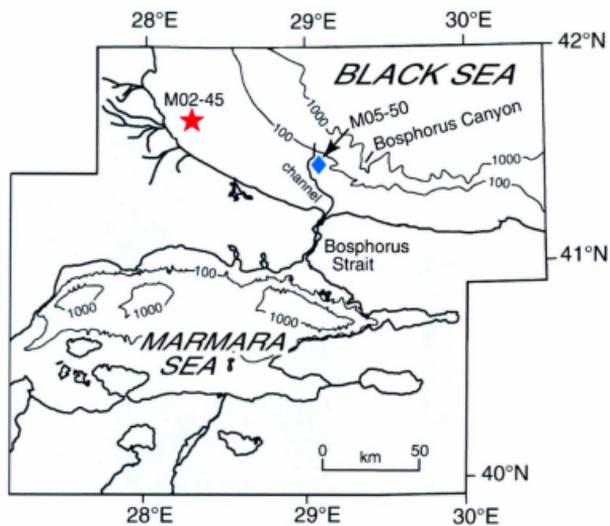
Figure 7.2. Regional map showing the locations of cores MAR05-50 (blue diamond) and MAR02-45 (red star) ~70 km northwest.
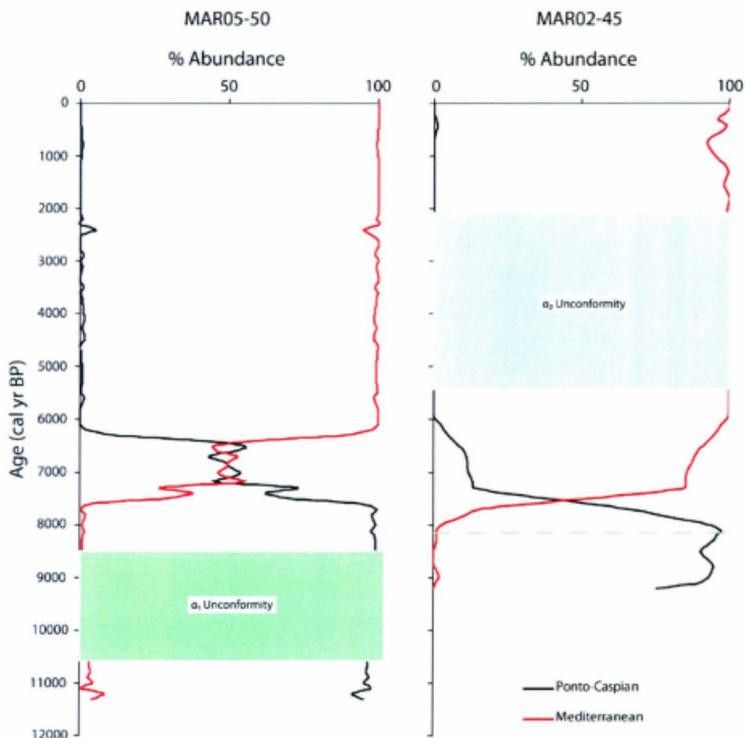
Figure 7.3. Comparison of changes in % abundance of Ponto-Caspian and Mediterranean ostracod species in cores MAR05-50 and MAR02-45. Both cores show an analogous turnover from brackish to marine ostracod species at approximately the same time. In core MAR02-45 the reflector which laterally correlates with the α_1 unconformity is a conformable surface (dashed green line). Likewise, in core MAR05-50 the lateral equivalent of the α_2 unconformity (dashed blue line) is a conformable surface while it is a clear unconformity in core MAR02-45.

147

the standard deviation for the dates bracketing 7500 cal yr BP is between ± 60 and ± 80 (Table 3.1; Hiscott et al., 2007, their Table 1) which could account for the observed difference. Also, the Ager program used to obtain the dates for all depths in core MAR05-50 has the fundamental limitation that it extrapolates and interpolates dates by assuming constant sedimentation rates between actual dated depths. If the actual sedimentation rate was fluctuating then the dates could be slightly too old or too young.

Another reason the brackish to marine faunal turnover at core site MAR05-50 is more irregular compared to core MAR02-45 (Fig. 7.3) is probably because of the immediate proximity of the former to the complex area of mixing near the Bosphorus Strait where the two water masses interact. The slightest variation in Mediterranean water input or Black Sea water output could have affected the abundance of marine and brackish species. Core site MAR02-45 is relatively far from the Bosphorus Strait and thus, not as sensitive to small variations in the water masses passing through the Bosphorus Strait.

Finally, it must be remembered that while salinity is a major control on the distribution of ostracods it is not the only factor. The substrate, availability of food and predation also influence distribution. Therefore, if these parameters were more favorable at core site MAR02-45 it could also explain why the Mediterranean ostracods colonized that area earlier than at core site MAR05-50.

7.3.1.2. Comparison of Species Found in Cores MAR02-45 and MAR05-50

Most of the ostracod species present in core MAR02-45 (Evans, 2004) are also present in core MAR05-50. Although some have differing or unidentified species names

in core MAR02-45, the author believes they are the same based on SEM images published in Evans (2004). *C. edwardsi*, *P. jonesii*, and *P. polita* are three notable Mediterranean species from Bio-zones 5 and 6 (~4350 cal yr BP onward) in core MAR05-50 which were not recorded in core MAR02-45. The transitional species *L. littoralis* appears in core MAR02-45, but makes a far more significant show in core MAR05-50 (Fig. 6.1). Although *L. littoralis* was found in core MAR02-45 (indentified as *Loxoconcha* sp. 3 by Evans) it was only present in very low abundances at only 3 widely spaced sample depths (Evans, 2004). In core MAR05-50 *L. littoralis* has a much more significant role essentially dominating the whole transitional interval and Bio-zone 3.

The reason that *L. littoralis* is abundant in core MAR05-50 and not in MAR02-45 is simply that this species was only able to rapidly colonize the immediate area at the northern exit of the Bosphorus Strait into the Black Sea for ~1000 years. This species did not make its way to core site MAR02-45 in such massive numbers. *P. agilis* (called *P. guttata* by Evans, 2004) became the dominant species after the turnover in core MAR02-45, just as in core MAR05-50, essentially skipping over the *L. littoralis* initial colonization "step".

The Mediterranean species *C. edwardsi*, *P. jonesii* and *P. polita* apparently enjoy high salinities as indicated by their late arrival to the core site MAR05-50 (Fig. 6.1). As with *L. littoralis*, these species are present at core site MAR05-50 but not at core site MAR02-45 simply due to the close proximity of core MAR05-50 to the Bosphorus Strait. A slightly lower salinity at core site MAR02-45 is not likely to be a contributing factor because these species were present since ~4300 cal yr BP (Fig 6.1) when the salinity on

149

the Black Sea shelf was likely lower than modern levels, because shelf waters are generally well mixed by waves and currents.

7.4. Comparison of Depth and Age Data Factor Analysis Results

Factor analysis extracted five R-factors in both the depth (Fig. 5.6) and age (Fig. 6.2) domains. The plots of R-factors 1–4 and Q-factors 1–4 in both the depth and age domains yielded essentially the same results (Fig. 7.4; Fig. 7.5). A discrepancy arises at the extraction of the R-factor 5 and Q-factor 5. The R-factor 5 (and Q-factpr 5) extracted from the depth data is not similar to the R-factor 5 (and Q-factor 5) extracted from the age data (Fig. 7.6).

From the depth data, analysis shows that R-factor 5 is controlled by *L. multipunctata* and *C. variablis* with a negative correlation with *P. agilis*. In this case, Q-factor 5 (Fig. 5.7) looks similar to the abundance plots of *L. multipunctata* and *C. variabilis* (Fig. 5.5a). If this is truly the R-factor 5 then R-factor 5 is a component of Bio-zones 4 and 5.

However, R-factor 5 extracted from the age data is controlled mainly by the occurrence of *C. carinata* and *H. rubra* and the corresponding Q-factor 5 (Fig. 6.3) does indeed have a trend very similar to that of *C. carinata* (Fig. 6.1). In this case, R-factor 5 is a component of all three marine Bio-zones 4–6.

These results most likely mean that in this study the factors begin to lose their meaning at the 5th factor level. The program is forced to extract as many factors as requested by the user. As more factors are extracted, the less significant and interpretable they become.

150
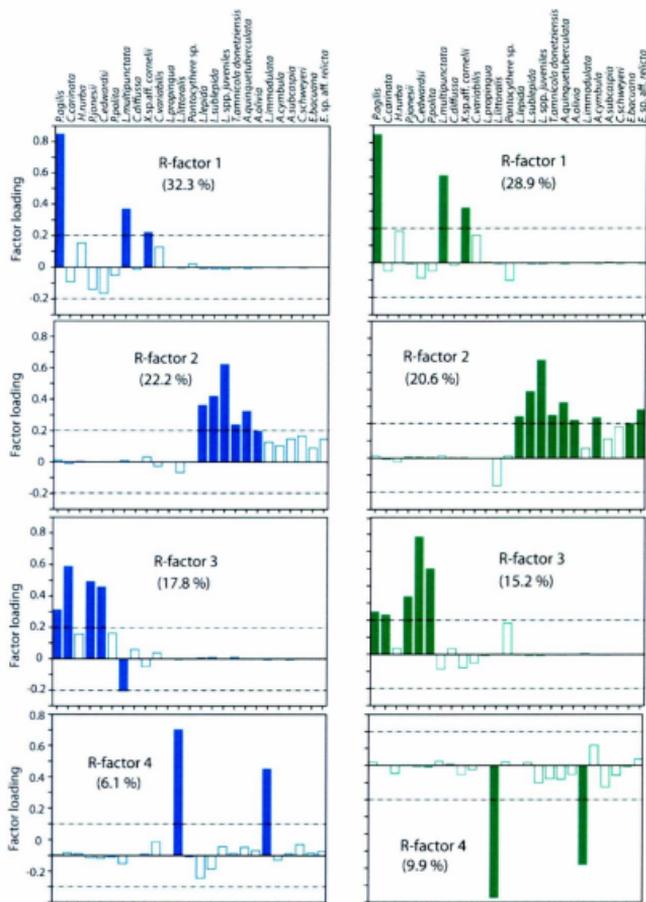
Figure 7.4. R-factor analysis of the depth (blue) and age (green) data yielded essentially the same results for the first four extracted factors.

151
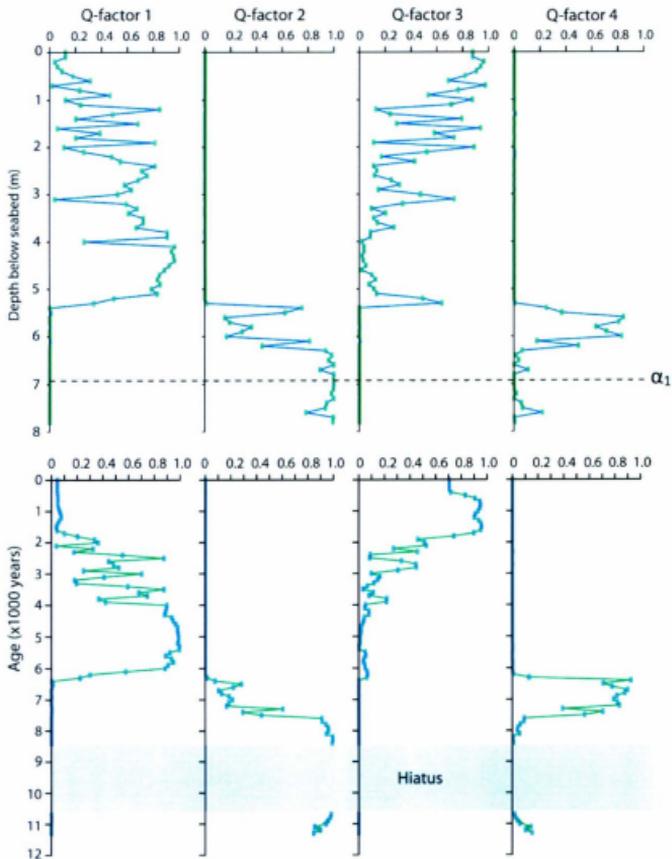
Figure 7.5. Q-factor plots from depth (top) and age (bottom) data are essentially the same for the first four extracted factors, showing distinct lower, middle and upper divisions.
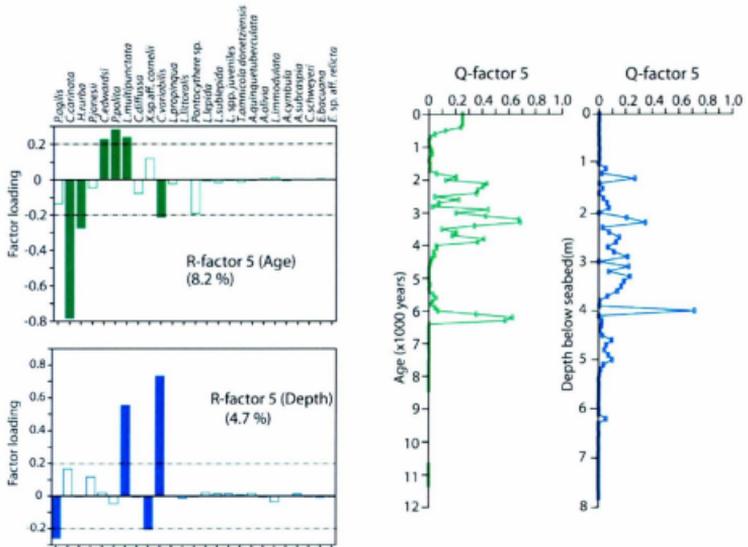
Figure 7.6. A comparison of R-factor 5 (left) and Q-factor 5 (right) from the depth data (blue) and age data (green) shows that these results do not concur.

7.5. Summary and Comment on Validity of Three Hypotheses of Reconnection

In summary, detailed identification and interpretation of ostracods in 89 samples from core MAR05-50 revealed that during the early Holocene, from ~11400 to ~7500 cal yr BP the southwestern Black Sea shelf was part of a brackish water "lake" which had no large or continuous input of water from the World Ocean. The ostracod fauna show the presence of a diverse and thriving brackish water ostracod community dominated by *L. sublepida* and *L. lepida* until 7580 cal yr BP. After 7450 cal yr BP the first Mediterranean species *L. littoralis* began to aggressively colonize the southwestern Black Sea shelf north of the Bosphorus Strait. For ~1000 years the original Ponto-Caspian ostracod species and the new Mediterranean immigrant species lived at the MAR05-50 core site in more or less equal abundances. After ~6400 cal yr BP the Mediterranean species began to diversify and dominate the core site on the southwestern Black Sea shelf. The Ponto-Caspian ostracod species and the Mediterranean species *L. littoralis* were replaced by new Mediterranean ostracod species, the most abundant being *P. agilis*.

The sedimentological data from core MAR05-50 and the findings of other authors suggests that a two-way flow between the Black Sea and the Mediterranean Sea was initiated at ~8500 cal yr BP. Therefore, there is a lag of ~1000 years between the first persistent entry of Mediterranean water into the Black Sea at ~8500 cal yr BP and the discernible colonization of the area by Mediterranean ostracod species at ~7500 cal yr BP. This lag is interpreted as the amount of time necessary for the water at the MAR05-50 core site to reach salinity levels favorable to ostracods migrating from the more saline environment of the Mediterranean Sea. Statistical analyses of the ostracod data show 6 Bio-zones with distinct ostracod assemblages; changes in those assemblages indicate a

gradual and sequential salinization of the Black Sea bottom water as a result of steady inflow of Mediterranean waters since ~8500 cal yr BP. The uppermost Bio-zone 6 contains ostracods which favor marine salinities, some of which can inhabit depths of 100 m or more, suggesting that sealevel and salinity values in the Black Sea were near modern values by ~2300 cal yr BP.

The main objective of this thesis was to delineate the paleoenvironmental evolution of the post-glacial Black Sea and to evaluate the validity of the three existing hypotheses regarding the post-glacial reconnection of the Black Sea with the Mediterranean Sea (i.e., the Flood Hypothesis, which argues for a catastrophic flooding of an isolated Black Sea by Mediterranean water at ~9150 cal yr BP; the Outflow Hypothesis, which argues for Black Sea outflow since at least ~11900 cal yr BP and a systematic reconnection with the Mediterranean Sea through the Bosphorus Strait sometime between 8500 cal yr BP and 8000 cal yr BP and a subsequent gradual salinization of the Black Sea bottom water; and the Oscillating Hypothesis which argues for neither a catastrophic nor a gradual reconnection but a cycle of transgressions and regressions over the Holocene after a temporary lowstand of ~ -50 m sometime between ~12700 cal yr BP and ~10000 cal yr BP (Chepalyga, 2002; Yanko-Hombach et al., 2007; Ivanova et al., 2007).

The ostracod data do not support the Flood Hypothesis. The statistical analysis clearly indicates an ordered and progressive replacement of Ponto-Caspian ostracod species by Mediterranean species. First of all, the ostracod data show that the core location was transgressed by brackish water and not subaerially exposed or covered by fresh water as the Flood Hypothesis would require. Furthermore, the marine Bio-zones 4-

155

6 strongly suggest that the post-reconnection salinization of the Black Sea was gradual and involved steps of increasing salinity over ~5000 years. The first Mediterranean species to appear is a single immigrant (*L. littoralis*), not the introduction of many new species which would be expected with a catastrophic inundation. The ostracod data do not suggest a catastrophic flooding of the Black Sea by Mediterranean water at 9150 cal yr BP from a lowstand of ~-95 m as proposed by Ryan et al. (2003).

With regard to the Oscillating Hypothesis, the ostracod data do not support or refute a regression and disconnection from the Marmara Sea between ~12700 cal yr BP and ~10000 cal yr BP. First of all, core MAR05-50 only contains sediments beginning at ~11500 cal yr BP, so the ostracod data cannot suggest what was happening on the southwestern Black Sea shelf before that time. Also, there are no ostracod data from 10600 cal yr BP to 8500 cal yr BP because there was a depositional hiatus at that time. The ostracod data from 11400 cal yr BP to 10600 cal yr BP do not conflict with a drawdown of water to -50 m during that time. Proponents of the Outflow Hypothesis also agree that the Black Sea level was as shallow as ~-40 m during the early Holocene but that it remained high enough that outflow was continuous. Sealevel oscillations outlined by Chepalyga (2002) for the Holocene are only on the order of a few tens of meters up to ~-40 m. These water depths would have still been suitable for the ostracods living there.

Furthermore, modelling by Soulet et al. (2010) indicated that a catastrophic marine breakthrough into the Black Sea (i.e., the Flood Hypothesis) would have had little effect on salinity. Salinity changes associated with relatively gradual and smaller sealevel transgressions and regressions (i.e., the Oscillating Hypothesis) would not have caused discernible changes in the ostracod assemblage. Therefore, the ostracod data from core

156

MAR05-50 neither contradicts nor confirms the sealevel oscillations in the Black Sea through the Holocene and the author agrees that the oscillating scenario suggested by Chepalyga (2002), Yanko-Hombach et al. (2007) and Ivanova et al. (2007) is entirely plausible.

With regard to the Outflow Hypothesis, the ostracod data from core MAR05-50 do support the scenario of a transgressed southwestern Black Sea shelf at least by ~11500 cal yr BP. Furthermore, the Outflow Hypothesis argues for a low salinity Black Sea before a gradual and progressive reconnection with the Mediterranean sometime between 8500 cal yr BP and 8000 cal yr BP which is supported by the ostracod data from core MAR05-50. Most importantly, the statistical data point to a successive and gradual turnover from brackish to marine ostracod species starting at 7450 cal yr BP after an ~1000 salinization lag and subsequent step-wise changes in the ostracod assemblages reflecting a progressive salinization of the Black Sea bottom water as argued by the Outflow Hypothesis. However, a caveat is necessary because Soulet et al. (2010) showed that a catastrophic inundation of the Black Sea by Mediterranean water would have had little effect on salinity, and even with such a catastrophic flood the subsequent salinity variations would still have been gradual up to ~2000 cal yr BP.

7.6. Future Work

7.6.1. Ostracod Geochemistry

Considerable information can be gained from ostracod shell chemistry. Because the ostracod moults quickly its carapace preserves a precise record of the ambient water conditions at that time. Also, because ostracod shells do not have chambers they are

often smooth and are less likely to be contaminated than other types of shells (Dwyer et al., 2002). Holmes and Chivas (2002) and Dwyer et al. (2002) give good overviews of applications of ostracod shell chemistry.

Trace elements are partitioned into the ostracod valve at the time of shell secretion. The main trace elements in the ostracod shell are Mg, Sr, Na, K, and Ba (Anadón et al., 2002). Mg/Ca and Sr/Ca ratios and oxygen isotopes in the ostracod valve can be used to interpret paleotemperature and paleosalinity but this application is not yet fully understood (Holmes and Chivas, 2002; Boomer et al., 2003) and there may be inter- and intra-specific variation in trace element uptake (Dwyer et al., 2002). Ostracods might also have the potential to be valuable indicators of water pollution by measuring the content of heavy metals such as Co, Ni, Cu, Zn, Cd and Pb in their valves but so far this has not been studied adequately (Holmes and Chívas, 2002).

An ostracod carapace is made of carbonate and thus, if younger than 50000 years, contains a proportion of radiogenic ^{14}C. Therefore, radiocarbon dates can be obtained from ostracod shells. According to Holmes and Chivas (2002) it is possible to obtain a radiocarbon date from a single large ostracod valve.

For geochemical results to be meaningful, the most pristine material must be used. Pristine ostracod valves of most species are abundant in cores MAR05-50P and MAR05-51G. For future work, extraction of geochemical data from the ostracod valves from these cores is recommended to further illuminate the Holocene paleoclimatic and paleoceanographic evolution of the Black Sea. The original material (i.e., ostracod valves) used in this thesis is archived at the Earth Sciences Department at Memorial

University of Newfoundland for such studies in the future.

7.6.2. Cores

In future, it would be interesting to examine ostracod valves from older sediments than those recovered in core MAR05-50 (i.e., older than ~11500 cal yr BP) and particularly from along the Bosphorus "corridor" heading southeast into the Marmara Sea to investigate whether ostracod records could point to a continuous or interrupted Black Sea outflow during the Late-Glacial–Holocene transition.

CHAPTER 8

CONCLUSIONS

The main objective of this thesis was to further elucidate the post-glacial paleoclimatic and paleoceanographic evolution of the Black Sea using the microfossil *Ostracoda* while also highlighting Black Sea ostracod taxonomy and the use of the ostracods in paleoenvironmental studies. The following salient conclusions were reached in this thesis:

1. A chronostratigraphic framework was constructed for the latest glacial to Recent sediments recovered in a 737 cm-long piston core (MAR05-50P) and its 157 cm-long gravity core (MAR05-51G) raised from 91 m depth on the southwestern Black Sea shelf on the eastern levee of a channel which accommodates the inflow of dense, saline Mediterranean water into the Black Sea. A 787 cm-long Composite core MAR05-50 was constructed from the two above cores by adding the top 50 cm of core MAR05-51G to the top of core MAR05-50P to account for an estimated core top loss of 50 cm from core MAR05-50P. Fourteen radiocarbon dates were obtained from fossil material from the above cores and an age model was constructed for core MAR05-50 using nine of the fourteen radiocarbon dates, omitting dates considered to be unreliable. MAR05-50 recovered a sedimentary record of the southwestern Black Sea shelf for essentially the entire Holocene epoch from ~11500 cal yr BP to present. An unconformity known as α_1 occurs at 695 cm depth in core MAR05-50. The sediments directly below and above unconformity α_1 were dated by extrapolation to delineate a depositional hiatus at the core site on the southwestern Black Sea shelf from ~10600 cal yr BP to ~8500 cal yr BP.

Based on sedimentological data from core MAR05-50 and geochemical data from core MAR02-45, a persistent inflow from the Mediterranean Sea is interpreted to have begun at ~8500 cal yr BP.

2. Ostracod valves were collected from 89 samples extracted from cores MAR05-50P and MAR05-51G at 10 cm intervals. With the aid of taxonomic literature 45 individual ostracod species were identified on the basis of gross morphology of the valves. From the base of core MAR05-50 dated at 11490 cal yr BP to 7580 cal yr BP the ostracod assemblage is clearly dominated by species known to be Ponto-Caspian types. This ostracod assemblage from this lower interval of core MAR05-50 is referred to as the "brackish assemblage". At 7450 cal yr BP there is an abrupt change in the ostracod assemblage in core MAR05-50. The Mediterranean species *Loxoconcha littoralis* becomes the dominant species in the interval from 7450 cal yr BP to 6410 cal yr BP. The ostracod assemblage from this interval is referred to as the "transitional assemblage". During this interval *L. littoralis* co-exited with the brackish water species in more or less equal abundances. At 6280 cal yr BP another change occurs in the ostracod assemblage. The first Mediterranean species *L. littoralis* and the Ponto-Caspian species are replaced by new species from the Mediterranean Sea. This interval from 6280 cal yr BP to the present is fully dominated by Mediterranean species and is known as the "marine assemblage".

3. There was a time lag of ~1000 years between the initiation of persistent inflow from the Mediterranean Sea at ~8500 cal yr BP and the colonization of the Black Sea shelf by the first Mediterranean ostracod species *L. littoralis*. This lag is interpreted as

the time needed for enough water to enter the Black Sea to mix with the bottom water to raise the salinity to levels favorable to Mediterranean ostracod species.

4. CONISS cluster analyses was able to further divide the above observed assemblages into 6 Bio-zones where distinct changes in the ostracod assemblages occurred reflecting ecological changes which evolved at the MAR05-50 core site since 11490 cal yr BP. Bio-zone 1 and Bio-zone 2 together constitute the lower, brackish assemblage. The main species that comprise this assemblage are *L. sublepida*, *L. lepida*, *T. amnicola donetziensis*, *C. schweyeri*, *A. olivia* and *A. quinquetuberculata*. Small changes in abundances separate Bio-zones 1 and 2 but the main species present remain the same. Based on the modern occurrences of Bio-zone 1 and 2 species in the Caspian and Azov Seas and estuarine areas around the Black Sea, the ecology of the Black Sea during the interval 11490–7580 cal yr BP is thought to have been low salinity, possibly as low was 5 psu up to ~10 psu, and the sea level was probably a few tens of meters shallower than today.

5. Bio-zone 3 equates to the transitional assemblage where salinities were raised enough for the Mediterranean species *L. littoralis* to rapidly move into the area. *L. littoralis* might indicate that the salinity of the Black Sea bottom water at that time (7450–6410 cal yr BP) could have been around 13–15, with an upper limit of ~18 psu, which would seem to be at the upper tolerance limits for the brackish water species which prefer more reduced salinities.

6. CONISS separated the upper, marine assemblage into Bio-zones 4, 5 and 6. Bio-zone 4 is the first marine bio-zone where the Mediterranean species *P. agilis*, *H. rubra*, *C. carinata*, *L. multipunctata* and *C. variabilis* first dominate the core site from

162

6280 cal yr BP to 4350 cal yr BP.   At 4350 cal yr BP Bio-zone 5 begins with the introduction of two new sublittoral Mediterranean species: *P. jonesii* and *C. edwardsi*. The introduction of these two species to the MAR05-50 core site is interpreted to reflect an increase in salinity and possibly an increase in water depth.   Based on the salinity tolerance given by (Neal, 1988) for *P. jonesii* of 26–35 psu the salinity might have been near or in this range during the Bio-zone 5 interval.   The uppermost Bio-zone 6 is marked by the introduction of another new marine species *P. polita*, which lives today in the Mediterranean and North Atlantic waters, and an increase in the abundances of *P. jonesii* and *C. edwardsi* and the virtual disappearance of Bio-zone 4 and 5 species *L. multipunctata* and *C. variabilis*.   This clear assemblage change must indicate ongoing ecological change and probably corresponds to salinity levels approaching levels modern values.   The results of statistical analyses described above clearly shows that the ostracod assemblage of core MAR05-50 underwent progressive, step-wise changes driven by salinity changes over ~5000 years.

      7.   The final objective of this thesis was to evaluate the validity of the three existing hypotheses regarding the post-glacial reconnection of the Black Sea with the Mediterranean Sea.   The three prevailing hypotheses are: the Flood Hypothesis, which argues for a catastrophic flooding of an isolated Black Sea by Mediterranean water at ~9150 cal yr BP; the Outflow Hypothesis, which argues for Black Sea outflow since at least ~11900 cal yr BP and a reconnection with the Mediterranean Sea through the Bosphorus Strait sometime between 8500 cal yr BP and 8000 cal yr BP and a subsequent gradual salinization of the Black Sea bottom water; and the Oscillating Hypothesis which argues for neither a catastrophic nor a gradual reconnection but an oscillating Black Sea

level between -50 and approximately current level after a temporary Early Holocene lowstand as early as ~12700 cal yr BP to ~10000 cal yr BP. The ostracod data do not agree with the Flood Hypothesis. After Mediterranean inflow was established at ~8500 cal yr BP, the area around the core site was colonized by one Mediteranean species (*L. littoralis*) which had been present in low abundances pre-reconnection. When the saline water began to flow in this species was able to thrive. If there had been a sudden inundation of Mediterranean water, an influx of many Mediteranean species would be expected. The ostracod data do not suggest a catastrophic flooding of the Black Sea by Mediterranean water at 9150 cal yr BP as proposed by Ryan et al. (2003). The regression proposed by Yanko-Hombach et al. (2007) between ~12700 cal yr BP and ~11200 cal yr BP cannot be refuted because core MAR05-50 only contains sediments as old as ~11490 cal yr BP, so the ostracod data cannot suggest what was happening on the southwestern Black Sea shelf before that time. More data from older sediments is needed to further shed light on the latest glacial to Holocene transition. The ostracod data neither contradicts nor confirms the sealevel oscillations in the Black Sea through the Holocene as suggested by Chepalyga (2002), Yanko-Hombach et al. (2007) and Ivanova et al. (2007). The author acknowledges that an oscillating Holocene Black Sea level is entirely possible. Similarly, the ostracod data are in general agreement with the Outflow Hypothesis in that the southwestern Black Sea shelf was covered by brackish water by the early Holocene and a reconnection with the Mediterranean Sea happened in a gradual and ordered manner. However, the ostracod data cannot confirm or refute the scenario of an uninterrupted post-glacial Black Sea outflow. Future work is needed to further test the validity of the Outflow Hypothesis and the Oscillating Hypothesis.

References

Abdi, H. (2003). Factor Rotations in Factor Analysis. In: M. Lewis-Beck., A. Bryman, & T. Futing (Eds.), *Encyclopedia of social sciences research methods.* Thousand Oaks: Sage.

Abe, K. (1990). What the sex ratio tells us: a case from marine ostracods. In R. Whatley, & C. Maybury (Eds.), *Ostracoda and global events* (pp. 175–185). Cambridge: Chapman Hall.

Agalarova, D.A., Kadyrova, Z.K., & Kulieva, S.A. (1961). *Ostracoda from Pliocene and post-Pliocene deposits of Azerbaijan, Baku.* Baku: Azerbaijan State Publisher. [in Russian]

Aksu, A.E., Hiscott, R.N., & Yaşar, D. (1999). Oscillating Quaternary water levels of the Marmara Sea and vigorous outflow into the Aegean Sea from the Marmara Sea-Black Sea drainage corridor. *Marine Geology (153),* 275–302.

Aksu, A.E., Hiscott, R.N., Kaminski, M.A., Mudie, P.J., Gillespie, H., Abrajano, T., & Yaşar, D. (2002a). Late-Glacial-Holocene paleoceanography of the Black Sea and Marmara Sea: stable isotopic, foraminiferal and coccolith evidence. *Marine Geology, 190,* 119–149.

Aksu, A.E., Hiscott, R.N., Yaşar, D., Işler, F.I., & Marsh, S. (2002b) Seismic stratigraphy of Late Quaternary deposits from the southwestern Black Sea shelf: evidence for non-catastrophic variations in sea-level during the last ~10 000 yr. *Marine Geology, 190,* 61–94.

Aladin, N.V. (1993). Salinity tolerance, morphology and physiology of the osmoregulatory organ in Ostracoda with special reference to Ostracoda from the Aral Sea. In P. Jones, & K. McKenzie (Eds.), *Ostracoda in the earth and life sciences* (pp. 387–403).

Anadón, P., Gliozzi, E., & Mazzini, I. (2002). Paleoenvironmental reconstruction of marginal marine environments from combined paleoecological and geochemical analyses on ostracods. In J.A. Holmes, & A.R. Chivas (Eds.), *the Ostracoda: Applications in Quaternary research* (pp. 227–247). Washington: American Geophysical Union.

Athersuch, J. (1979). The ecology and distribution of the littoral ostracods of Cyprus. *Journal of Natural History, 13*(2), 135–160.

Athersuch, J., & Whittaker, J.E. (1987). On *Carinocythereis carinata* (Roemer). *Stereo-Atlas ostracod shells, 14,* 97–102.

Athersuch, J., & Horne, D.J. (1987). Some species of the genus *Sclerochilus* Sars(Crustacea: Ostracoda) from British waters. *Zoological Journal of the Linnean Society, 91,* 197–222.

Athersuch, J., Horne, D.J., & Whittaker, J.E. (1989). *Marine and brackish water ostracods*. Bath: E.J. Brill.

Baird, W. (1850). *The natural history of the British Entomostraca*. London: Ray Society.

Balkas, T.G., Dechev, R., Mihnea, P.E.., & Serbanescu, O. (1990). State of the marine environment in the Black Sea region. *UNEP Regional Seas Report and Studies*, No. 124.

Ballard, R.D., Coleman, D.F., & Rosenberg, G.D. (2000). Further evidence of abrupt Holocene drowning of the Black Sea shelf. *Marine Geology, 170,* 253-261.

Benson, R.H. (1976). Changes in the ostracods of the Mediterranean with the Messinian Salinity Crisis. *Palaeogeography, Palaeoclimatology, Palaeoecology, 20, 147–170.*

Birks, H.J.B., & Gordon, A.D. (1985). *Numerical methods in Quaternary pollen analysis*. London: Academic Press.

Bonaduce, G., Ciampo, G., & Masoli, M. (1975). *Distribution of Ostracoda in the Adriatic Sea*. Naples: Stazione Zoologica di Napoli.

Boomer, I., Whatley, R.C. & Aladin, N. (1996). Aral Sea Ostracoda as environmental indicators. *Lethaia, 29*, 77-85.

Boomer, I., Horne, D.J., & Slipper, I.J. (2003). The use of ostracods in palaeoenvironmental studies, or what can you do with an ostracod shell? *Paleontological Society Papers, 9*,153–179.

Boomer, I., von Grafenstein, U., Guichard, F. & Bieda, S. (2005). Modern and Holocene sublittoral ostracod assemblages (Crustacea) from the Caspian Sea: A unique brackish, deep-water environment. *Palaeogeography, Palaeoclimatology, Palaeoecology, 225*, 173–186.

Boomer, I., Guichard, F., & Lericolais, G. (2010). Late Pleistocene to Recent ostracod assemblages from the western Black Sea. *Journal of Micropalaeontology, 29*, 119–133.

Brady, G.S. (1868). A monograph of the of the Recent British Ostracoda. *Transactions of the Linnean Society of London, 26*, 353–495.

Brady, G.S., & Robertson D. (1869). Notes of a week's dredging in the west of Ireland. *Annals and magazine of Natural History, series 4 (3)*.

Brady, G.S., & Norman, A.M. (1889). A monograph of the marine and freshwater Ostracoda of the North Atlantic and of northwestern Europe. Section I. Podocopa. *Scientific Transactions of the Royal Dublin Society, series 2, (4)*, 63–270.

Brady, G.S., & Robertson, D. (1872). Contributions to the study of the Entomostraca. No. 9. On the Ostracoda taken amongst the Scilly Isles, and on the anatomy of *Darwinula stevensoni*. *Annals and Magazine of Natural History, series 4(9)*, 48–70, pls 1–2.

Cabral, M.C., Luz, C., & Fatela, F. (2011). First survey of Recent ostracods from the continental shelf of Western Algarve, South Portugal. In M. Gross (Ed.), European Ostracodologists Meeting 7, Abstract Volume (pp. 39–41). Graz: Universalmuseum Joanneum.

Caraion, F.E. (1963). St. cerc. biol., Seria biol. anim.

Cattell, B. (1966). The scree test for the number of factors. Multivariate Behavioral Research, 1, 245-276.

Chepalyga, A.L. (1984). Inland Sea Basins. In: A.A. Velichkno (Ed.), Late Quaternary Environments of the Soviet Union (pp. 229–247). Minneapolis: University of Minnesota Press.

Chepalyga, A.L. (2002). The Black Sea. In A.A. Velichko (Ed.), Development of the northern landscapes and climate: Last Pleistocene-Holocene – Perspectives of the future (pp. 205–285). Moscow: GEOS. [in Russian]

Cohen, A.C., Martin, J.W., & Kornicker, L.S. (1998). Homology of Holocene ostracode biramous appendages with those of other crustaceans: the protopod, epipod, exopod and endopod. Lethaia, 31(3), 251–265.

Danielpol, D.L., Ito, E., Wansard, G., Kamiya, T., Cronin, T.M., & Baltanás, A. (2002). Techniques for collection and study of Ostracoda. In J.A. Holmes, & A.R. Chivas (Eds.), the Ostracoda: Applications in Quaternary research (pp. 65–97). Washington: American Geophysical Union.

Davis, J.C. (1973). Statistics and data analysis in geology. United Sates: John Wiley & Sons.

De Deckker, P. (2002). Ostracod palaeoecology. In J.A. Holmes, & A.R. Chivas (Eds.), the Ostracoda: Applications in Quaternary research (pp. 121–134). Washington: American Geophysical Union.

Dubowsky, N.W. (1939). On the ostracod fauna of the Black Sea. *Trudy. Karadah. Nauch. Sta. T.I. Vyazemskoho, 5,* 1–68.

Dwyer, G.S., Cronin, T., & Baker, P. (2002). Trace elements in marine ostracods. In J.A. Holmes, & A.R. Chivas (Eds.), *the Ostracoda: Applications in Quaternary research* (pp. 205–225). Washington: American Geophysical Union.

Elofson, O. (1941). Zur Kenntnis der marinen Ostracoden Schwedens mit besonderer Berucksichtigung des Skageraks. *Zoologiska Bidrag Fran Uppsala, 19,* 217–534.

Evans, J.M. (2004). *Noah's flood: Fact or fiction? A paleoenvironmental study of Holocene Black Sea Ostracoda* (master's project report). University College London, London.

Eriş, K.K., Ryan, W.B.F., Çagatay, M.N., Sancar, U., Lericolais, G., Ménot, G., & Bard, E. (2007). The timing and evolution of the post-glacial transgression across the Sea of Marmara shelf south of İstanbul. *Marine Geology 243,* 57–76.

Filipova-Marinova, M. (2007). Archaeological and paleontological evidence of climate dynamics, sea-level change, and coastline migration in the Bulgarian sector of the Circum-Pontic region. In V. Yanko-Hombach, A.S. Gilbert, N. Panin, & P.M. Dolukhanov (Eds.), *The Black Sea flood question: Changes in coastline, climate and human settlement* (pp. 453–482). Heidelberg: Springer.

Finetti, I., Bricchi, G., Del Ben, A., Papin, M., & Xuan, Z. (1988). Geophysical study of the Black Sea area. *Bollettino di Geofisica Teorica e Applicata, 30*(117–118), 197–324.

Flood, R.D., Hiscott, R.N., & Aksu, A.E. (2009). Morphology and evolution of an anastomosed channel network where saline underflow enters the Black Sea. *Sedimentology, 56,* 807–839.

Frenzel, P., & Boomer, I. (2005). The use of ostracods from marginal marine, brackish waters as bioindicators of modern and Quaternary environmental change. *Palaeogeography, Palaeoclimatology, Palaeoecology,225*(1–4), 68–92.

Giosan, L., Donnelly, Constantinescu, S., Filip, F., Ovejanu, I., Vespremeanu-Stroe, A., Vespremeanu, E., & Duller, G.A.T. (2006). Young Danube delta documents stable Black Sea level since the middle Holocene: Morphodynamic, aleogeographic, and archaeological implications. *Geological Society of America, 24,* (9) 757–760.

Giosan, L., Filip, F., & Constatinescu, S. (2009). Was the Black Sea catastrophically flooded in the early Holocene? *Quaternary Science Reviews, 28,* 1–6.

Giunta, S., Morigi, C., Negri, A., Guichard, F., & Lericolais, G. (2007). Holocene biostratigraphy and paleoenvironmental changes in the Black Sea based on calcareous nannoplankton. *Marine Micropaleontology, 63,* 91–110.

Glenn, C.R., & Arthur, M.A. (1984). Sedimentary and geochemical indicators of productivity and oxygen contents in modern and ancient basins: the Holocene Black Sea as the "type" anoxic basin. *Chemical Geology, 48,* 325–354.

Gordon, A.D., & Birks, H.J.B. (1972). Numerical methods in Quaternary palaeoecology. I. Zonation of pollen diagrams. *New Phytologist 71,* 961–979.

Grimm, E.C. (1987). CONISS: A FORTRAN 77 program for stratigraphically constrained cluster analysis by the method of incremental sum of squares. *Computers & Geosciences, 13*(1), 13–35.

Hiscott, R.N., Aksu, A.E., Yaşar, D., Kaminski, M.A., Mudie, P.J., Kostylev, V.E., MacDonald, J.C., Işler, F.I., & Lord, A.R. (2002). Deltas south of the Bosphorus strait record persistent Black Sea outflow to the Marmara Sea since ~10 ka. *Marine Geology, 190,* 95–118.

Hiscott, R.N., Aksu, A.E., Mudie, P.J., Marret, F., Abrajano, T., Kaminsli, M.A., ...Yaşar, D. (2007). A gradual drowning of the southwestern Black Sea shelf: evidence for

a progressive rather than abrupt Holocene reconnection with the eastern Mediterranean Sea through the Marmara Sea Gateway. *Quaternary International, 167–168,* 19–34.

Hiscott, R.N., Aksu, A.E., & Mudie, P.J. (2008). Comment on "The timing and evolution of the post-glacial transgression across the Sea of Marmara shelf south of İstanbul" by Eriş et al., Marine Geology 243, 57–76. *Marine Geology, 248,* 228–236.

Hiscott, R.N., & Aksu, A.E. (2002). Late Quaternary history of the Marmara Sea and Black Sea from high-resolution seismic and gravity-core studies. *Marine Geology, 190,* 261–282.

Holmes, J.A., & Chivas, A.R. (2002a). Ostracod shell chemistry: overview. In J.A. Holmes, & A.R. Chivas (Eds.), *the Ostracoda: Applications in Quaternary research* (pp. 185–204). Washington: American Geophysical Union.

Holmes, J.A., & Chivas, A.R. (2002b). Introduction. In J.A. Holmes, & A.R. Chivas (Eds.), *the Ostracoda: Applications in Quaternary research* (pp. 1–4). Washington: American Geophysical Union.

Horne, D.J., Cohen, A., & Martens, K. (2002). Taxonomy, morphology and biology of Quaternary and living Ostracoda. In J.A. Holmes, & A.R. Chivas (Eds.), *the Ostracoda: Applications in Quaternary research* (pp. 5–36). Washington: American Geophysical Union.

Imbrie, J., Hays, J. D., Martinson, D. G., McIntyre, A., Mix, A. C., Morley, J. J., Pisias, N. G., Prell, W. L., Shackleton, N. J. (1984). The orbital theory of Pleistocene climate : support from a revised chronology of the marine δ^{18}O record. In A. Berger, J. Imbrie, H. Hays, G. Kukla, & B. Saltzman (Eds.), Milankovitch and Climate: Understanding the Response to Astronomical Forcing, Proceedings of the NATO Advanced Research Workshop held 30 November - 4 December, 1982 in Palisades, NY. (p.269). Dordrecht: D. Reidel Publishing.

Ivanova, E.V., Murdmaa, I.O., Chepalyga, A.L., Cronin, T.M., Pasechnik, I.V., Levchenko, O.V.,...Platonova, E.A. (2007). Holocene sea-level oscillations and environmental changes on the Eastern Black Sea shelf. *Palaeogeography, Palaeoclimatology, Palaeoecology, 246,* 228–259.

Kaminski, M.A., Aksu, A.E., Box, M., Hiscott, R.N., Filipescu, S., & Al-Salameen, M. (2002). Late glacial to Holocene benthic foraminifera in the Marmara Sea: Implications for Black Sea-Mediterranean Sea connections following the last deglaciation. *Marine Geology, 190,* 165–202.

Keen, M.C. (1982). Intraspecific variation in Tertiary ostracods. In R.H. Bates, E. Robinson, & L.M. Sheppard (Eds.), *Fossil and Recent Ostracods* (pp. 381–405). Chichester: Ellis Horwood Ltd.

Kerey, I.E., Meriç, E., Tunoğlu, C., Kelling, G., Brenner, R.L., & Doğan, A.U. (2004). Black Sea-Marmara Sea Quaternary connections: new data from the Bosphorus, İstanbul, Turkey. *Palaeogeography, Palaeoclimatology, Palaeoecology, 204,* 277–295.

Kılıç, M. (2000). Recent Ostracoda (Crustacea) fauna of the Black Sea coasts of Turkey. *Turkish Journal of Zoology, 25,* 375–388.

Klovan, J.E., & Imbrie, J. (1971). An algorithm and FORTRAN-IV program for large scale Q-mode factor analysis and calculation of factor scores. *Mathematical Geology, 3,* 61–77.

Lane-Serff, G.F., & Rohling, E.J. (1997). Postglacial connection of the Black Sea to the Mediterranean and its relation to the timing of sapropel formation. *Paleoceanography, 12*(2), 169–174.

Latif, M.L., Özsoy, E., Salihoğlu, I., Gaines, A.F., Başturk, Ö., Yılmaz, A., & Tuğrul, S. (1992). Monitoring via direct measurements of the modes of mixing and transport

of waste-water discharges into the Bosphorus underflow. *Middle East Technical University, Institute of Marine Sciences, Technical Report, 92-2*, 98 pp.

Lericolais, G., Bulois, C., Gillet, H., & Guichard, F. (2009). High frequency sea level fluctuations recorded in the Black Sea since the LGM. *Global and Planetary Change, 66,* 65–75.

Lericolais, G., Guichard, F., Morigi, C., Minereau, A., Popescu, I., & Radan, S. (2010). The post Younger Dryas Black Sea regression identified from sequence stratigraphy correlated to core analysis and dating. *Quaternary International, 225*(2), 199–209.

Letouzey, J., Biju-Duval, B., Dorkel, A., Gonnard, R., Kristchev, K., Montadert, , L., & Sungurlu, O. (1977). The Black Sea: a marginal basin; geophysical and geological data. In B. Biju-Duval, & L. Montadert (Eds.), *International symposium on the structural history of the Mediterranean basins* (pp. 363–376). Paris: Editions Technip.

Linegar, A. (2012). *Paleoenvironmental history of the southwestern Black Sea: an elemental and stable isotopic study* (master's thesis). Memorial University of Newfoundland, Canada.

Livental, V.E. 1929. Ostracoda of Akchagilian and Apsheronian beds of the Babazan Section. *Izvestiya Azerbajdzahnskogo Politekhnischeskogo Instituta, 1,* 1-58. [In Russian]

Livental, V.E. (1938). Deposits and microfaunaof the Baku area. *Azerbaijan Scientific Research Institute for Petroleum, Transactions, 1,* 46–67. [in Russian]

Major, C., Ryan, W., Lericolais, G., & Hajdas, I. (2002). Constraints on Black Sea outflow to the Sea of Marmara during the last glacial-interglacial transition. *Marine Geology, 190,* 19–34.

Major, C.O., Goldstein, S.L., Ryan, W.B.F., Lericolais, G., Piotrowski, A.M., & Hajdas, I. (2006). The co-evolution of Black Sea level and composition through the last deglaciation and its paleoclimate significance. *Quaternary Science Reviews, 25,* 2031–2047.

Mandelstam, M.I., Markova, L., Rosyeva, T., & Stepanaitys, N. (1962). *Ostracoda of the Pliocene and post-Pliocene deposits of Turkmenistan*. Ashkhabad: Turkmenistan Geological Institute.

Marret, F., Mudie, P.J., Aksu, A.E., & Hiscott, R.N. (2009). A Holocene dinocyst record of a two-step transformation of the Neoeuxinian brackish water lake into the Black Sea. *Quaternary International, 197,* 72–86.

Martin, R.E., Leorri, E., & McLaughlin, P.P. (2007). Holocene sea level and climate change in the Black Sea: Multiple marine incursions related to freshwater discharge events. *Quaternary International, 167–168,* 61–72.

Merten, K.N., Bradley, L.R., Takano, Y., Mudie, P.J., Marret, F., Aksu, A.E.,...Matsuoka, K. (2012). Quantitative estimation of Holocene surface salinity variation in the Black Sea using dinoflagellate cyst process length. *Quaternary Science Reviews, 39,* 45–59.

Morin, J.J., & Cohen, A.C. (1991). Bioluminescent displays, courtship, and reproduction in ostracods. In R.T. Bauer, & J.W. Martin (Eds.), *Crustacean sexual biology* (pp. 1–16). New York: Columbia University Press.

Mudie, P.J., Rochon, A., & Aksu, A.E. (2002). Pollen stratigraphy of Late Quaternary cores from Marmara Sea: land-sea correlation and paleoclimatic history. *Marine Geology, 190,* 233–260.

Mudie, P.J., Rochon, A., Aksu, A.E., & Gillespie, H. (2004). Late glacial, Holocene and modern dinoflagellate cyst assemblages in the Aegean-Marmara-Black Sea

corridor: statistical analysis and re-interpretation of the early Holocene Noah's Flood hypothesis. *Review of Palaeobotany and Palynology 128,* 143-167.

Mudie, P.J., Marret, F., Aksu, A.E., Hiscott, R.N., & Gillespie, H. (2007). Palynological evidence for climate change, anthropogenic activity and outflow of Black Sea water during the late Pleistocene and Holocene: Centennial- to decadal- scale records from the Black and Marmara Seas. *Quaternary International, 167–168,* 73–90.

Murray J.W., Top, Z., & Özsoy, E. (1991). Hydrographic properties and ventilation of the Black Sea. *Deep-Sea Research, 38,* (2), S663–S689.

Murray, J.W., & Izdar, E. (1989). The 1988 Black Sea Oceanographic Expedition: overview and new discoveries. *Oceanography,* 2, 15–16.

Müller, G.W. (1894). *Die Ostracoden des Golfes von Neapel und der angrenzenden meeres-abschnitte, flora und fauna.* Berlin: R. Friedlander

Neale, J.W. (1988). Ostracods and palaeosalinity reconstruction. In P. De Deckker, J.P. Colin, & J.P. Peypouquet (Eds.), *Ostracoda in the earth sciences* (pp. 125–155). Netherlands: Elsevier.

Neprochnov, Yu. P. (1958). The results of seismic investigation in the Black sea in the neighborhood of Anapa. *Dokl. Acad. Sc. USSR 121*(6), 1001-1004.

Nevesskaya, L. A. (1970). On the classification of enclosed and semienclosed basins based on their fauna characteristics. In D. B. Obruchev, & V. N. Shimanskiy (Eds.), *Modern Problems of the Paleontology* (pp. 258-278). Moscow: Nauka [in Russian]

Norman, A. M. (1865). Report on the Crustacea. In G.S. Brady (Ed.), Reports of deepsea dredging on the coasts of Northumberland and Durham, 1862–1864. *Natural History Transactions of Northumberland and Durham, 1*(1), 12–29.

Oğuz, T., Latun, V.S., Latif, M.A., Vladimirov, V.V., Sur, H.I., Markov, A.A., Özsoy, E., Kotovshchikov, B.B., Eremeev, V.V., & Ünlülata, Ü. (1993). Circulation in the surface and intermediate layers of the Black Sea. *Deep-Sea Research I, 40*(8), 1597–1612.

Olteanu, R. (1978). Ostracoda from DSDP Leg 42B. In J.L. Usger, & P., Supko (Eds.), *Initial reports of the deep-sea drilling project, 42*(2), 1017–1038.

Opreanu, P.A. (2003/4). Some data on the Recent ostracod fauna from the continental shelf of the Black Sea in the Crimea and Sinop areas. *Geo-Eco-Marina, 9–10,* 1–4.

Opreanu, P.A. (2005). Contributions to the knowledge of Recent Ostracoda (Crustacea) distribution in the northwestern Black Sea. *Analele Ştiinţifice ale Universităţii "Al.I. Cuza" Iaşi, s. Biologie animal.* 63–70.

Opreanu, P.A. (2008). Ostracode relicte Ponto-Caspice in sectorul Romanecs Aal Marii Negre. *Geo Eco Marina, 14*(1), 57–62. [in Romanian]

Ostrovsky, A.B., Izmailov, Ya. A. & Shcheglov, A.P. (1977). New data on stratigraphy and geochronologyof Pleistocene marine terraces of the Caucasian Black Sea coast and of the Kerch-Taman region. In: Paleogeography and the Deposits of Southern Seas of the USSR, 61–68. Moscow: Nauka. [in Russian]

Özsoy, E., Latif, M.A., Tuğrul, S, & Ünlülata, Ü. (1995). Exchanges with the Mediterranean, fluxes and boundary mixing processes in the Black Sea. In: F. Briand (Ed.), *Mediterranean Tributary Seas. Spec. Publ. 15, CIESME Science Series, Vol. 1* (pp. 1–25). Monaco: Bulletin de l'Institut Océanographique.

Özsoy, E., Di Iorio, D., Gregg, M., & Backhaus, J.O. (2001). Mixing in the Bosphorus Strait and the Black Sea continental shelf: observations and a model of the dense water outflow. *Journal of Marine Systems, 31,* 99–135.

Panin, N., & Strechie, C. (2006). Late Quaternary sea-level and environmental changes in the Black Sea: A brief review of published data. *The Journal of Archaeomythology, 2(1),* 3–16.

Penny, D.N. (1993). Northern North Sea benthic Ostracoda: modern distribution and paleoenvironmental significance. *The Holocene 3*(3), 241–254.

Puri, H., Bonaduce, G., & Malloy, J. (1964). Ecology of the Gulf of Naples. *Pubblicazioni della Stazione Zoological di Napoli, 33,* 87–199.

Robinson, A. (Ed.). (1997). *Regional and petroleum geology of the Black Sea and surrounding region.* Tulsa: The American Association of Petroleum Geologists.

Roemer, F.A. (1838). Die Cytherinen des Molassegebirges. *Neues Jahrbuch für Mineralogie,* 514–519.

Rögl, F. (1999). Mediterranean and Paratethys. Facts and hypotheses of an Oligocene to Miocene paleogeography (short overview). *Geologica Carpathica, 50*(4), 339–349.

Ruggieri, G. (1964). Ecological remarks on the present and past distribution of four species of *Loxoconcha* in the Mediterranean. *Pubblicazioni della Stazione Zoologica di Napoli, 33,* 515–528.

Ruggieri, G. (1967). Due ostracofaune del Miocene allocto dell val Mareccia (Appennino Settentrionale). *Rivista Italiana di Paleontologia e Stratigrafia, 73*(1), 351–384.

Ruggieri, G. (1962). Alcuni Ostracodi quaternari e recenti pertinenti al genere Costa Neviani. *Bollettino della Societa Paleontologica Italiana, 1*(2), 3–9.

Ryan, W.B.F., Pitman, W.C., III, Major, C.O., Shimkus, K., Maskalenko, V., Jones, G.A.,...Yüce, H. (1997). An abrupt drowning of the Black Sea shelf. *Marine Geology, 138,* 119–126.

Ryan, W.B.F., & Pitman, W.C. (1998). Noah's flood: The new scientific discoveries about the event that changed history. New-York : Simon & Schuster.

Ryan, W.B.F., Major, C.O., Lericolais, G., & Goldstein, S.L. (2003). Catastrophic Flooding of the Black Sea. *Annual Review of Earth and Planetary Sciences 31,* 525-554.

Sars, G.O. (1866). *Oversigt af Norges marine Ostracoder.* Brøgger & Christie.

Schornikov, E.I. (1964). An experiment on the distinction of the Caspian elements of the ostracod fauna in the Azov-Black Sea basin. *Zoologicheski Zurnal, 43,* 1276–1293.

Schornikov, E.I. (1966). *Leptocythere (Crustacea, Ostracoda)* of the Azov-Black Sea basin. *Zoologicheski Zurnal, 45,* 32–49.

Schornikov, E.I. (1967). *Identification key to the fauna of the Black Sea and Azov Sea. Vol. 2: Free living invertebrates. Crustacean.* Kiev.

Schornikov, E. I. (1969). Subclass Ostracoda, shelled Crustacea-Ostracoda. In *Opredelitel' fauny Chernogo i Azovskogo morey, tom 2, Rakoobraznye (Key to the Fauna of the Black and Azov Seas, 2. Free Living Invertebrates-Crustacea,* pp. 163–260).Kiev: Naukova dumka. [in Russian]

Schornikov, E.I. (2011). Ostracoda of the Caspian origin in the Azov-Black Sea basin. In M. Gross (Ed.), European Ostracodologists Meeting 7, Abstract Volume (pp.180–184). Graz: Universalmuseum Joanneum.

Schweyer, A.V. (1949). On the Pliocene Ostracoda of the northern Caucasus and lower Volga region. *Trudy Vesoyuznogo Neftyanogo Naucho-Isseldovatelskogo Geologo-Razvedochnogo Instituta, 30,* 9–68.

Siani, G., Paterne, M., Arnold, M., Bard, E., Métiver, B., Tisnerat, N., & Bassinot, F. (2000). Radiocarbon reservoir ages in the Mediterranean Sea and Black Sea. *Radiocarbon, 42,* 271–280.

Skene, K.I., Piper, D.J.W., Aksu, A.E., & Syvikski, J.P.M. (1998). Evaluation of the glocal oxygen isotope curve as a proxy for quaternary for quaternary sea level by modeling of delta progradation. *Journal of Sedimentary Research, 68* (6), 1077–1092.

Smith, A.J., & Horne, D.J. (2002). Ecology of marine, marginal marine and nonmarine ostracods. In J.A. Holmes, & A.R. Chivas (Eds.), *the Ostracoda: Applications in Quaternary research* (pp. 37–64). Washington: American Geophysical Union.

Soulet, G., Delaygue, G., Vallet-Coulomb, C., Böttcher, M.E., Sonzogni, C., Lericolais, G., & Bard, E. (2010). Glacial hydrologic conditions in the Black Sea reconstructed using geochemical pore water profiles. *Earth and Planetary Science Letters 296,* 57-66.

Soulet, G., Ménot, G., & Bard, E. (2011). A revised calendar age for the last reconnection of the Black Sea to the global ocean. *Quaternary Science Reviews, 30*(9–10), 1019–1026.

Sperling, M., Schmiedl, G., Hemleben, Ch., Emeis, K.C., Erlenkeuser, H., & Grootes, P.M. (2003). Black Sea impact on the formation of eastern Mediterranean sapropel S1? Evidence from the Marmara Sea. *Palaeogeography, Palaeoclimatology, Palaeoecology, 190,* 9–21.

Stancheva, M. (1989). Taxonomy and Biostratigraphy of the Pleistocene ostracods of the Western Black Sea Shelf. *Geologica Balcanica, 19*(6), 3–39.

Stanev, E.V., Le Traon, P.Y., & Peneva, E.L. (2000). Sea level variations and their dependency on meteorological and hydrological forcing: Analysis of altimeter and surface data for the Black Sea. *Journal of Geophysical Research, 105* (C7), 17,203-17,216.

Stepanaitys, N. (1958). New forms of ostracods from the Bakunian deposits of western Turkmenistan. *Izvestiya Akademia Nauk Turkmenistan SSR, 2,* 11–20.

Tunoğlu, C. (2002). The Recent Ostracoda association of İstanbul Strait exit, and Zonguldak and Amasra coastal areas of Black Sea. *Yerbilimleri, 26,* 27–43.

Van Morkhoven, F.P.C.M. (1962). *Post-Palaeozoic Ostracoda: Their morphology, taxonomy, and economic use Vol.1.* London: Elsevier.

Van Morkhoven, F.P.C.M. (1963). *Post-Palaeozoic Ostracoda: Their morphology, taxonomy, and economic use Vol.2.* London: Elsevier.

Vidal, L., Ménot, G., Joly, C., Bruneton, F., Rostek, F., Çağatay, M.N., Major, C.O., & Bard, E. (2010). Hydrology in the Sea of Marmara during the last 23 ka: Implications for timing of Black Sea connections and sapropel deposition. *Paleoceanography, 25,* PA1205.

Wagner, C. W. (1957). *Sur les Ostracodes du Quaternaire recent des Pays-Bas et leur utilisation dans l'étude géologique des depots Holocénes.* The Hague: Mouton & Co.

Whatley, R. (1990). Ostracoda and Global Events. In R. Whatley & C. Maybury (Eds.), *Ostracoda and Global Events.* (p. 3–24). London: Chapman and Hall.

Whittaker, J.E. (1972). *The taxonomy, ecology and distribution of Recent brackish and marine Ostracoda from localities along the coast of Hampshire and Dorset (Christchurch Harbour, the Fleet and Weymouth Bay).* (Doctoral dissertation, unpublished). University of Wales, United Kingdom.

Yanko-Hombach, V. (2004). The Black Sea flood controversy in light of the geological and foraminiferal evidence. In V. Yanko-Hombach, M. Görmüş, A. Ertunç, M. McGann, R. Martin, J. Jacob, & S. Ishman (Eds.). Program and extended abstracts of the fourth international congress on environmental micropalaeontology, microbiology, and meiobenthology. Isparta, Turkey.

Yanko-Hombach, V. (2007). Controversy over Noah's Flood in the Black Sea: geological and foraminiferal evidence from the shelf, In V. Yanko-Hombach, A.S. Gilbert,

N. Panin, & P.M. Dolukhanov (Eds.), *The Black Sea flood question: Changes in coastline, climate and human settlement* (pp. 149–203). Heidelberg: Springer.

Yanko-Hombach , V., Gilbert, A.S., & Dolukhanov, P. (2007) Controversy over the great flood hypotheses in the Black Sea in light of geological, paleontological, and archaeological evidence. *Quaternary International, 167–168,* 91–113.

Appendix A - Original Sample Data

MAR05-50P

Samp	Dry Wt	>63 µm	# V	Con	A	B	C	D	E	F	G	H	I
0	31.21	0.60	235	7.53	78	65	18	8	42	7	7	1	0
10	25.68	0.82	191	7.44	104	16	15	10	23	7	1	2	2
20	28.79	0.22	58	2.01	18	8	1	2	28	0	1	0	0
30	27.75	0.18	77	2.78	35	2	2	6	25	2	1	0	4
40	31.79	0.32	98	3.08	52	2	2	8	21	7	1	0	2
50	27.85	0.41	34	1.22	13	3	2	5	9	0	0	0	0
60	22.91	0.28	147	6.42	70	12	6	11	39	0	1	1	1
70	29.00	0.21	262	9.03	101	3	2	13	24	2	0	14	43
80	29.80	0.22	282	9.46	140	8	11	34	32	17	0	12	4
90	25.60	0.05	34	1.33	11	1	3	5	7	0	0	5	0
100	29.54	0.13	39	1.32	27	1	0	3	5	1	0	0	0
110	28.71	0.09	99	3.45	41	11	16	10	15	6	0	0	0
120	27.95	0.15	69	2.47	36	3	5	13	8	0	2	0	0
130	26.81	0.20	32	1.19	14	4	5	0	3	0	0	2	0
140	27.12	0.10	5	0.18	4	0	1	0	0	0	0	0	0
150	26.79	0.13	48	1.79	20	2	7	8	10	0	0	0	0
160	29.21	0.09	26	0.89	13	0	2	2	7	0	0	0	0
170	30.22	0.25	182	6.02	113	5	5	8	20	3	0	6	1
180	29.24	1.16	192	6.57	108	4	6	20	39	3	0	5	0
190	28.87	0.09	11	0.38	5	0	0	0	6	0	0	0	0
200	31.06	0.16	70	2.25	43	0	1	7	9	0	0	3	0
210	32.14	0.32	128	3.98	72	1	2	21	14	0	0	10	0
220	31.11	0.14	99	3.18	69	2	1	7	11	0	0	1	0
230	30.64	0.15	122	3.98	70	2	4	10	21	2	1	5	0
240	32.33	0.15	140	4.33	83	1	2	17	14	2	0	5	0
250	32.33	0.15	205	6.34	126	5	5	23	39	1	0	0	0
260	29.09	0.14	30	1.03	9	2	2	1	14	0	0	0	0
270	32.12	0.43	255	7.94	152	4	11	25	31	7	1	6	2
280	32.01	0.76	403	12.59	236	8	8	32	53	0	0	43	0
290	29.49	0.56	346	11.73	210	5	11	28	47	1	0	17	0
300	34.76	0.52	553	15.91	326	4	12	48	67	14	0	47	0
310	32.54	0.42	317	9.74	181	6	10	27	47	1	1	34	0
320	30.34	0.38	354	11.67	205	6	21	34	45	5	0	23	0
330	33.15	0.63	661	19.94	330	1	5	56	12	12	0	32	0
340	36.54	2.75	2221	60.78	0	0	0	0	35	18	0	89	0
350	34.48	0.22	1046	30.34	0	0	0	4	10	0	0	56	0
360	30.86	0.13	681	22.07	555	0	0	37	6	8	0	52	0
370	31.61	0.10	561	17.75	467	0	0	18	2	4	0	44	0
380	32.32	0.51	1127	34.87	0	0	0	79	19	3	0	117	0
390	31.28	0.16	823	26.31	622	0	0	67	11	1	0	67	0
400	31.29	0.12	541	17.29	394	0	0	59	6	4	0	27	0
410	30.99	0.07	258	8.32	176	0	0	24	0	0	0	27	0
420	29.30	0.36	643	21.94	517	0	0	84	11	2	0	10	0
430	31.91	0.56	65	2.04	47	0	0	13	2	0	0	1	0
440	29.13	0.86	220	7.55	182	0	0	16	6	0	0	4	0
450	33.69	0.32	297	8.82	231	0	0	39	13	0	0	0	0
460	30.58	0.95	191	6.25	134	0	0	35	13	0	0	4	0
470	31.35	0.92	19	0.61	6	0	0	10	3	0	0	0	0
480	35.55	0.90	161	4.53	46	0	0	48	50	0	0	0	0

490	31.62	0.54	148	4.68	2	0	0	2	0	0	0	0	0
500	31.66	0.36	74	2.34	0	0	0	4	0	0	0	0	0
510	35.15	0.99	251	7.14	5	0	0	0	0	0	0	0	0
520	33.06	0.90	168	5.08	2	0	0	0	0	0	0	0	0
530	35.28	0.78	129	3.66	10	0	0	2	1	0	0	0	0
540	35.87	1.17	190	5.30	2	0	0	1	1	0	0	0	0
550	33.65	0.34	203	6.03	6	0	0	0	1	0	0	0	0
560	34.63	0.42	97	2.80	6	0	1	0	3	0	0	0	0
570	41.45	0.32	128	3.09	2	0	0	0	1	0	0	0	0
580	36.03	0.41	58	1.61	2	0	0	0	0	0	0	0	0
590	35.84	1.00	282	7.87	0	0	0	0	0	0	0	0	0
600	34.69	0.47	148	4.27	1	0	0	0	0	0	0	1	0
610	40.28	0.78	486	12.07	0	0	0	0	0	0	0	0	0
620	34.63	0.65	192	5.54	2	0	0	0	0	0	0	0	0
630	40.27	0.60	193	4.79	2	0	0	0	0	0	0	0	0
640	42.39	0.99	509	12.01	1	0	0	0	0	0	0	0	0
650	35.23	0.59	92	2.61	3	0	0	0	0	0	0	0	0
660	36.87	0.21	70	1.90	2	0	0	0	0	0	0	0	0
670	41.56	2.14	250	6.01	0	0	0	0	1	0	0	0	0
680	36.60	0.60	96	2.62	5	0	0	0	0	0	0	0	0
690	36.03	2.40	244	6.77	1	0	0	0	0	0	0	0	0
700	34.04	0.42	48	1.41	1	0	0	0	0	0	0	0	0
710	35.92	0.52	32	0.89	0	0	0	0	0	0	0	0	0
720	35.48	0.94	223	6.29	2	0	0	0	1	0	0	0	0
730	35.52	1.59	128	3.60	0	0	0	1	0	0	0	0	0
MAR05-51G													
10	21.09	0.14	95	4.50	39	10	6	7	20	1	2	0	2
20	24.62	0.52	150	6.09	57	28	13	12	21	0	12	1	0
30	24.02	0.10	108	4.50	47	27	6	7	19	2	0	0	0
40	24.49	0.09	116	4.74	46	23	6	6	14	1	13	0	0
50	24.09	0.11	66	2.74	38	1	2	3	16	1	1	1	2
60	24.36	0.24	54	2.22	18	12	2	4	8	0	3	0	2
70	24.05	0.16	56	2.33	32	5	4	6	8	0	1	0	0
80	22.61	0.13	64	2.83	32	4	6	6	11	1	1	0	0
90	22.59	0.38	158	7.00	75	8	16	13	44	0	1	0	0
100	24.34	0.14	243	9.98	100	7	21	19	81	3	3	1	4
110	25.92	0.29	81	3.12	40	1	7	13	8	1	0	3	6
120	25.45	0.10	56	2.20	12	3	7	10	22	0	0	1	0
130	24.67	0.61	156	6.32	56	13	11	25	40	1	3	1	0
140	24.49	0.16	70	2.86	35	2	3	15	14	0	0	1	0
150	26.42	0.15	65	2.46	37	3	7	6	10	0	2	0	0
MAR05-50													
	J	K	L	M	N	O	P	Q	R	S	T	U	V
0	0	1	0	0	3	0	0	0	4	0	0	0	0
10	1	1	0	0	1	0	0	0	4	0	0	0	0
20	0	0	0	0	0	0	0	0	0	0	0	0	0
30	0	0	0	0	0	0	0	0	0	0	0	0	0
40	1	1	0	0	0	0	0	0	0	0	0	0	0
50	0	0	1	0	0	0	0	0	0	0	0	0	1
60	0	5	0	0	0	0	0	0	0	0	0	0	0
70	3	31	2	13	0	1	0	1	0	0	0	0	0
80	0	19	0	0	0	0	0	0	0	0	0	0	2
90	1	0	0	0	0	0	0	6	0	0	0	0	0
100	0	2	0	0	0	0	0	0	0	0	0	0	0

110	0	0	0	0	0	0	0	0	0	0	0	0	0
120	2	0	0	0	0	0	0	0	0	0	0	0	0
130	0	0	0	0	0	0	0	0	0	1	0	0	0
140	0	0	0	0	0	0	0	0	0	0	0	0	0
150	0	0	0	0	0	0	0	0	0	0	0	0	0
160	0	2	0	0	0	0	0	0	0	0	0	0	0
170	0	20	0	0	0	1	0	0	0	0	0	0	0
180	0	4	1	0	0	0	0	0	0	0	0	0	0
190	0	0	0	0	0	0	0	0	0	0	0	0	0
200	2	5	0	0	0	0	0	0	0	0	0	0	0
210	1	4	0	0	0	0	0	0	0	0	0	0	0
220	0	6	0	0	0	1	1	0	0	0	0	0	0
230	0	5	0	0	0	1	0	0	0	0	1	0	0
240	1	10	2	0	0	0	0	0	0	0	0	0	0
250	0	4	0	0	0	0	0	0	0	0	0	0	0
260	0	2	0	0	0	0	0	0	0	0	0	0	0
270	0	11	1	0	0	0	0	0	0	0	0	0	0
280	1	16	0	0	0	0	0	1	0	0	0	0	0
290	1	21	0	0	0	4	0	0	0	0	1	0	0
300	4	21	1	0	0	0	0	0	0	0	0	0	0
310	1	4	0	0	0	1	0	0	0	0	0	0	0
320	3	6	2	0	0	0	0	0	0	0	0	0	0
330	3	15	0	0	0	0	0	0	0	0	0	0	0
340	15	10	3	0	0	3	1	0	0	0	1	3	0
350	6	19	0	0	0	0	0	0	0	0	1	1	0
360	17	3	0	0	0	0	0	0	0	0	0	0	0
370	6	14	2	0	0	0	0	0	0	0	1	0	0
380	25	9	4	0	0	0	0	0	0	0	0	2	0
390	30	13	2	0	0	0	0	0	0	0	3	1	1
400	20	25	0	0	0	0	0	0	0	0	1	0	0
410	24	6	0	0	0	0	0	0	0	0	0	0	0
420	16	0	0	0	0	0	0	0	0	0	0	0	1
430	1	0	0	0	0	0	0	0	0	0	0	0	0
440	12	0	0	0	0	0	0	0	0	0	0	0	0
450	14	0	0	0	0	0	0	0	0	0	0	0	0
460	5	0	0	0	0	0	0	0	0	0	0	0	0
470	0	0	0	0	0	0	0	0	0	0	0	0	0
480	4	0	0	0	0	0	0	0	0	0	0	0	4
490	0	0	0	0	0	0	0	0	0	0	0	0	82
500	2	1	0	0	0	0	0	0	0	0	0	0	22
510	0	0	0	0	0	0	0	0	0	0	0	0	139
520	0	0	0	0	0	0	0	0	0	0	0	0	82
530	0	0	0	0	0	0	0	0	0	0	0	0	49
540	0	0	0	0	0	0	0	0	0	0	0	0	80
550	0	3	0	0	0	0	0	0	0	0	0	0	107
560	0	1	0	0	0	0	0	0	0	0	0	0	11
570	0	4	0	0	0	0	0	0	0	0	0	0	52
580	0	0	0	0	0	0	0	0	0	0	0	0	1
590	0	0	0	0	0	0	0	0	0	0	0	0	0
600	0	0	0	0	0	0	0	0	0	0	0	0	2
610	1	0	0	0	0	0	0	0	0	0	0	0	1
620	0	0	0	0	0	0	0	0	0	0	0	0	1
630	0	0	0	0	0	0	0	0	0	0	0	0	0
640	2	0	0	0	0	0	0	0	0	0	0	0	0

650	0	0	0	0	0	0	0	0	0	0	0	0
660	1	0	0	0	0	0	0	0	0	0	0	0
670	2	0	0	0	0	0	0	0	0	0	0	1
680	0	0	0	0	0	0	0	0	0	0	0	0
690	0	0	0	0	0	0	0	0	0	0	0	1
700	0	0	0	0	0	0	0	0	0	0	0	3
710	0	0	0	0	0	0	0	0	0	0	0	2
720	0	0	0	0	0	0	0	0	0	0	0	0
730	0	0	0	0	0	0	0	0	0	0	0	1

MAR05-51G

10	0	1	0	0	2	1	0	0	0	0	0	0
20	0	0	0	0	1	0	0	0	4	0	0	0
30	0	0	0	0	0	0	0	0	0	0	0	0
40	0	1	1	0	0	3	0	0	3	0	0	0
50	0	0	0	0	0	0	0	0	0	0	0	0
60	0	5	0	0	0	0	0	0	0	0	0	0
70	0	0	0	0	0	0	0	0	0	0	0	0
80	1	2	0	0	0	0	0	0	0	0	0	0
90	0	1	0	0	0	0	0	0	0	0	0	0
100	1	0	2	0	0	0	0	0	0	0	0	0
110	0	1	0	1	0	0	0	0	0	0	0	0
120	0	0	0	0	0	1	0	0	0	0	0	0
130	2	0	0	0	0	3	0	0	0	0	0	0
140	0	0	0	0	0	0	0	0	0	0	0	0
150	0	0	0	0	0	0	0	0	0	0	0	0

MAR05-50P

	W	X	Y	Z	AA	BB	CC	DD	EE	FF	GG	HH	I
0	0	0	0	0	0	0	1	0	0	0	0	0	0
10	0	1	0	0	0	0	0	0	0	0	0	0	0
20	0	0	0	0	0	0	0	0	0	0	0	0	0
30	0	0	0	0	0	0	0	0	0	0	0	0	0
40	0	0	0	0	0	0	0	0	1	0	0	0	0
50	0	0	0	0	0	0	0	0	0	0	0	0	0
60	0	0	1	0	0	0	0	0	0	0	0	0	0
70	0	8	0	0	0	0	0	0	1	0	0	0	0
80	0	0	0	0	0	0	0	0	2	0	0	1	0
90	1	0	0	0	0	0	0	0	0	0	0	0	0
100	0	0	0	0	0	0	0	0	0	0	0	0	0
110	0	0	0	0	0	0	0	0	0	0	0	0	0
120	0	0	0	0	0	0	0	0	0	0	0	0	0
130	0	0	0	0	0	0	0	0	0	0	0	0	0
140	0	0	0	0	0	0	0	0	0	0	0	0	0
150	0	0	0	0	0	0	0	0	1	0	0	0	0
160	0	0	0	0	0	0	0	0	0	0	0	0	0
170	0	0	0	0	0	0	0	0	0	0	0	0	0
180	0	0	0	0	0	0	0	0	2	0	0	0	0
190	0	0	0	0	0	0	0	0	0	0	0	0	0
200	0	0	0	0	0	0	0	0	0	0	0	0	0
210	0	0	0	0	0	0	0	1	0	0	0	0	0
220	0	0	0	0	0	0	0	0	0	0	0	0	0

230	0	0	0	0	0	0	0	0	0	0	0	0
240	0	0	0	0	0	1	0	1	0	0	0	0
250	0	0	0	0	0	1	1	0	0	0	0	0
260	0	0	0	0	0	0	0	0	0	0	0	0
270	0	0	0	0	0	0	2	1	1	0	0	0
280	0	0	0	0	0	0	0	0	3	0	0	0
290	0	0	0	0	0	0	0	0	0	0	0	0
300	0	0	0	0	0	0	0	1	4	0	1	0
310	0	0	0	0	0	0	0	1	2	0	1	0
320	0	0	0	0	0	0	1	0	3	0	0	0
330	0	0	0	0	0	0	1	1	0	0	0	0
340	0	0	0	0	0	5	11	4	17	3	2	2	0
350	0	0	0	0	0	0	1	0	0	0	0	0
360	0	0	0	0	0	0	0	2	1	0	0	0
370	0	0	0	0	0	1	0	0	2	0	0	0
380	0	0	0	0	0	0	0	5	1	0	0	0
390	0	0	0	0	0	0	0	2	2	0	1	0
400	0	0	0	0	0	0	0	5	0	0	0	0
410	0	0	0	0	0	0	0	0	0	0	0	0
420	0	0	0	0	0	0	0	2	0	0	0	0
430	0	0	0	0	0	0	0	1	0	0	0	0
440	0	0	0	0	0	0	0	0	0	0	0	0
450	0	0	0	0	0	0	0	0	0	0	0	0
460	0	0	0	0	0	0	0	0	0	0	0	0
470	0	0	0	0	0	0	0	0	0	0	0	0
480	0	0	0	0	0	0	2	3	4	0	0	0
490	0	0	0	0	0	2	3	37	0	5	2	4	0
500	0	0	0	0	0	2	34	5	2	1	0	0
510	0	0	2	0	0	18	39	18	5	5	8	0
520	0	0	3	0	0	3	6	40	11	1	0	7	2
530	0	0	0	0	0	3	6	32	2	2	4	2	0
540	0	0	0	0	0	2	6	45	23	6	7	6	0
550	0	0	0	0	0	0	6	51	6	7	1	6	0
560	0	0	0	0	0	2	8	39	9	1	2	2	0
570	0	0	0	3	0	3	5	34	7	4	2	6	0
580	0	0	1	0	0	0	5	37	3	4	0	1	0
590	0	0	0	0	0	7	43	124	22	15	9	4	0
600	0	0	0	0	0	1	14	95	7	8	2	2	0
610	0	0	0	0	0	6	62	328	38	20	7	2	2
620	0	0	1	0	0	2	40	88	12	11	6	3	8
630	0	0	0	0	0	6	23	101	12	7	5	0	17
640	0	0	0	0	0	7	70	305	22	15	10	2	26
650	0	0	0	0	0	5	5	46	9	4	8	0	2
660	0	0	0	0	0	2	3	28	10	4	6	0	0
670	0	0	0	0	0	21	38	66	87	0	13	2	0
680	0	0	0	0	0	8	10	44	16	2	7	1	0
690	0	0	3	0	0	4	16	137	38	9	5	5	5
700	0	0	0	0	0	3	1	21	5	5	1	1	2
710	0	0	0	0	0	0	1	17	0	1	5	0	0
720	0	0	2	0	0	17	15	127	23	5	13	0	0
730	0	0	0	0	1	9	15	40	25	4	23	0	0
MAR05-51G												
10	0	4	0	0	0	0	0	0	0	0	0	0
20	0	0	0	0	0	0	0	0	1	0	0	0

30	0	0	0	0	0	0	0	0	0	0	0	0	0
40	0	0	0	0	0	0	0	0	0	0	0	0	0
50	0	0	0	0	0	0	0	0	0	0	0	0	0
60	0	0	0	0	0	0	0	0	0	0	0	0	0
70	0	0	0	0	0	0	0	0	0	0	0	0	0
80	0	0	0	0	0	0	0	0	0	0	0	0	0
90	0	0	0	0	0	0	0	0	0	0	0	0	0
100	0	0	0	0	0	0	0	0	1	1	0	0	0
110	0	0	0	0	0	0	0	0	0	0	0	0	0
120	0	0	0	0	0	0	0	0	0	0	0	0	0
130	0	0	1	0	0	0	0	0	1	0	0	0	0
140	0	0	0	0	0	0	0	0	0	0	0	0	0
150	0	0	0	0	0	0	0	0	0	0	0	0	0

MAR05-50P

	JJ	KK	LL	MM	NN	OO	PP	QQ	RR	SS
0	0	0	0	0	0	0	0	0	0	0
10	0	0	0	0	0	0	0	0	0	0
20	0	0	0	0	0	0	0	0	0	0
30	0	0	0	0	0	0	0	0	0	0
40	0	0	0	0	0	0	0	0	0	0
50	0	0	0	0	0	0	0	0	0	0
60	0	0	0	0	0	0	0	0	0	0
70	0	0	0	0	0	0	0	0	0	0
80	0	0	0	0	0	0	0	0	0	0
90	0	0	0	0	0	0	0	0	0	0
100	0	0	0	0	0	0	0	0	0	0
110	0	0	0	0	0	0	0	0	0	0
120	0	0	0	0	0	0	0	0	0	0
130	0	0	0	0	0	0	0	0	0	0
140	0	0	0	0	0	0	0	0	0	0
150	0	0	0	0	0	0	0	0	0	0
160	0	0	0	0	0	0	0	0	0	0
170	0	0	0	0	0	0	0	0	0	0
180	0	0	0	0	0	0	0	0	0	0
190	0	0	0	0	0	0	0	0	0	0
200	0	0	0	2	0	0	0	0	0	0
210	0	0	0	0	0	0	0	0	0	0
220	0	0	0	0	0	0	0	0	0	0
230	0	0	0	0	0	0	0	0	0	0
240	0	0	0	0	0	0	0	0	0	0
250	0	0	0	0	0	0	0	0	0	0
260	0	0	0	0	0	0	0	0	0	0
270	0	0	0	2	0	0	0	0	0	0
280	0	0	0	0	0	0	0	0	0	0
290	0	0	1	1	0	0	0	0	0	0
300	0	0	0	0	0	0	0	0	0	0
310	0	0	0	0	0	0	0	0	0	0
320	0	0	0	0	0	0	0	0	0	0
330	0	0	1	0	0	5	0	1	0	0
340	0	0	0	0	0	0	0	0	0	0
350	0	0	0	0	0	0	0	0	0	0
360	0	0	0	0	0	0	0	0	0	0
370	0	0	0	0	0	0	0	0	0	0
380	0	0	0	0	0	0	0	0	0	0

390	0	0	0	0	0	0	0	0	0
400	1	0	0	0	0	0	0	0	0
410	0	0	0	0	0	0	0	0	0
420	0	0	0	0	0	0	0	0	0
430	0	0	0	0	0	0	0	0	0
440	0	0	0	0	0	0	0	0	0
450	0	0	0	0	0	0	0	0	0
460	0	0	0	0	0	0	0	0	0
470	0	0	0	0	0	0	0	0	0
480	2	0	5	0	0	0	0	0	0
490	1	0	0	0	0	0	0	0	0
500	2	0	6	0	0	2	0	1	1	0
510	0	0	2	0	0	2	0	0	0	0
520	1	0	10	2	1	0	0	0	0	0
530	0	0	8	0	0	1	1	1	0	0
540	1	0	3	0	0	0	1	4	0	0
550	5	0	4	0	0	3	0	0	0	0
560	1	0	4	0	0	0	0	0	0	0
570	0	1	1	0	0	0	0	2	0	0
580	1	0	56	0	0	1	0	0	0	0
590	1	0	2	0	1	1	1	8	0	0
600	0	0	3	5	0	4	4	2	1	0
610	0	0	8	1	1	3	1	2	1	0
620	3	3	6	0	0	4	3	1	0	0
630	4	2	26	1	0	5	4	7	0	0
640	1	1	5	2	0	0	0	1	0	0
650	3	0	2	1	0	5	1	2	0	0
660	0	0	15	2	0	2	0	0	0	0
670	0	0	3	0	0	0	0	0	0	0
680	4	0	11	1	1	0	1	1	1	0
690	0	0	2	0	1	0	0	2	0	0
700	0	0	2	0	0	0	0	1	0	0
710	0	0	15	2	0	1	0	0	1	0
720	2	0	4	0	0	1	0	1	0	1
730	0	0	0	0	0	0	0	0	0	0
MAR05-51G									
10	0	0	0	0	0	0	0	0	0
20	0	0	0	0	0	0	0	0	0
30	0	0	0	0	0	0	0	0	0
40	0	0	0	0	0	0	0	0	0
50	0	0	0	0	0	0	0	0	0
60	0	0	0	0	0	0	0	0	0
70	0	0	0	0	0	0	0	0	0
80	0	0	0	0	0	0	0	0	0
90	0	0	0	0	0	0	0	0	0
100	0	0	0	0	0	0	0	0	0
110	0	0	0	0	0	0	0	0	0
120	0	0	0	0	0	0	0	0	0
130	0	0	0	0	0	0	0	0	0
140	0	0	0	0	0	0	0	0	0
150	0	0	0	0	0	0	0	0	0

KEY

Samp: Sample depth in the core (cm)
Dry Wt: Weight of sample after oven drying
>63 μm: Weight of >63 μm fraction after sieving
V: Number of valves in the sample
Con: Concentration (# of valves per gram of dry sediment)

SPECIES KEY

A   *P. agilis*
B   *C. edwardsi*
C   *P. jonesii*
D   *H. rubra*
E   *C. carinata*
F   *Bythocythere* sp.
G   *P. polita*
H   *L. multipunctata*
I   *C. diffusa*
J   *X.* sp. aff. *cornelii*
K   *C. variabilis*
L   *L. devexa*
M   *A. propinqua*
N   *Cytheropteron* sp.
O   *B. subulata rectangularis*
P   *Hemicytherura* sp.
Q   *Semicytherura* sp.
R   *C. semipunctata*
S   *Leptocythere* sp. 1
T   *S. gewemuelleri*
U   *P. simile*
V   *L. littoralis*
W   Unknown sp. 3
X   *Pontocythere* sp.
Y   Unknown sp. 1
Z   *C.* sp. aff. *fuscata*
AA   *C. acronasuta*

BB   *L. lepida*
CC   *L . sublepida*
DD   *L. spp. juveniles*
EE   *T. amnicola donetziensis*
FF   *A. quinquetuberculata*
GG   *A. olivia*
HH   *L. immodulata*
II   *A. cymbula*
JJ   *A. subcaspia*
KK   *A. caspia*
LL   *C. schweyeri*
MM   *E. (M.) lopatici*
NN   *A. striatocostata*
OO   *A. bacuana*
PP   *A. pediformis*
QQ   *E.* sp. aff. *relicta*
RR   *A. volgensis*
SS   Unknown sp. 2